universität wien

MASTERARBEIT

Titel der Masterarbeit

Synthesis and Evaluation of Arylcarbamoylated Cinchona-Based Chiral Anion Exchangers for HPLC

Verfasser

Hubert Hettegger, BSc

angestrebter akademischer Grad

Master of Science (MSc)

Wien, 2012

Studienkennzahl lt. Studienblatt:	A 066 862
Studienrichtung lt. Studienblatt:	Masterstudium Chemie
Betreuer:	o. Univ.-Prof. Dr. Wolfgang Lindner, Dr. Michal Kohout

Danksagung

Ich möchte mich an dieser Stelle ganz herzlich bei Herrn Prof. Dr. Wolfgang Lindner für die Möglichkeit bedanken, meine Masterarbeit in der Arbeitsgruppe für Hochleistungstrenntechniken und Materialien gemacht haben zu können. Mein Dank gilt auch der motivierenden Betreuung und Unterstützung während der ganzen Zeit der Masterarbeit. Die interessanten Diskussionen über Honigbienen und Fussball sollen hierbei natürlich nicht unerwähnt bleiben.

Ein weiteres großes Dankeschön gilt meinem Betreuer Michal Kohout, der mir bei jeder Fragestellung immer und überall zur Seite gestanden ist. Dank deiner hervorragenden Betreuung und hilfsbereiten Unterstützung im Labor hatte ich immer Freude am Arbeiten. Für das Korrekturlesen der vorliegenden Arbeit möchte ich dir ebenfalls danken.

Peter Frühauf danke ich speziell für das Packen der Säulen, den zahlreichen Hilfestellungen in Zusammenhang mit der Infinity und der Unterstützung bei vielen anderen Fragen.

Des Weiteren möchte ich mich von ganzem Herzen bei meiner Freundin Pálma bedanken. Ohne deinen Rückhalt wäre ich mit dem Studium sicher noch nicht fertig. Ich möchte dir auch für dein Verständnis und die Hilfsbereitschaft danken. Du hast immer ein offenes Ohr für mich gehabt und dafür möchte ich dir wirklich aufrichtig Danke sagen!

Ich möchte vor allem meinem Kumpel, Nachbar und „Laborabschnittspartner“ Roli danken, mit dem ich nicht nur den Großteil des Masterstudiums, sondern auch die gesamte Masterarbeit absolviert habe. Ich wünsche dir für die anstehende Dissertation alles Gute und viel Erfolg!

Weiters möchte ich mich bei Jano und Vebi bedanken, die immer für einen sehr abwechslungsreichen Alltag gesorgt haben.

Ein besonderes Dankeschön geht an meine Eltern für die Unterstützung während meiner ganzen Studienzeit. Ohne euch wäre mir das Studium nicht möglich gewesen. Danke sagen möchte ich auch meinen Studienkollegen, Schulkollegen und Freunden, meinen beiden Brüdern Tobias und Peter und Allen, die in den letzten Jahren für eine abwechslungsreiche und schöne Zeit gesorgt haben.

Table of Contents

I. Aims

The first aim of the present master thesis is the synthesis of a series of novel chiral stationary phases (CSPs) for high performance liquid chromatography (HPLC). In particular the focus is placed on weak anion exchange (WAX) type CSPs. Therefore two different types of linkers (one allylated and one propargylated), which are supposed to serve as immobilization anchor onto preactivated silica, should be synthesized. These linkers should be connected to two basic modules derived from cinchona alkaloids, namely dihydroquinine and dihydroquinidine, via carbamoyl bond with the secondary hydroxylic group. We assume that these reactions would lead to four different selectors, from which a series of CSPs should be prepared.

The second aim is the subsequent evaluation of the synthesized CSPs in terms of their chiral separation ability towards chiral acidic compounds, in particular *N*-protected amino acids, *N*-protected aminosulfonic acids, *N*-protected aminophosphonates and carboxylic acids. A small set of basic and zwitterionic compounds serves as a proof of principle to ascertain an anion exchange mechanism.

Moreover, the influence of different immobilization strategies, endcapping as well as immobilization controllability should be evaluated. Assuming controlled loading of the selectors, we aim to evaluate the influence of the selector density on the silica surface on the overall performance of the new CSPs. Subsequently, the column with the best enantioseparation capabilities should be compared to commercially available chiral anion exchangers.

1. Introduction

The separation of chiral compounds into single enantiomers is an important aspect of analytical and preparative issues including the enantioseparation of chiral drugs [1-6], purity determination of pharmaceutical products [7-11], drug development [12, 13], separation of chiral synthons [14] or bioactive compounds [15-17] and in the flavor and fragrance field [18, 19]. The chiral separation is also required for the analysis of food contaminants [20] and environmental pollutants [21-23]. Nowadays, all pharmacokinetic profiles of optically active drugs need to be determined stereoselectively [14].

Besides liquid chromatography, various methods such as capillary electrophoresis (CE) [11], supercritical fluid chromatography (SFC) [14], gas chromatography (GC) [24], simulated moving bed technology (SMB) [25], enzymatic resolution [26] and crystallization [27] are used to separate enantiomers either on analytical or preparative scale.

1.1. Principles of Chirality

The term chirality is derived from the Greek word $\chi\varepsilon\iota\rho$ (hand) and means handedness. Chiral molecules do have the same atomic composition, they are structural isomers, which have the same constitution, but are not superimposable. Stereoisomers can be classified into diastereomers and enantiomers. Both differ in terms of symmetry and energy level. Diastereomers possess no mirror images in terms of symmetry and they have distinct energy content. Enantiomers are structurally non-superimposable mirror images with identical level of energy. A left and a right hand represent an ideal model of enantiomers. Chiral molecules contain no rotation-reflection axis, mirror plane or a center of inversion [14, 28].

We cannot distinguish enantiomers in an achiral environment. They have the same physical properties (e.g. melting point) except for the behavior towards polarized light, which in turn represents a chiral environment. A 1:1 molar mixture of two enantiomers is called racemate or racemic mixture. The overall optical rotation for a racemic mixture is zero because both of the enantiomers are optical isomers with exactly opposite rotation of polarized light [14, 29].

Chirality is grounded in various chiral elements [14, 30]:

- center of chirality (e.g. tetra-coordinated carbon with four different substituents)
- chiral axes (e.g. ortho-substituted biphenyls)
- chiral planes (e.g. substituted paracyclophanes)
- chiral helices (e.g. deoxyribonucleic acid - DNA)
- topologically chiral elements (e.g. iron-sulfur proteins [31])

Chiral molecules do have a key role in living systems. Almost all natural strains of amino acids and sugar molecules consist of only one enantiomer. Naturally occurring proteinogenic amino acids largely consist of the (*S*)-form, while the majority of sugar molecules found in living organisms have the (*R*)-form. Since amino acids are building components for proteins and sugars are building blocks of polysaccharides like cellulose (helical structure) or starch, chirality can be found throughout all living systems [32, 33].

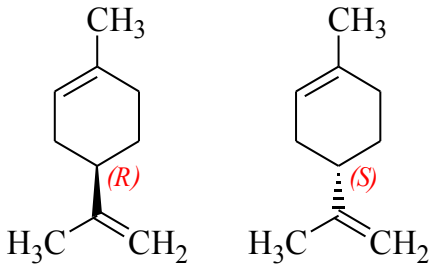

Figure 1.1.: The two stereoisomers of limonene;
left hand side: (*R*)-limonene, right hand side: (*S*)-limonene.

Due to the chiral nature of all living systems exogenic chiral compounds like food additives (e.g. flavors) and drugs are recognized by sensory organs and metabolized by enzymes stereoselectively. One renowned example for the different recognition of enantiomers by sensory organs is limonene. In **figure 1.1.** the structures of the two enantiomers are given. The (*R*)-enantiomer has a fragrant smell of orange, the (*S*)-enantiomer of this flavor has turpentine odour [14].

Another prominent examples for the different effect of enantiomers in terms of pharmaceutical responses are levopropoxyphen and dextropropoxyphene. The first mentioned (*2R*,*3S*)-levopropoxyphene has antitussive activity, whereas the

(*2S,3R*)-enantiomer dextropropoxyphene is an analgesic agent. Due to the different medical effects of enantiomers it is of utmost importance to administer the right stereoisomer [14].

The drug Contergan® is probably the most famous and tragic example for the importance of chirality in terms of drug effects. The active substance thalidomide (the structure is depicted in **figure 1.2.**) exists in two enantiomeric forms. Thalidomide was prescribed in the late 1950s as a sedative with anti-nausea effect for treating insomnia and morning sickness of pregnant women. In those days thalidomide was administered as racemic mixture. The drug was withdrawn in 1961 due to the terrible teratogenic effect [34]. In later investigations it could be shown that only the (*R*)-enantiomer shows beneficial effects (so-called eutomer) and the (*S*)-enantiomer (so called isomeric ballast or distomer [26]) is responsible for the teratogenic behavior. However, the administration of the single (*R*)-enantiomer would not contribute to a less teratogenic effect because thalidomide shows rapid *in vivo* chiral inversion and therefore racemization [35].

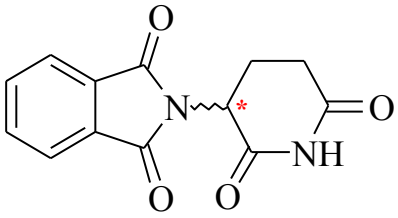

Figure 1.2.: Structure of thalidomide.

1.2. Separation of Enantiomers

As already mentioned above enantiomers do have identical physical and chemical properties [30] except their exactly opposite behavior towards polarized light. In an achiral environment one cannot distinguish between enantiomers or separate them from each other. Basically there are two main strategies for separating enantiomers. Both deal with the general approach of forming diastereomers, either via covalent bonding or formation of labile diastereomeric associates. **Figure 1.3.** illustrates these two basic concepts.

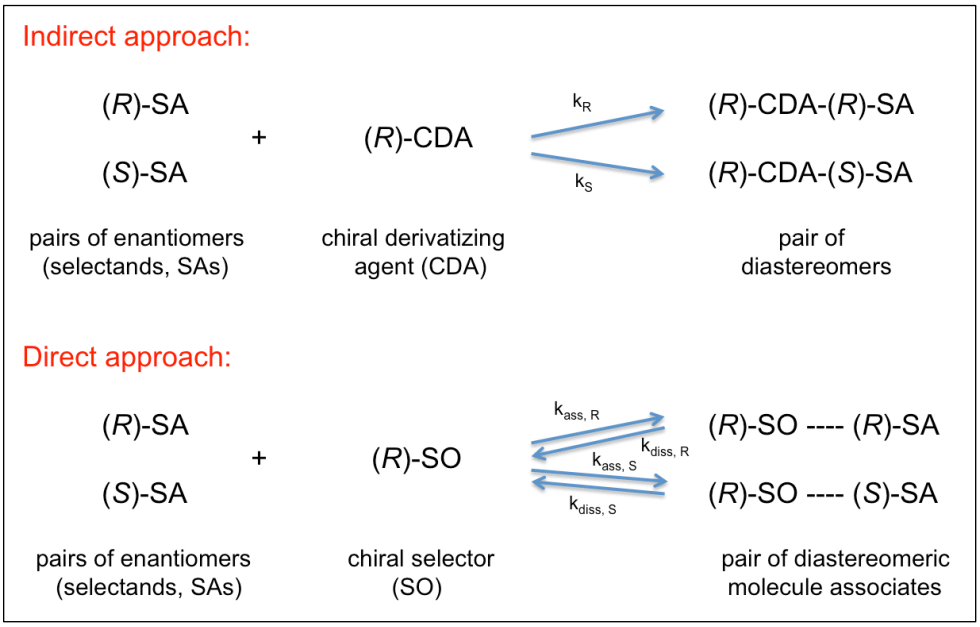

Figure 1.3.: The two basic concepts of enantioseparation; adapted and modified from [14].

In the indirect approach a pair of chemically stable diastereomers with an enantiomerically pure auxiliary, a chiral derivatizing agent (CDA), is formed. This reaction must proceed quantitatively. Since a covalent bond between selectand (SA) and CDA is formed, the separated diastereomers must be cleaved after separation to give an enantiomerically pure product. This is one drawback of the indirect method. Of course no racemization of the starting compounds and no kinetic racemate resolution must happen. For the separation no chiral environment and separation system is necessary because diastereomers differ in their physicochemical properties. Therefore reversed phase (RP) or normal phase (NP) chromatography is often sufficient for the separation of organic molecules [14, 30, 36].

The direct approach is based on the formation of a diastereomeric pair of molecule associates. This formation must be reversible (non-covalent binding). Two enantiomeric SAs interact with the enantiomerically pure chiral selector (SO), which is e.g. immobilized on a silica surface for chiral stationary phase (CSP) mode in an HPLC separation system. If the binding strength differs for both of the SAs (due to differences in energy content and therefore unequal thermodynamic complex stabilities and equilibrium constants) they are separable due to different retention. Another experimental mode for the direct approach would be the chiral additive mobile phase mode, which is of little importance nowadays [14, 30].

The interaction of SA with SO in the direct approach for the separation of enantiomers can be explained by thermodynamic considerations (*van´t Hoff* analysis) and a basic interaction model called three-point attachment [37].

1.3. Three-point Interaction Model

This model was proposed in 1952 by K. Dalgliesh [14, 38]. Although this model is not free of criticism and its validity is still under debate (e.g. a four-location model was proposed by Mesecar and Koshland in 2000 for describing the enantiodiscrimination ability of proteins and enzymes [39]), it visualizes the direct approach of enantioseparation using liquid chromatography and chiral stationary phases.

In **figure 1.4.** the three-point interaction model is illustrated. An enantiomerically pure selector (SO) is immobilized on a silica surface representing a chiral stationary phase. This selector contains three theoretical interaction sides (A, B and C), which can interact with a potential chiral selectand via three binding sites (SA; a, b and c). These non-covalent interactions and bonds can be of electrostatic nature like ionic interaction, Van der Waals forces like dipole-dipole, dipole-induced dipole and ion-dipole interactions and/or hydrogen bonding, π-π-interactions, hydrophobic interactions and a steric influence as well. The interaction must not be of attractive nature; repulsive interaction can also be involved in the three-point interaction [40].

In case of an “ideal fit“ all three interactions are complementary and match perfectly. One example for a complementary interaction would be e.g. an interaction between a hydrogen donating amino group of a SO and a hydrogen accepting carbonyl group of a SA. The “ideal fit” situation results in strong non-covalent bonding of SO and SA, and therefore high retention for the (*S*)-SA in the case shown below.

A “non-ideal fit” situation results in for example just one complementary interaction and therefore the interaction strength is weaker in comparison to the “ideal fit”. Therefore the (*R*)-SA is lower retained and elutes before the (*S*)-SA.

This result is also indicated by a lower association constant ($K_S > K_R$). Due to the resulting difference in retention times enantioseparation can be observed [14, 41].

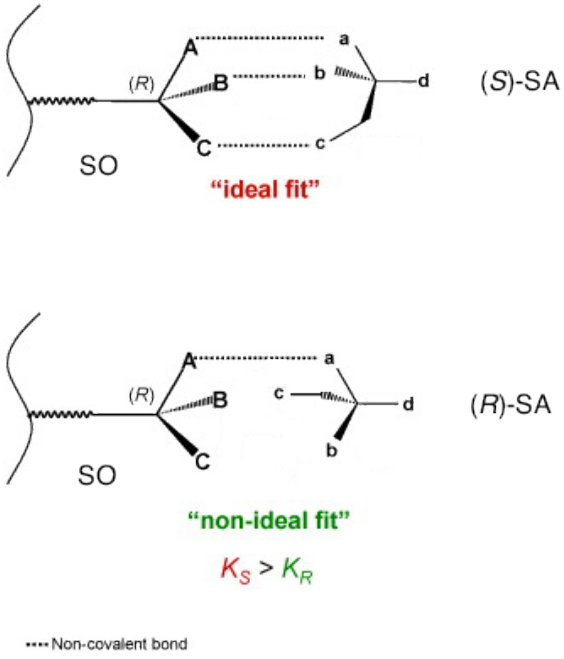

Figure 1.4.: Visualization of the three-point interaction model; adapted and modified from [40].

1.4. Thermodynamic Aspects of Enantioseparation

Enantioseparation is of course influenced by temperature. All chromatographic parameters like column efficiency, resolution, enantioselectivity and retention are influenced by changes in temperature. Thermodynamic considerations can be applied for the reversible formation of a SO--SA complex both for the (*R*)-SA and the (*S*)-SA. Different affinities of enantiomeric SAs to a chiral SO are described by changes of the Gibbs free energy $\Delta G^0_{(R)}$ and $\Delta G^0_{(S)}$ in the free and complexed form. The equilibrium processes can be described with the equilibrium binding constant K_i according to **equation [1.1]** (subscript *i* denotes the respective enantiomer), which combines the difference in free energy $\Delta G^0_{(i)}$ and K_i, wherein *R* is the universal gas constant (8.314 $J.K^{-1}.mol^{-1}$) and *T* the absolute temperature in Kelvin:

$$\Delta G_i^o = -RT \cdot lnK_i \qquad \textbf{[1.1]}$$

The Gibbs free energy consists of an enthalpic ($\Delta H_{(i)}$) and entropic part ($\Delta S_{(i)}$). This fact is represented by the *Gibbs-Helmholtz equation* (see **equation [1.2]**):

$$\Delta G_i^o = \Delta H_i^o - T\Delta S_i^o \quad \textbf{[1.2]}$$

A simple combination of **equation [1.1]** and **[1.2]** results in the *van´t Hoff equation*, which is depicted in **equation [1.3]**:

$$\ln K_i = -\frac{1}{T}\frac{\Delta H_i^o}{R} + \frac{\Delta S_i^o}{R} \quad \textbf{[1.3]}$$

This linear equation can be used for *van´t Hoff* thermodynamic analysis by simply plotting *ln* K_i vs. *1/T*. The intercept reflects the change of entropy $\Delta S^0_{(i)}$, whereas the slope represents the change of entropy $\Delta H^0_{(i)}$. The enantioselectivity α, which is the quotient between the retention factors k_i of one pair of enantiomers (see **equation [3.2]** in **chapter 3.4.** and **equation [1.6]**), is described as the difference between Gibbs free energy changes upon interaction of one SA with the SO over the other SO--SA associate. Under the assumption that $K_S > K_R$ (retention for the (*S*)-enantiomer is higher) one can deduce **equation [1.4]**:

$$\Delta\Delta G^o_{S,R} = \Delta G^o_S - \Delta G^o_R = -RT \cdot ln\frac{K_S}{K_R} = -RT \cdot ln\alpha \quad \textbf{[1.4]}$$

This equation can again be combined with the *Gibbs-Helmholtz* relationship, which results in **equation [1.5]**:

$$\ln\alpha = -\frac{1}{T}\frac{\Delta\Delta H_i^o}{R} + \frac{\Delta\Delta S_i^o}{R} \quad \textbf{[1.5]}$$

The expression above links the experimentally determinable enantioselectivity coefficient α and the absolute temperature with the differential enthalpy $\Delta\Delta H^0_{(i)}$ and entropy $\Delta\Delta S^0_{(i)}$ of enantioseparation. Note that the enantioselectivity coefficient α depends on two chromatographic parameters - the retention factor k_i and the phase ratio Φ (quotient between the volume of the stationary and the mobile phase) - as presented in **equation [1.6]:**

$$\alpha = \frac{k_S}{k_R} = \frac{K_S \cdot \Phi}{K_R \cdot \Phi} \quad \textbf{[1.6]}$$

Based on experimental results one can assume that enantioseparation processes are usually controlled by enthalpic contributions [40, 42, 43].

1.5. Chiral Stationary Phases

For a successful separation of enantiomers two major parameters are important. The first is the selection of an appropriate chiral stationary phase (CSP), which is able to separate the selected compounds. The second important parameter is the choice of the mobile phase conditions to yield retention and separation. In this chapter the main groups of CSPs and chiral selectors (SOs), respectively, are briefly described.

In principal one can distinguish between three different types of CSPs:

- Brush type: The chiral selector is immobilized via a spacer on an organic or inorganic support like silica. For chiral anion exchange purposes the most common type is the brush type CSP.
- Organic polymer type: Either the pure crosslinked chiral polymer serves as CSP or an organic polymer is coated onto the surface of a support material. Grafted polymers on a support material are also possible.
- Molecular imprinted polymer type: In this case either the pure polymer itself is imprinted and serves as CSP or the imprinted polymer is surface-grafted onto silica [14].

The chiral selectors can be grouped into low-molecular mass selectors, macrocyclic and macromolecular selectors.
An overview of these chiral selectors is depicted in **figure 1.5.**, for a more detailed description also with respect to advantages and disadvantages of every single CSP and selector type see [14, 40, 41]. Hereafter only the chiral anion exchange type is discussed in a more detailed view because the aim of the thesis was the synthesis and evaluation of weak anion exchange (WAX) type CSPs for liquid chromatography.

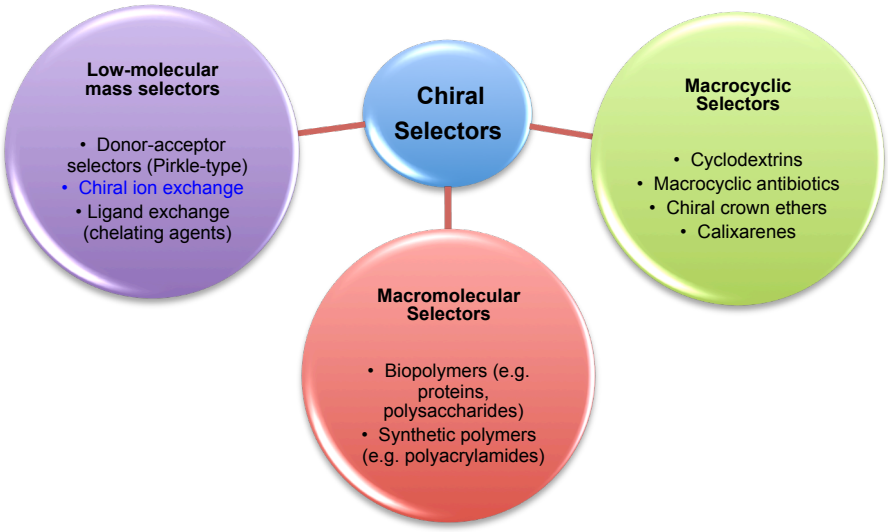

Figure 1.5.: Overview of the different types of chiral selectors; data collected from [14].

1.6. Chiral Ion Exchange

In the field of chiral ion exchangers one can distinguish between anion, cation and zwitterionic type CSPs. All three types were developed, among others, in our working group.

1.6.1. Cation Exchange type CSPs

For a chiral cation exchange stationary phase a chiral acidic SO has to be immobilized on a silica surface. Acidic compounds, which are suitable for cation exchange, are e.g. carboxylic acids used as weak cation exchangers (WCXs). Strong cation exchangers (SCXs) can be based e.g. on sulfonic acids. Other possibilities would be the use of sulfinic, phosphoric, phosphonic or phosphinic acids. Hoffmann and Lindner have recently developed a novel type of SCX-CSPs [44]. They immobilized a SO based on a chiral 2-aminocyclohexanesulfonic acid (ACHSA) derivative and were able to separate basic compounds (chiral organic amines) such as common drugs like bupranolol, clenbuterol, quinine, terbutalin and others under a polar organic mode mobile phase condition. The structure of one SCX-CSP is shown in **figure 1.6.** with (*1R*,*2R*) configuration of the ACHSA residue.

This selector contains two chiral centers in position 1 and 2. The same selector with just opposite configuration (*1S*,*2S*) was as well synthesized and immobilized on silica by Hoffmann et al. [44] and successfully employed as CSP. Between these two CSPs it was possible to achieve reversal of the elution order due to enantiomeric behavior of the two selectors.

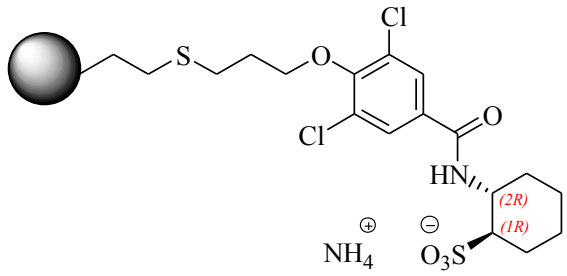

Figure 1.6.: Structure of the SCX-CSP; adapted and modified from [44].

Under basic mobile phase conditions (e.g. addition of diethylamine DEA or diisopropylethylamine DIPEA as a buffer component) the selector is deprotonated and therefore cation exchange as a primary retention effect is possible. Further on hydrogen bonding via the amide -NH as donor and the amide carbonyl as acceptor is possible. The π-acidic dichloro-substituted aromatic moiety is capable of π-π-interactions.

1.6.2. Zwitterion type CSPs

This type of CSPs contains both anion exchange type structural motifs as well as cation exchange type motifs. The fusion of them results in zwitterionic exchange type (ZWIX) CSPs, which were recently developed by Hoffmann et al. [33, 45] in our working group. A big advantage of this type of CSPs is the broad applicability in terms of separable compounds. Both anions as well as cations can be separated. The list can further be extended to zwitterionic SAs such as proteinogenic amino acids, drugs like DOPA (3,4-dihydroxyphenylalanine) and aminosulfonic acids (e.g. ACHSA).

In **figure 1.7.** the structure of a selected ZWIX-CSP invented by Hoffmann et al. in 2008 [45] is shown. It is a synthetic combination of quinine-type WAX (red colored) and ACHSA-type SCX (blue colored).

The selector itself is a zwitterion in protonated form of the quinuclidine ring of the quinine moiety and deprotonated form of the sulfonic group at the ACHSA moiety.

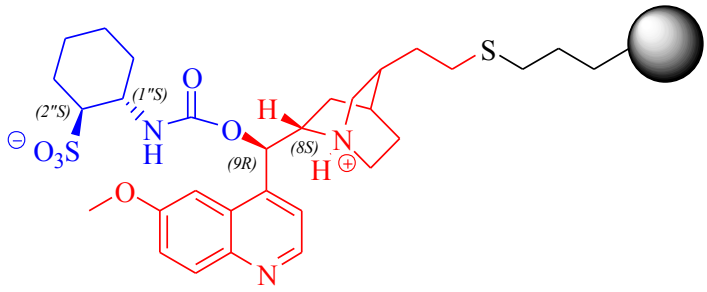

Figure 1.7.: ZWIX-CSP developed by Hoffmann et al. 2008; adapted and modified from [45].

The charge state is dependent on the mobile phase conditions. During retention one charged moiety can act as an intramolecular counterion and therefore the concentration of buffer salts in the mobile phase can be reduced [46].

In the case of the ZWIX-CSP shown in **figure 1.7.** various interactions with a potential chiral analyte are possible. Primary ionic interaction due to the charged quinuclidine ring and the sulfonic acid group of the ACHSA residue, hydrogen bonding via the carbonyl and -NH of the carbamate bridge, π-π-interaction because of the aromatic quinoline ring and a sterical influence as well. The overall interaction results in a potential ability for chiral recognition and therefore enantioseparation.

1.6.3. Anion Exchange type CSPs

Because of a broad range of chiral acidic compounds used e.g. as drugs or agrochemicals (see above) separation of these compounds and analysis of the enantiomeric ratio is an important task in analytical chemistry. The enantioseparation is possible via anion exchange type CSPs with immobilized selectors containing ionizable primary, secondary, tertiary or constantly charged quaternary amines, whereas quaternary amines represent the strongest anion exchange type SOs.

One important group of weak anion exchangers (WAXs), namely *O9-tert*-butyl carbamate derivatives of the cinchona alkaloids quinine and quinidine, were invented by Lindner and Lämmerhofer and have been commercialized under the trade name

CHIRALPAK® QN-AX and QD-AX by Chiral Technologies [13]. In **figure 1.8.** the structures of these two CSPs are shown.

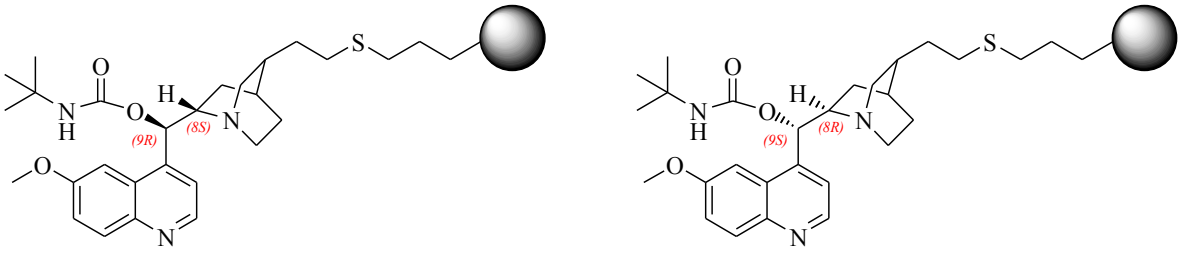

Figure 1.8.: Structures of CHIRALPAK® QN-AX and QD-AX CSPs; adapted and modified from [47, 48].

With this type of CSP various interactions are possible which are discussed below (see **chapter 1.7.**). Primary ionic interaction takes place via the protonated tertiary amine in the quinuclidine ring under acidic mobile phase conditions. The only conformational difference between QN-AX and QD-AX are the centers of chirality in position 8 and 9. QN-AX possesses (*8S*,*9R*) whereas the pseudoenantiomeric QD-AX [13] has (*8R*,*9S*) configuration. All the other centers of chirality (located at the quinuclidine ring, position 1 = chiral tertiary amine) are of the same absolute configuration (*1S*,*3R*,*4S*).

The selectors in case of QN-AX and QD-AX are immobilized via the vinyl group (positions C10, C11) of the quinuclidine ring. One advantage of the naturally occurring and relatively cheap quinine (QN) and quinidine (QD) is that immobilization is possible without further derivatization. The immobilization is carried out with radical thiol-ene addition onto mercaptopropyl-modified silica.

In former studies, native QN and other cinchona alkaloids have been used as chiral selectors with rather inadequate performance [13]. Therefore the secondary alcohol group of cinchona alkaloids at position 9 was derivatized with a vast number of functional groups resulting in the formation of ethers, amides, esters, sulfonamides and hydrazine derivatives. All these selectors where evaluated in terms of their applicability for chiral separations, but the carbamate derivatives, especially *t*Butyl carbamate of QN and QD, provided high enantioselectivities for a broad range of selectands including *N*-protected amino acids, *N*-protected aminosulfonic acids, *N*-protected aminophosphonates and carboxylic acids (see **chapter 3**) [13].

1.7. Retention Mechanism for *N*-protected amino acids

A retention mechanism for chiral acidic analytes can be explained on the basis of a strongly retained compound. As a model CSP in former studies commercially available Chiralpak® QN-AX *t*Butyl carbamoylated quinine (the structure is given in **figure 1.8.** above) has been used. This CSP demonstrates extraordinary high enantioselectivities, e.g. for *N*-3,5-dinitrobenzoylated (DNB) amino acids like DNB-Leu ($\alpha > 15$ [13]). In this case the (*S*)-enantiomer of DNB-Leu shows much higher retention compared to the respective (*R*)-enantiomer.

Due to the very strong interaction between stationary phase and the above-mentioned (*S*)-compound it was possible to elucidate a tentative chiral molecular recognition mechanism via a multidisciplinary approach using complementary methods like X-ray crystal structure analysis of co-crystallized selector and enantiomerically pure DNB-(*S*)-Leu, molecular modeling approaches, density functional theory calculations, FTIR, ^{1}H-NMR, VCD, CD, UV spectroscopy and thermodynamic studies [13].

The primary driving force for retention is the formation of an ion-pair at the quinuclidine ring of the selector. Therefore the bicyclic tertiary amine ring has to be positively charged due to protonation under slightly acidic mobile phase conditions and the associated SA must be simultaneously deprotonated and therefore negatively charged under the same conditions. The protonated amine is then capable of forming non-directed, strong and long ranged Coulomb attraction with the SA. This ion pairing mechanism is the dominating factor for retention.

Besides this primary attraction various intermolecular interactions (all of them of non-covalent nature) stabilize the SO-SA complex:

- Face-to-face π-π-stacking between the electron rich π-basic quinoline ring of the SO and the electron poor π-acidic aromatic moiety of the SA.
- Directed intermolecular hydrogen bonding between the C=O of the SA and the carbamoyl -NH of the SO.
- Van der Waals interactions.
- A second hydrogen bonding between the amide -NH of the SA and the carbonyl of the SO carbamate.

- Steric interaction due to the sterically demanding *t*Butyl residue of the SO and the flexible leucine moiety of the SA [13, 49, 50].

All these interactions together with the tight ion pairing primary force result in a high degree of enantioselectivity. In **figure 1.9.** a complexation model for the interaction between the carbamoylated QN selector and DNB amino acids as well as DNP amino acids is shown.

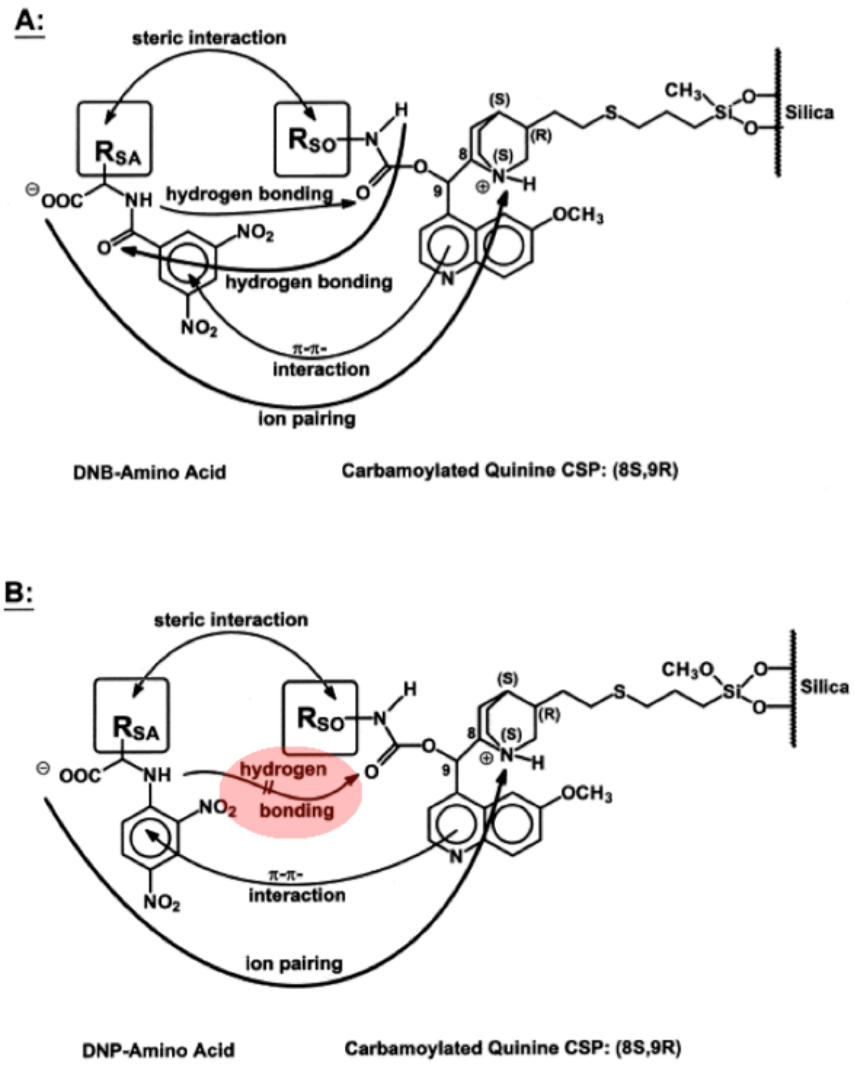

Figure 1.9.: Tentative chiral recognition model for a carbamoylated QN selector; (A) DNB amino acids; (B) DNP amino acids; R_{SA} = 2-methylpropane (Leu); R_{SO} = *t*Butyl; adapted and modified from [50].

The respective DNB-(*R*)-Leu enantiomer is much less retained in comparison to the (*S*)-enantiomer. The reason for this observation is a steric exclusion process. The (*R*)-enantiomer is not capable of forming a strong SO--SA complex, because of the

lack of accommodation in the well-defined binding pocket of the selector. Therefore stabilizing secondary interactions like hydrogen bonding and π-π-stacking cannot be achieved by the SA and the resulting overall retention is weak [13].

The importance of hydrogen bonding for enantioselectivity can be shown with DNB-*N*-methyl leucine. The only structural difference in comparison to DNB-Leu is, that the hydrogen of the amide is replaced by a methyl group. For this compound no enantioseparation was possible, a result that clearly shows the importance of hydrogen bonding in terms of chiral recognition or selectivity [49].

Another example for the hydrogen bonding influence is the interaction of the SO with a structurally similar compound, namely *N*-2,4-dinitrophenyl (DNP) leucine (see **figure 1.9.**). The lack of a carbonyl in the protecting group of leucine results in a significantly lower enantioselectivity coefficient and a reversal of elution order in comparison to the structurally related DNB-Leu compound [50].

1.8. Stoichiometric Displacement Model

As already mentioned above an ion exchange retention mechanism is reasonable for describing the interactions between cinchona based chiral selectors and acidic analytes. Besides the interactions taking place between SO and SA the mobile phase and its composition contributes to retention in a crucial way. Therefore the so-called stoichiometric displacement model allows explaining the dependency of retention times on the buffer concentration in the mobile phase, assuming that the pH-value stays constant (if one can speak of pH-value in polar organic mode consisting for example of MeOH as a bulk phase). A linear relationship between *log k* vs. *log [X]* (log of the counterion concentration in [mol.L^{-1}]) indicates an ion exchange mechanism (**equation [1.7]**).

$$\log k = \log K_Z - Z \cdot \log[X] \qquad \textbf{[1.7]}$$

This linear relationship demonstrates an important aspect of the stoichiometric displacement model. The higher the counterion-concentration, the lower the retention is. The counterions are also retained and act as a displacer for SA molecules. Due to this equation it is easily possible to adjust the retention times by simply diluting the mobile phase or adding buffer in a higher concentration.

However, for preparative purposes and mass spectrometric detection high buffer concentrations (and especially non-volatile buffers) should be avoided.
The slope *Z* in **equation [1.7]** is an empirical coefficient that contains information on how many charges in the ion-exchange process are involved (**equation [1.8]**):

$$Z = \frac{m}{n} \qquad \textbf{[1.8]}$$

The divisor *n* is the effective charge number of the mobile phase counterion and the dividend *m* is the effective charge number of the selectand ion. One can see that an increase of the charge number of the counterion results in a flatter slope (e.g. citrate in comparison to acetate). In terms of elution strength the order citrate > phosphate > formate ≥ acetate can be seen as a rule of thumb [13, 51].
If the slope is as steep/flat for both enantiomers, they both respond with the same sensitivity to an alteration of the counterion concentration in the mobile phase. Therefore the linear regressions are parallel for both stereoisomers. One additional aspect is that the selectivity coefficient stays almost constant, independent of the counter ion concentration. This allows an easy adjustment of the retention times.
The intercept K_Z in **equation [1.7]** is a system-specific constant, which is related to the mobile phase volume V_0 [L], the number of available ion-exchange sites q_x (representing the surface charge density [mol.m^{-2}], the area of the surface *S* [m^2.g^{-1}] and the ion-exchange equilibrium constant *K* [L.mol^{-1}]. All these parameters are expressed in **equation [1.9]** [40, 51]:

$$K_Z = \frac{K \cdot S \cdot (q_x)^z}{V_0} \qquad \textbf{[1.9]}$$

In the case of cinchona alkaloid based selectors one should not forget that the anion-exchanger itself is a weak base and therefore acid-base equilibria have to be considered. In **equation [1.10]** the retention factor *k* is expressed taking these dissociation equilibria into account by the mass action model:

$$k = \phi \cdot \frac{K \cdot [SO^+] \cdot [SA^-]}{[X^-] \cdot ([SA^-] + [SAH])} \qquad \textbf{[1.10]}$$

ϕ	phase ratio
K	ion-exchange equilibrium constant
$[SO^+]$	concentration of protonated active ion-exchange sites
$[SA^-]$	ionized, deprotonated SA
$[X^-]$	concentration of counterions in the mobile phase
$[SAH]$	concentration of non-ionized SA

A more simplified version of **equation [1.10]** is given in **equation [1.11]**, which again indicates the inverse proportionality of the retention factor *k* and the counterion concentration $[X^-]$.

$$k = \phi \cdot \frac{1}{[X^-]} \cdot K \cdot \alpha_{SA}^{*} \cdot \alpha_{SO}^{*} \cdot [SO]_{tot} \qquad \textbf{[1.11]}$$

Please note that in this case α is the degree of dissociation of SA and SO and $[SO]_{tot}$ means the total concentration of selector immobilized on the silica support, which is equivalent to q_x in **equation [1.9]** [51].

1.9. Immobilization Strategies

In the present master thesis two different strategies for the immobilization of the selectors on silica were employed:

- Radical activated thiol-ene “click” reaction
- Copper catalyzed azide-alkyne cycloaddition (Huisgen click chemistry)

1.9.1. Radical mediated thiol-ene addition

This reaction is often described as click reaction, although it does not always meet the prerequisites for a click reaction. Kolb et al. defined that “*the reaction must be modular, wide in scope, give very high yields, generate only inoffensive byproducts that can be removed by nonchromatographic methods, and be stereospecific (but not necessarily enantioselective)*” [52].

Besides the thiol-ene addition exist several other reactions with “click chemistry” characteristics such as metal-free dipolar cycloadditions, Diels-Alder reactions and thiol-based reactions like thiol-isocyanate, thiol-bromo and thiol-yne processes. In the present case azobisisobutyronitrile (AIBN) has been used as a radical starter for mediating the reaction. Apart from the radical pathway the thiol-ene reaction also works under a number of different conditions like catalytic processes mediated by nuleophiles, bases and acids [53] or supramolecular catalysis using *β*-cyclodextrin [54].

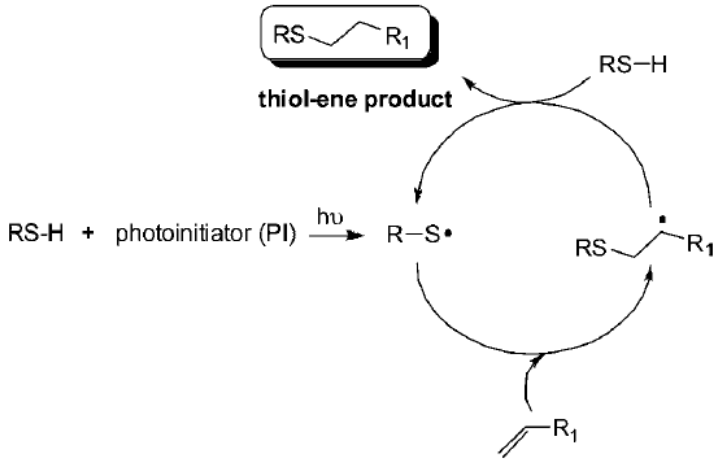

Figure 1.10.: Reaction mechanism for the thiol-ene addition; adapted from [53].

The reaction scheme for the hydrothiolation carried out via radical mediation is shown in **figure 1.10.**, in which the photoinitiator (PI) is AIBN and the radicals were formed via thermal activation of the radical starter in the present thesis. The reaction is a typical chain process consisting of initiation, propagation and termination. First the radical starter or photoinitiator decomposes due to heating or irradiation, respectively, and forms stable radicals, which treat thiols in order to form thiyl radicals. First step of the propagation is the addition of thiyl radical to an alkene compound yielding a carbon-centered radical as indicated above. The reaction is completed after the chain transfer of radical to another thiol-containing molecule. Thereby a new thiyl radical is generated and the reaction cycle is repeated. The third step of the radical chain process is the termination, which can be due to coupling processes of two radicals. The reaction can be carried out with almost any olefins, though terminal enes are more reactive in comparison to internal double bonds [53].

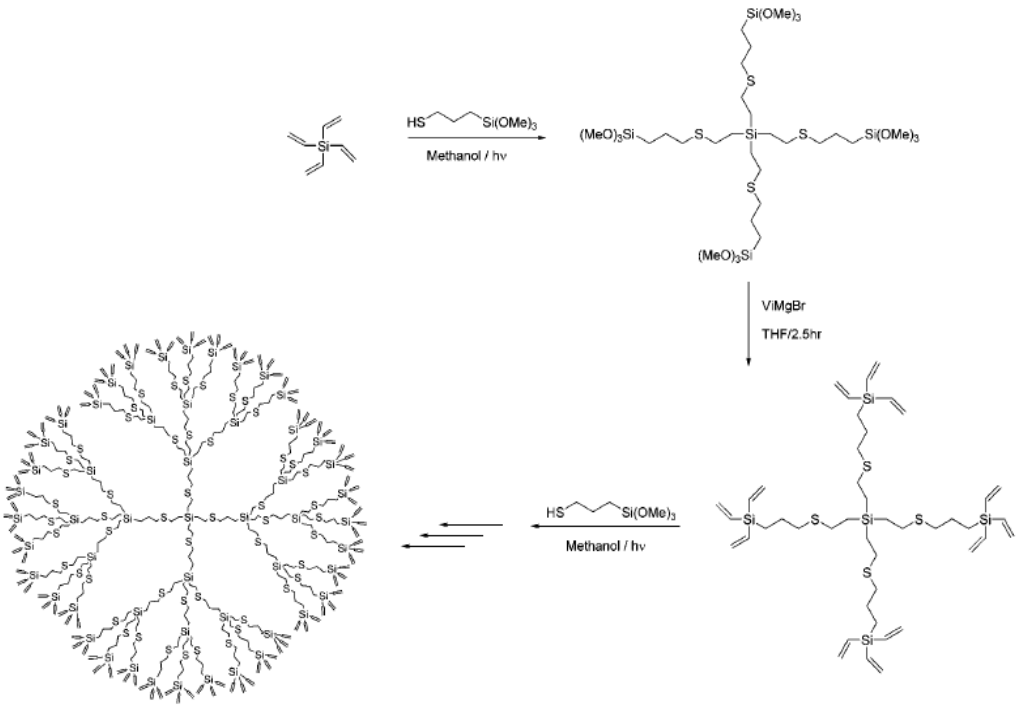

Figure 1.11.: Formation of carbosilane-thioether dendrimers via thiol-ene addition; adapted and modified from [55].

Due to the versatile application possibilities of the thiol-ene addition it is also used for immobilization of chiral selectors (containing olefins) onto mercaptopropyl-modified silica for example by Oberleitner et al. [42].

Further applications of this type of reaction are the synthesis of films and networks, the post-polymerization modification of polymers [53] and the formation of complex macromolecules such as dendrimers [56]. An illustrative example for this type of macromolecules is the formation of carbosilane-thioether dendrimers via photochemical induced hydrothiolation "click" chemistry followed by Grignard reaction (see **figure 1.11.)** [55].

1.9.2. Azide-alkyne cycloaddition

The copper(I) and base catalyzed Huisgen azide-alkyne click reaction has been discovered by Rostovtsev et al. in 2002 [57]. In this 1,3-dipolar cycloaddition 1,2,3-triazoles are formed from azides and terminal alkyne moieties [58]. The acceleration rate using a copper catalyst for this click reaction is tremendous in comparison to a non-catalyzed reaction (10^7 to 10^8) [59].

Copper can be used either directly as Cu(I) or as a coupled $CuSO_4$/ascorbate system in which Cu(II) as a precatalyst is reduced *in situ* by the ascorbate to the active Cu(I).

One disadvantage of Cu(I) salts like CuI is that they are sensitive to oxidation, which complicates operation and handling. Therefore research is focused on air-stable copper(I) complexes or copper(II) precatalysts only (without reducing agent). The latter is possible via oxidative homocoupling of alkynes (so-called Glaser reaction), in which considerable amounts of active Cu(I) are generated. One advantage of this procedure is that no external reductant is necessary [60].

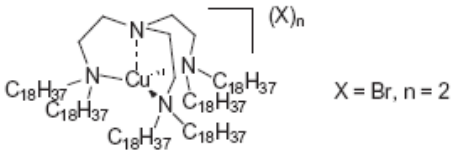

Figure 1.12.: Cu(II) precatalyst complex with $C18_6$tren ligand; adapted and modified from [60].

One example for a Cu(II) precatalyst with $C18_6$tren as a ligand (tren = tris(2-aminoethyl)amine), which works without reducing agent at room temperature (RT), is presented in **figure 1.12.** and was developed by Harmand et al. [60]. Fortunately this complex is stable towards ambient oxygen.

In the present thesis Cu(I) iodide was used as a catalyst and acetonitrile as a solvent. Under these conditions high immobilization rates could be achieved. Full conversion was also observed in previous studies in toluene, dichloromethane, *N*-diisopropylethylamine, tetrahydrofuran and *N*,*N*-dimethylformamide as solvents. Tornøe et al. observed no reaction in the absence of CuI [58].

In **figure 1.13.** a proposed reaction mechanism for the click reaction is shown. In the presence of a base the Cu(I) covalently attaches to the terminal alkyne and in a stepwise or concerted way to the polarized azide moiety (step 1 and 2). Due to rearrangement of the bindings a triazole ring is formed (step 3 and 4) in the non-regiospecific reaction.

However, this type of reaction does not work with internal alkynes. As additional sources of Cu(I) compounds CuCl, CuBr and CuI can be used [58].

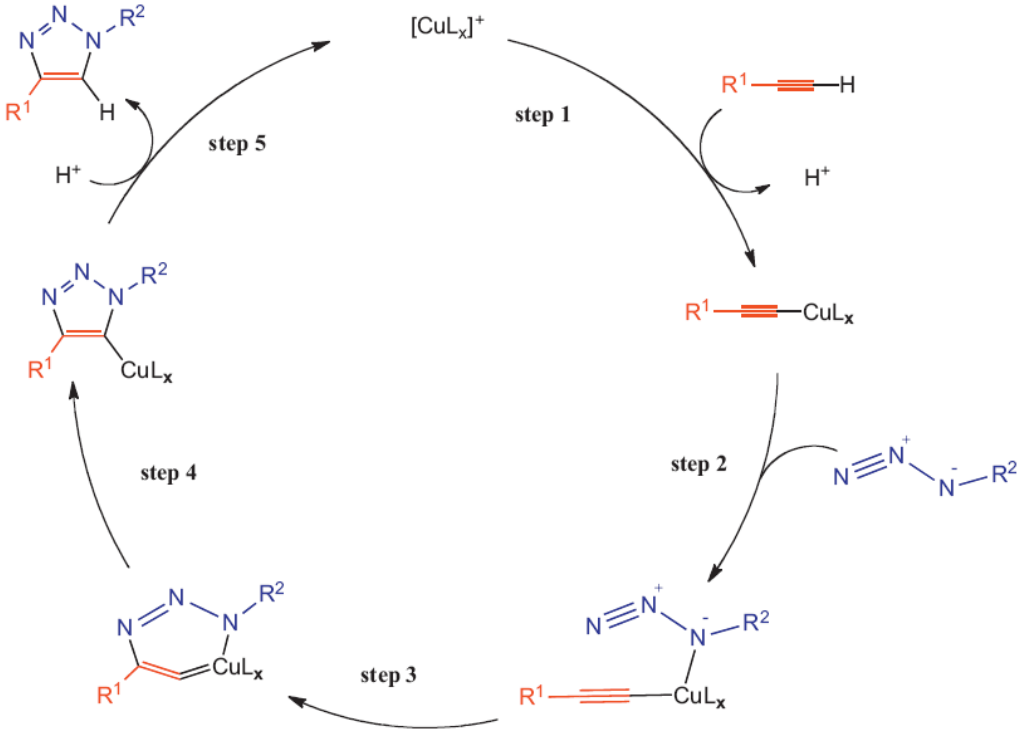

Figure 1.13.: Proposed catalytic mechanism for the formation of 1,2,3-triazoles; adapted from [61].

Besides the above mentioned copper catalysts it is also possible to use ruthenium(II)-based complexes for azide-alkyne cycloaddition catalysis. Boren et al. developed several complexes for the reaction of primary and secondary azides with both terminal and internal alkynes, whereas tertiary azides were not suitable [59]. Due to the simple feasibility of click reaction it is used for the immobilization of e.g. chiral selectors (containing alkynes) onto azidopropyl-modified silica [62].

2. Synthesis Results

2.1. Synthesis of Selectors and Chiral Stationary Phases

The first aim of the master thesis was the synthesis of new arylcarbamoylated cinchona-based chiral selectors (SOs) and chiral stationary phases (CSPs) for liquid chromatography. Four different types of chiral weak anion exchange (WAX) SOs (**SO1-4**) have been successfully synthesized. In combination with different SO loading on the silica support and different column dimensions, twelve columns (containing **CSP1-10**) have been prepared.

Therefore two different linkers (**L1**, **L2**), which enable the immobilization of the selector on the modified silica support were prepared. These isocyanates (**L1**, **L2**) were subsequently reacted with the hydroxyl group of cinchona alkaloids to afford our designed selectors. As building blocks dihydroquinine (**DHQN**) and dihydroquinidine (**DHQD**) were used.

The immobilization of the chiral SOs onto preactivated silica surfaces was carried out via the carbamoyl moiety implementing either radical addition with alkene thiol group or azide-alkyne Huisgen click chemistry, respectively.

2.1.1. Synthesis of Linker 1

Scheme 1 shows the synthetic route to **L1**. Commercially available 3,5-dichloro-4-hydroxybenzoic acid **1** was transformed into its 4-allyloxy-3,5-dichlorobenzoic acid allyl ester **2a** by reaction with allyl bromide. Purification of the product was achieved by flash column chromatography on silica. The ester group of the purified intermediate was then hydrolyzed with sodium hydroxide. Acidification with hydrochloric acid led to the carboxylic acid species **3a**. This intermediate was then treated with oxalyl chloride $(COCl)_2$ and dry *N,N*-dimethylformamide (DMF) as a catalyst to form the acyl halide **4a**. An alternative approach for activating the acid would be the reaction with thionyl chloride instead of oxalyl chloride, but $(COCl)_2$ is commonly milder [63]. One advantage of both reagents is that they produce only gaseous by-products.

The activated species was then converted into the acyl azide **5a** by nucleophilic substitution with sodium azide, which could be easily isolated by extraction. Heating

up the dry acyl azide led to the respective isocyanate **L1** via Curtius-rearrangement. The driving force of this reaction is the release of nitrogen. The crude product was purified by vacuum distillation and the colorless liquid product was stored at 4°C.

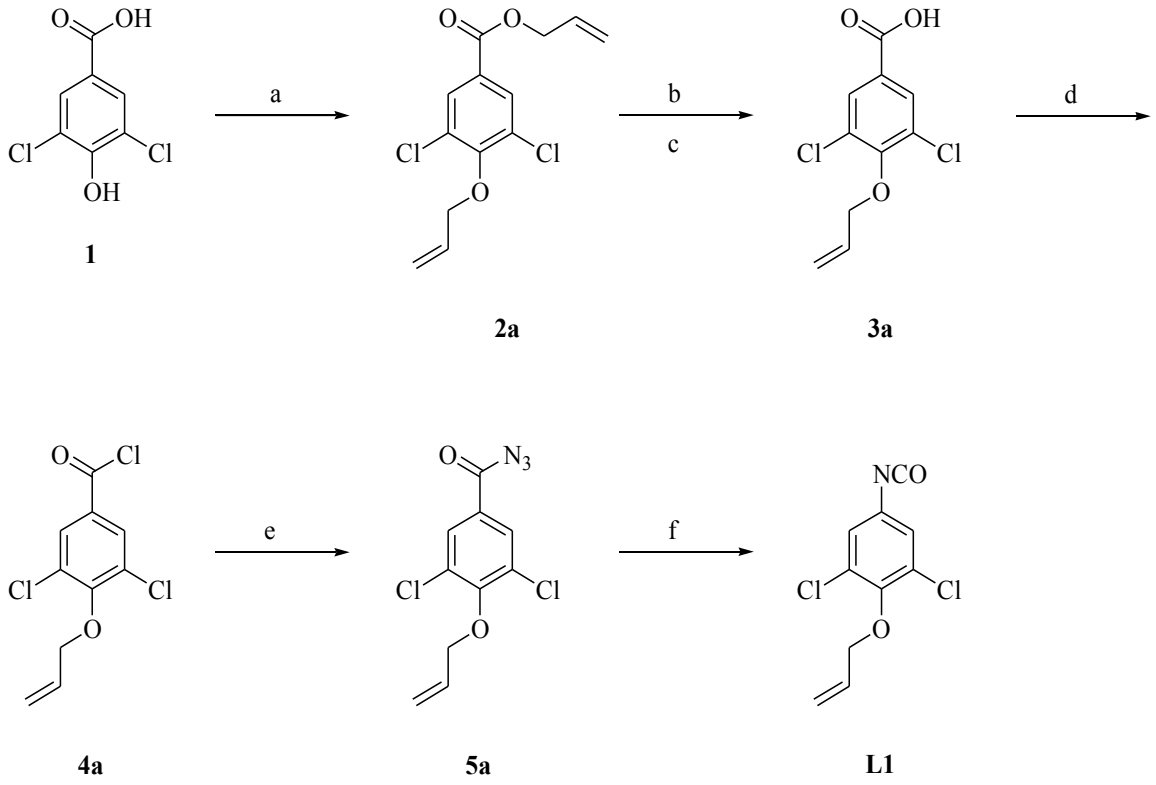

***Scheme 1**: Conditions: (a) allyl bromide, K_2CO_3, acetone, reflux, 18 h, (b) NaOH, ethanol, water, reflux, 1 h, (c) HCl, 0°C, (d) $(COCl)_2$, DMF(catalyst), reflux, 1 h, (e) NaN_3, acetone, water, 0°C, 1 h, (f) toluene, reflux, 2 h.*

2.1.2. Synthesis of Linker 2

Scheme 2 shows the synthetic route to **L2**. Analogously, commercially available 3,5-dichloro-4-hydroxybenzoic acid **1** was transformed into its 4-propargyloxy-3,5-dichlorobenzoic acid propargyl ester **2b** by reaction with propargyl bromide. Purification of the product was achieved by flash column chromatography on silica. The ester group of the purified intermediate was then hydrolyzed with sodium hydroxide. Acidification with hydrochloric acid led to the carboxylic acid form **3b**. This intermediate was then treated with oxalyl chloride and dry DMF as a catalyst providing the respective acyl halide **4b**, which was subsequently converted into acyl azide **5b** by reaction with sodium azide, which could be easily isolated by precipitation and extraction. The procedure for isolating the acyl azide **5b** is slightly

different in comparison to the work-up of the acyl azide species described for **L1** above.

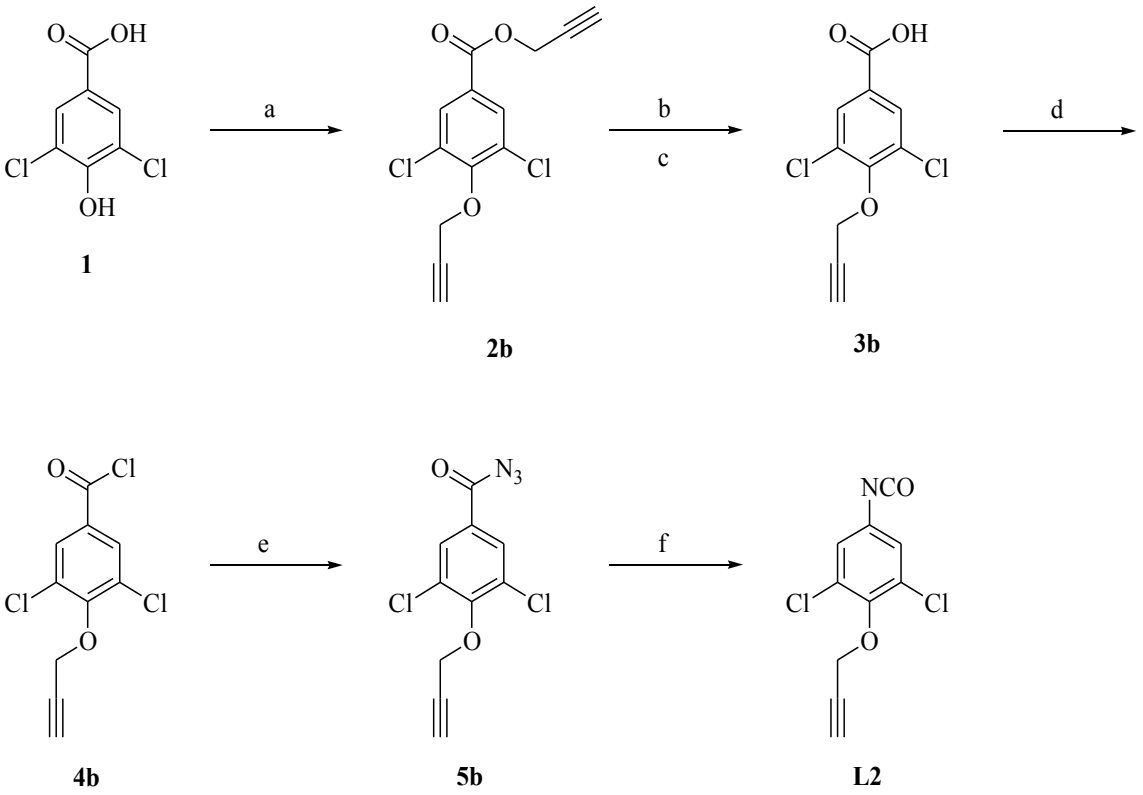

***Scheme 2**: Conditions: (a) propargyl bromide, K_2CO_3, acetone, reflux, 18 h, (b) NaOH, ethanol, water, reflux, 1 h, (c) HCl, 0°C, (d) $(COCl)_2$, DMF (catalyst), reflux, 1 h, (e) NaN_3, acetone, water, 0°C, 1 h, (f) toluene, reflux, 3 h.*

In the case of **L2** the acyl azide **5b** was first allowed to precipitate in an aqueous solution, afterwards filtered and washed in order to remove soluble by-products. The filtration cake was then dissolved in EtOAc, washed with water and saturated aqueous NaCl solution and dried over $MgSO_4$ to give a fully dry acyl azide **5b** after evaporation of the solvent. This work-up procedure is much more efficient with respect to drying than described above for the acyl azide species of **L1**.

Heating up the fully dry acyl azide led to the respective isocyanate **L2** via Curtius-rearrangement. Purification of the product by vacuum distillation was not possible due a high boiling point; hence the crude product was used directly for carbamoylation of cinchona derivatives.

2.1.3. Synthesis of Selector 1

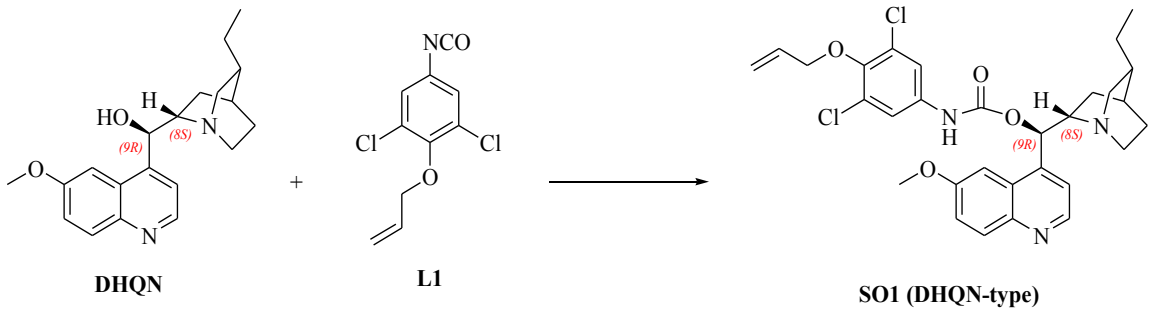

***Scheme 3**: Conditions: toluene, dibutyltin dilaurate (catalyst), reflux, N_2, 18 h.*

Scheme 3 shows the synthetic route to generate **SO1** (DHQN-type SO). Commercially available **DHQN** was dissolved in toluene and dried via azeotropic distillation. The carbamoylation of dihydroquinine was carried out under nitrogen atmosphere with isocyanate **L1** and dibutyltin dilaurate (DBTDL) as a catalyst [64]. Purification of the product **SO1** was achieved by flash column chromatography on silica.

2.1.4. Synthesis of Selector 2

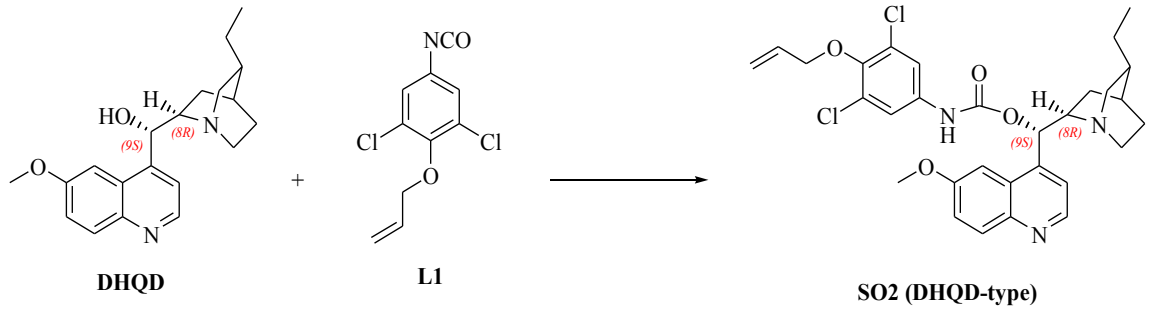

***Scheme 4**: Conditions: toluene, DBTDL (catalyst), reflux, N_2, 18 h.*

Scheme 4 shows the synthetic route to generate **SO2** (DHQD-type). Analogously to the procedure mentioned above, **DHQD** and **L1** were mixed together with the catalyst, the product was formed and afterwards purified by flash column chromatography on silica. **SO2** was then recrystallized from EtOH.

2.1.5. Synthesis of Selector 3

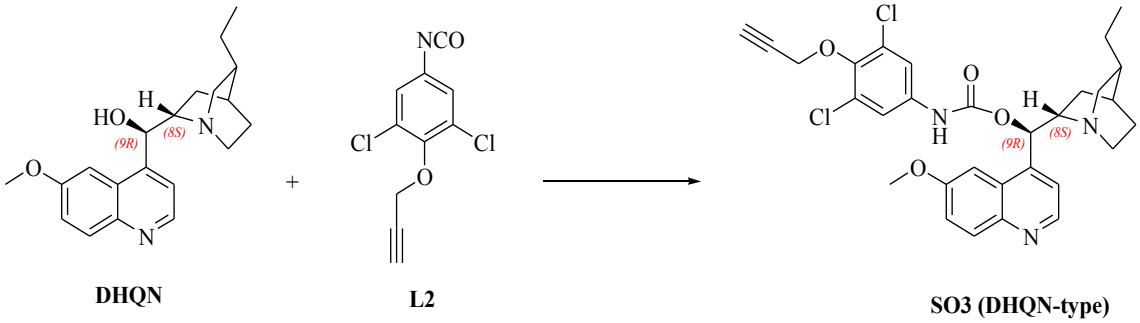

***Scheme 5**: Conditions: toluene, DBTDL (catalyst), reflux, N_2, 18 h.*

Scheme 5 shows the synthetic route to generate **SO3** (DHQN-type). Commercially available **DHQN** was dissolved in toluene and dried via azeotropic distillation. The carbamoylation of **DHQN** was carried out under nitrogen atmosphere with purified isocyanate **L2** and DBTDL as a catalyst. Purification of the product was achieved by flash column chromatography on silica. Crystallization of **SO3** was not possible.

2.1.6. Synthesis of Selector 4

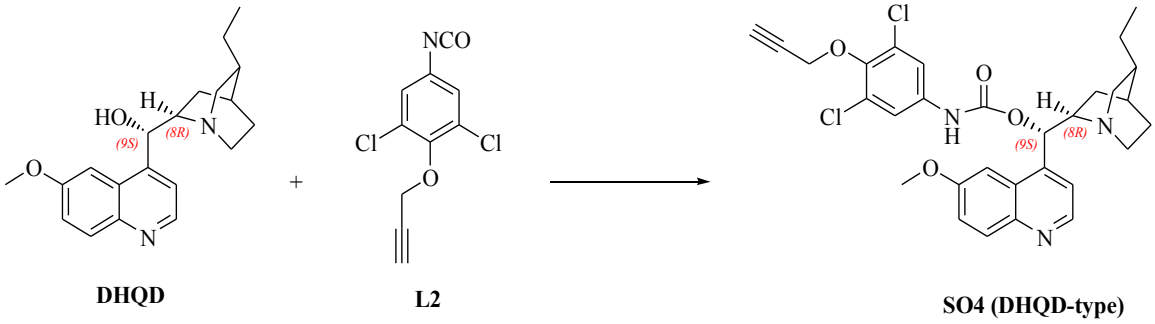

***Scheme 6**: Conditions: toluene, DBTDL (catalyst), reflux, N_2, 18 h.*

Scheme 6 shows the synthetic route to generate **SO4** (DHQD-type). Analogously to the procedure mentioned above, **DHQD** and **L2**, which was prepared *in situ* via Curtius rearrangement of acyl azide **5b**, were mixed, catalyst was added, the product was formed and afterwards purified by flash column chromatography on silica.

2.1.7. Immobilization of SO1 onto MP-Silica

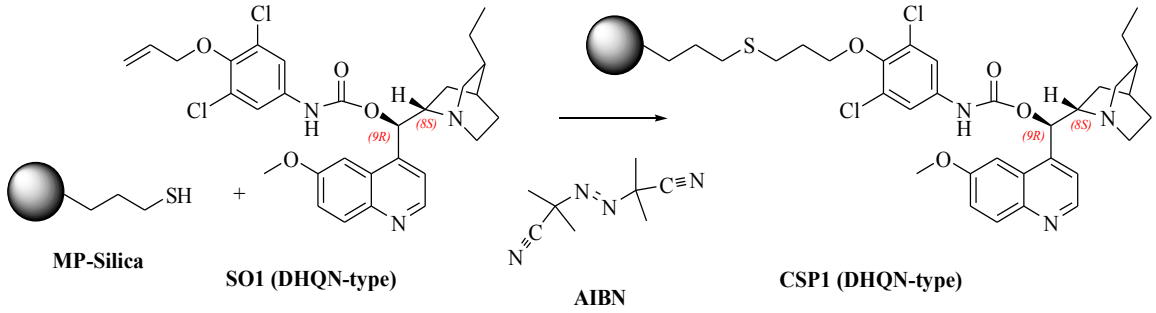

***Scheme 7**: Conditions: methanol, azobisisobutyronitrile (AIBN), reflux, N_2, 18 h.*

Scheme 7 shows the immobilization step for **CSP1** (DHQN-type) via radical thiol-ene addition. Mercaptopropyl-modified silica (**MP-Silica**, loading of thiol groups app. 650 µmol/g silica), **SO1** and AIBN as a radical starter were suspended in MeOH under nitrogen atmosphere. When AIBN is heated, it decomposes and forms two stable 2-cyanoprop-2-yl radicals and one molecule of nitrogen is released. The suspension was mechanically stirred in order to not damage the silica particles and heated under reflux. After 18 h the silica was filtered with a frit and washed. After drying under vacuum SO loading of **CSP1** was determined by elemental analysis (EA).

2.1.8. Immobilization of SO2 onto MP-Silica

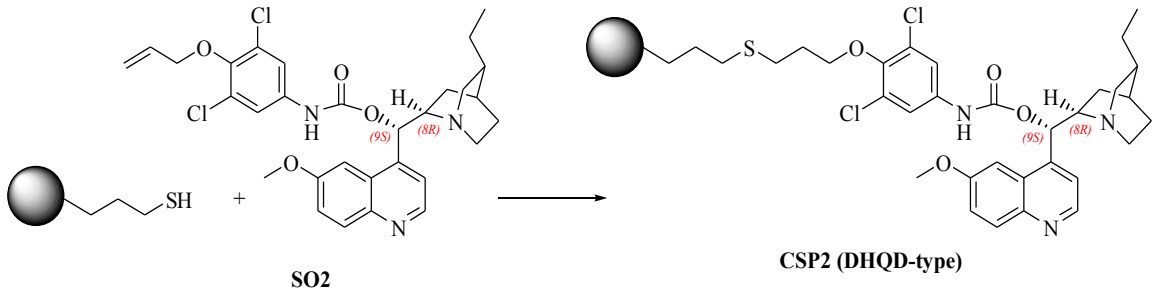

***Scheme 8**: Conditions: methanol, AIBN, reflux, N_2, 18 h.*

Scheme 8 shows the synthetic route to **CSP2** (DHQD-type) via radical addition. The reaction was carried out in the same manner as mentioned above for the immobilization of **SO1**. The reagents were suspended in MeOH, heated and after

18 h the modified silica was filtered, washed, dried and SO loading of **CSP2** was determined by elemental analysis.

2.1.9. Synthesis of AzP-Silica

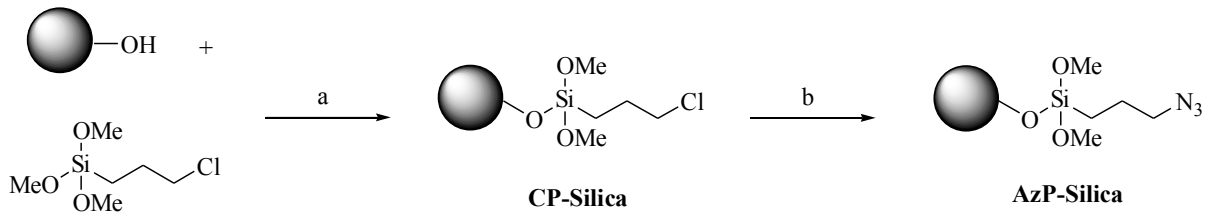

***Scheme 9**: Conditions: (a) toluene, p-toluenesulfonic acid (catalyst), reflux, 18 h, (b) NaN_3, dimethylsulfoxide (DMSO), tetrabutylammonium iodide (catalyst), 80°C, 72 h.*

Scheme 9 shows the two-step synthetic route to azidopropyl-modified silica **AzP-Silica**. The synthesis was carried out similarly to a procedure published by Kacprzak et al. [62].

Silica and the catalyst were suspended in toluene and dried via azeotropic distillation. For surface-preactivation the haloalkylsilane was added to the reaction mixture and the mixture was stirred under reflux. The suspension was then filtered and washed with toluene and methanol. Chloropropyl-modified silica (**CP-Silica**) was dried under vacuum and chloropropyl-loading was determined by elemental analysis. **CP-Silica** was treated with NaN_3 in DMSO and tetrabutylammonium iodide as a catalyst to substitute the chloro-group by an azide group via nucleophilic halide/azide exchange. **AzP-Silica** was filtered, washed and dried under vacuum. Azide-loading of **AzP-Silica** was determined by elemental analysis. The analysis results showed a successful conversion of 85% from **CP-Silica** (740 µmol/g) to **AzP-Silica** with an azide-alkylsilane loading of 630 µmol/g.

2.1.10. Immobilization of SO3 onto AzP-Silica

Scheme 10 shows the synthetic route to **CSP3** (DHQN-type) linked via 1,2,3-triazole group. The described procedure can be considered as a general synthetic pathway valid for **CSP5** (DHQN-type) as well. All azide click reactions were carried out in a way similar to the procedure published by Kacprzak et al. [47, 62, 65].

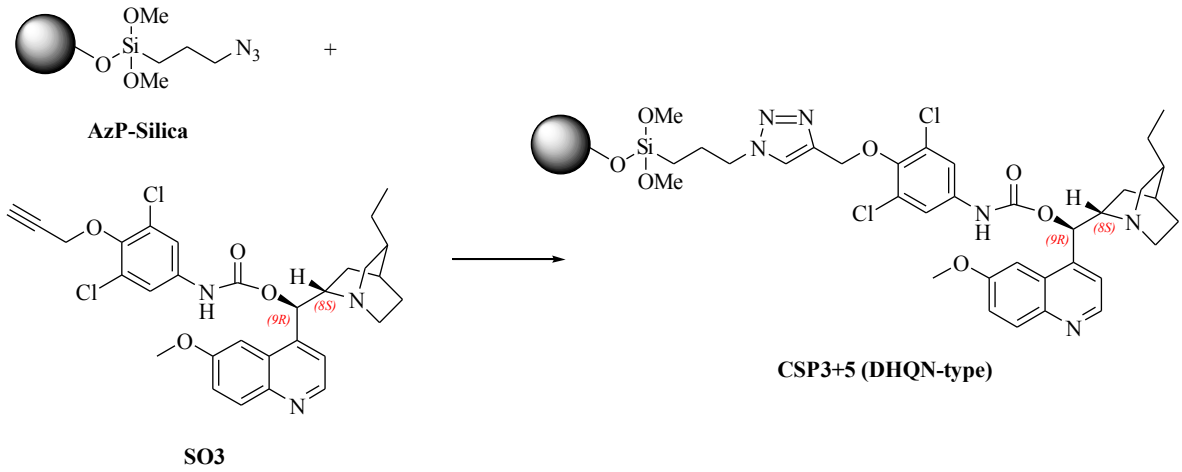

***Scheme 10**: Conditions: ACN, CuI (catalyst), N,N-diisopropylethylamine (DIPEA), room temperature (RT), 72 h.*

ACN was degassed together with **AzP-Silica**, **SO3** and DIPEA (Hünig´s base) in a resealable glass bottle. Catalyst was added under N_2 flushing and the sealed glass bottle was shaken for 72 h on an overhead shaker at room temperature. The reaction mixture was then filtered, washed and dried under vacuum. SO loading was determined by elemental analysis.

2.1.11. Immobilization of SO4 onto AzP-Silica

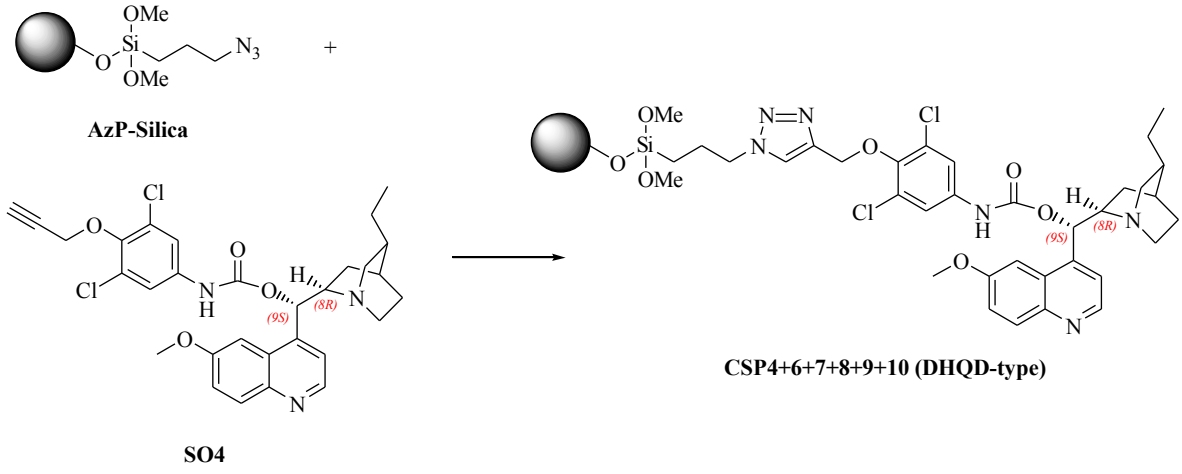

***Scheme 11**: Conditions: ACN, CuI (catalyst), DIPEA, RT, 72 h.*

Scheme 11 shows the synthetic route to **CSP4** (DHQD-type) via azide-alkyne Huisgen cycloaddition. This synthetic procedure was also applied for **CSP6+7+8+9+10** (all of them are DHQD-type CSPs). Analogously to the procedure

mentioned above, the reagents were mixed, degassed, shaken for 72 h and afterwards worked up. SO loading was again determined by elemental analysis.

2.2. Summary of all synthesized CSPs

In combination with different SO loading of **SO1-4** onto silica, 12 different columns were prepared. **Table 2.1.** shows a summary of all synthesized CSPs together with dimensions of the packed columns, type and loading of the SO.
SO loading for the radical thiol-ene addition was 144 and 179 µmol/g for **CSP1** (DHQN-type) and **CSP2** (DHQD-type), respectively. In comparison to the immobilization via Huisgen azide alkyne click reaction the SO loading achieved via thiol-ene addition was approximately three times lower. This could be due to the π-acidic character of the dichloro-substituted aromatic ring from the linker and the resulting radical scavenging property [66]. However, in former experiments of our working group the SO loading of about 200 µmol/g showed good enantioseparation properties for *N*-protected amino acids [65].

Table 2.1.: Summary of synthesized CSPs and the corresponding packed columns.

Column Number	CSP Number	SO	Type of SO	Dimensions of the column	Dimensions of Silica	SO loading [µmol/g]
1	CSP1	SO1	DHQN	150x4 mm ID	5 µm, 120 Å	179
2	CSP2	SO2	DHQD			140
3	CSP3	SO3	DHQN			477
4	CSP4	SO4	DHQD			490
5	CSP5	SO3	DHQN			214
6	CSP6	SO4	DHQD			232
7	CSP7	SO4	DHQD			238
8	CSP8	SO4	DHQD			314
9	CSP9	SO4	DHQD			150
10	CSP10	SO4	DHQD			138
11	CSP3	SO3	DHQN	75x4 mm ID	5 µm, 120 Å	477
12	CSP4	SO4	DHQD			490

CSP7 and **CSP10** (both of them DHQD-type) do have slightly different chemical and physical properties in comparison to the other synthesized CSPs. **CSP7** is almost a one to one physical mixture of **CSP4** and pure **AzP-Silica**. This CSP was made for

comparative purposes to **CSP6** (DHQD-type) because of similar overall SO loading per gram silica.

CSP10 is a modified version of **CSP9**. The only difference is that the free azido-groups of **CSP9** – after immobilizing **SO4** – were endcapped with propargyl alcohol to give **CSP10**. The reaction scheme for endcapping is shown in **scheme 12**.

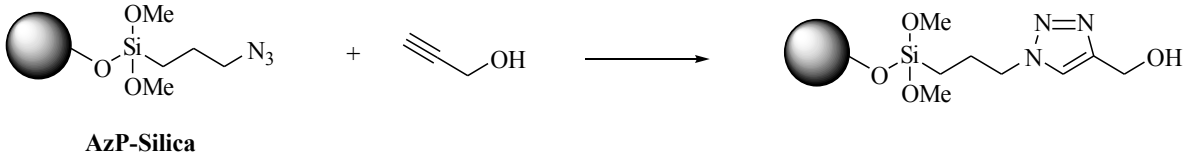

AzP-Silica

***Scheme 12**: Conditions: ACN, CuI (catalyst), DIPEA, RT, 72 h.*

All columns were packed “in-house” into stainless steel columns with 150 mm length and 4 mm inner diameter, except for **columns 11** and **12**, which were packed into 75x4 mm ID columns for comparative purposes and a loading study. Packing of the columns was carried out using the conventional slurry packing method with iPrOH as slurry solvent and MeOH as packing solvent at a pressure of approximately 650 bars.

After packing the columns were flushed with aqueous EDTA solution to remove remaining CuI catalyst (**column 3-12**), water and MeOH.

2.3. Properties of the SOs

All four SOs (**SO1-4**) are derived from well-established cinchona alkaloid weak anion exchange (WAX) type SOs, namely **QN-AX** and **QD-AX** [67] and thus they are potentially suitable for the separation of acidic chiral compounds. Due to the pseudoenantiomeric behavior of the building blocks **DHQN** and **DHQD** [13, 49, 68, 69].

reversal of the elution order is possible. The immobilization can be carried out via two different strategies, either radical thiol-ene addition with AIBN or V65 as radical starter or copper(I)-catalyzed Huisgen alkyne-azide click chemistry.

There are multiple interactions with potential analytes (selectands, SAs) possible:

- Primary ionic interaction via the ionizable bicyclic tertiary amine in the quinuclidine ring at acidic mobile phase conditions (p*K* app. 9.8, entirely protonated at pH-values lower than 7.8 [70]). The quinoline amine (p*K* is app. 3.9) is mainly deprotonated under weakly acidic mobile phase conditions [70].
- Hydrogen-bonding via the carbamate -NH as donor and the carbonyl as an acceptor.
- Intermolecular π-π interactions via the aromatic π-basic quinoline ring and the aromatic ring of the linker.
- Steric interaction because of the sterically demanding aromatic dichloro-substituted linker.

All these interactions result in a potential ability for chiral recognition and make the SOs suitable for enantiomeric separation of chiral acidic SAs.

2.4. Immobilization Efficiency

In **table 2.2.** and **figure 2.1.** the dependency of the immobilization efficiency of offered SO is shown. All immobilizations were carried out using the same conditions for Huisgen click chemistry.

Table 2.2.: Dependency of immobilization efficiency of offered SO.

CSP	Offered SO [µmol/g Silica]	Actual Loading [µmol/g Silica]	Loading Efficiency [%]
3	1044	477	///
4	1014	490	///
8	360	314	87
6	250	232	93
5	230	214	93
9	150	150	100

For **CSP3** (DHQN-type) and **CSP4** (DHQD-type) no selector loading efficiency is shown, because the SOs (**SO3** for **CSP3** and **SO4** for **CSP4**) were offered in app. 1.5 times molar excess referring to azidopropyl-loading on **AzP-Silica** with

629 µmol/g silica. For **CSP5+6+8+9** the SOs were offered in deficit. With higher amount of offered SO the loading efficiency decreases. At a very low level of offered SO (150 µmol/g for **CSP9**) immobilization can be regarded as quantitatively. In average 93% of the offered SO were immobilized.

The maximum of practical loading is approximately 500 µmol/g silica, achieved with excess offer of SO. The stoichiometric maximum of loading capacity at 629 µmol/g was never reached, even with a considerable excess of SO. This result reflects the impact of sterical hindrance.

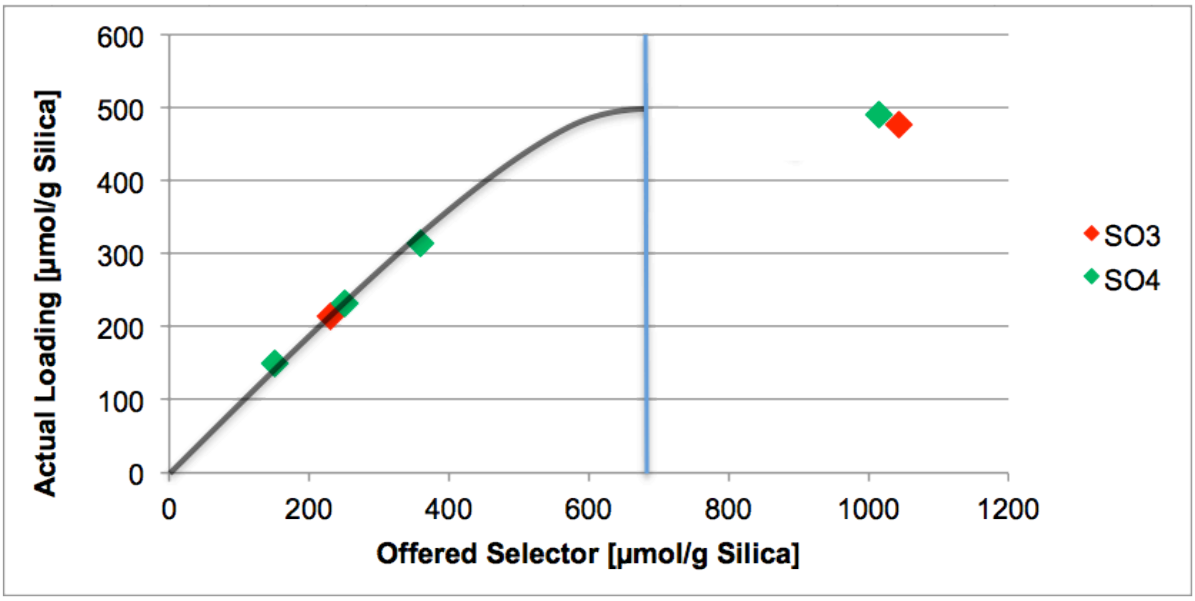

Figure 2.1.: Actual loading vs. offered SO3 or SO4; blue line: stoichiometric maximum (629 µmol/g).

Similar effects have been observed by Marshall et al. [71]. In the present case, the sterically demanding cinchonan derived SO leads to saturation phenomena at surface densities higher 500 µmol/g, rendering the preparation of more densely loaded CSP surfaces elusive.

3. Evaluation of the WAX-CSPs

3.1. Reference CSPs and Columns

For comparative purposes and the loading study as well, four additional columns were used (see **table 3.1.**). Three columns were packed with commercially available Chiralpak® QN-AX and QD-AX selector type silica materials [13]. In **figure 3.1.** the structures of these cinchona-derivatives-based weak anion exchange CSPs are depicted. These two quinine and quinidine derived carbamoylated reference materials show high capabilities in terms of resolution of chiral acidic compounds [49, 50, 67, 72, 73].

To further discover the influence of free azido-groups on the retention of analytes (selectands, SAs), one 150x4 mm ID column was packed with pure AzP-Silica as a non-chiral stationary phase (SP1).

Table 3.1.: Further used columns for Evaluation.

Column Number	Type of Selector	Dimensions of the column	Dimensions of Silica	Selector loading [µmol/g]
13	QN-AX	150x4 mm ID	5 µm, 120 Å	app. 340
14	QD-AX	150x4 mm ID		
15	QD-AX	75x4 mm ID		
16	AzP	150x4 mm ID	5 µm, 120 Å	629

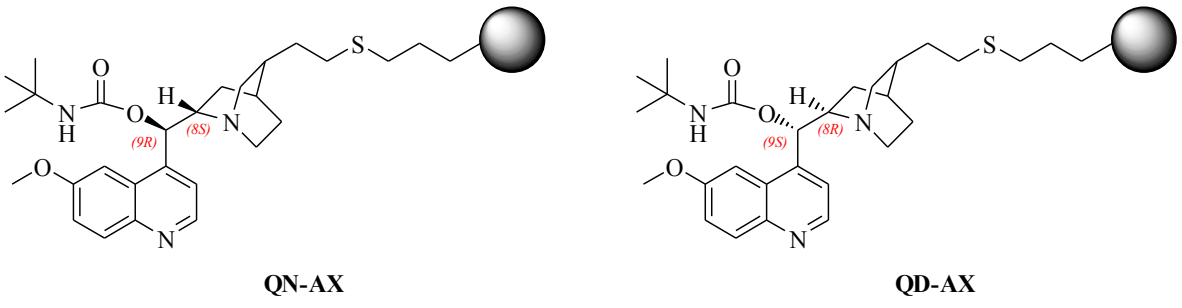

Figure 3.1.: Structures of CHIRALPAK® QN-AX and QD-AX CSPs; adapted and modified from [47, 48].

3.2. Analytes

For the evaluation of the CSPs a broad set of chiral SAs was used. Since all the synthesized CSPs are weak anion exchange type CSPs based on cinchona alkaloids and the retention is primarily driven by an ion exchange mechanism [42, 49, 67], the majority of the SAs consists of chiral organic acids and acid derivatives including 31 *N*-protected amino acids (BOC-Gly and DNZ-Gly as achiral compounds), 17 carboxylic acids, nine *N*-protected aminophosphonates and three *N*-protected aminosulfonic acids. For determining the elution order single enantiomers were used if they were available. To further proof the concept of anion exchange four zwitterionic and three basic compounds, which should stay non-retained [42], were also used for the evaluation of the CSPs. In **figures 3.2.** to **3.9.** the structures of all SAs used for evaluation are shown. The SAs were commercially available, synthesized earlier in the working group of Prof. Lindner or were kind gifts of other working groups [74, 75].

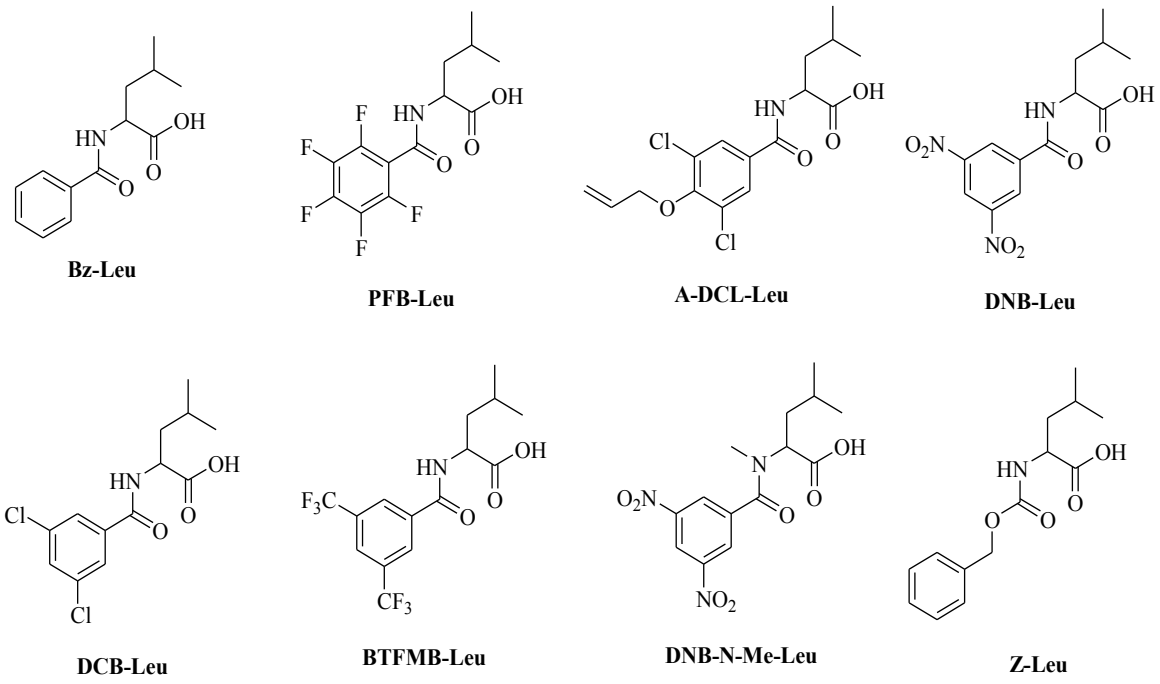

Figure 3.2.: *N*-protected amino acids (leucine derivatives).

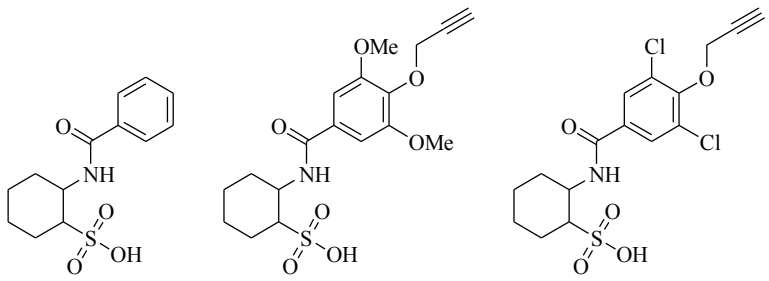

Figure 3.3.: *N*-protected amino sulfonic acids.

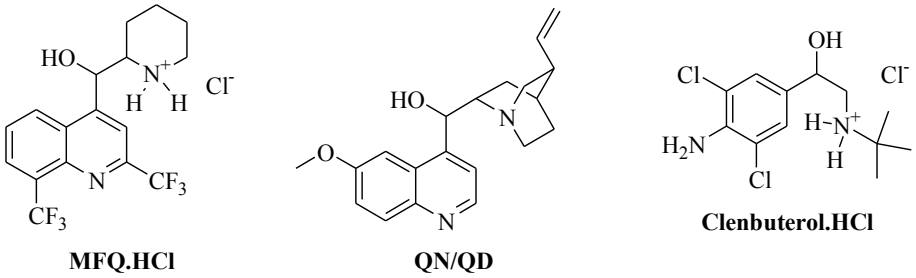

Figure 3.4.: Basic compounds.

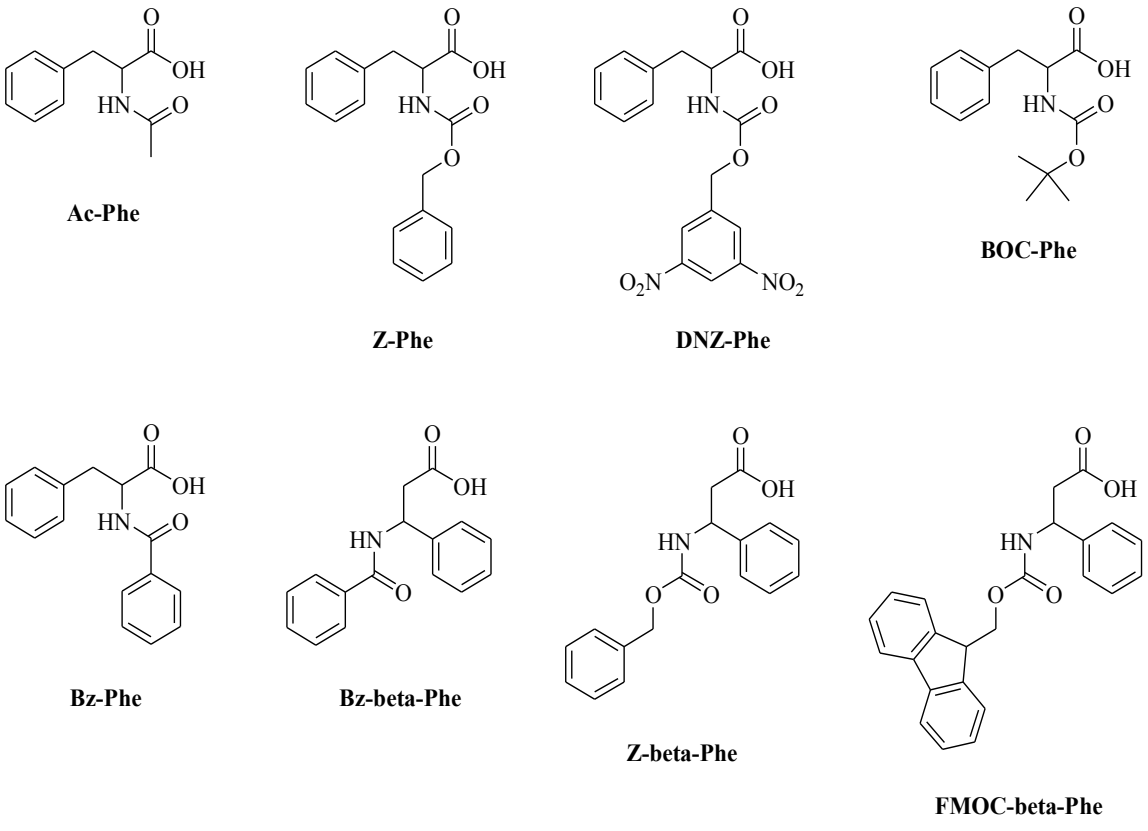

Figure 3.5.: *N*-protected amino acids (phenylalanine derivatives).

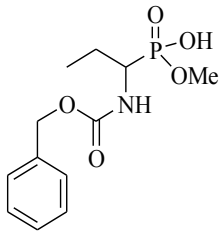

PI-2-38-1

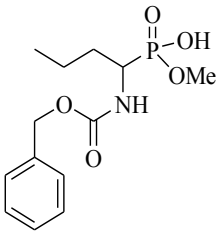

PI-2-34-1

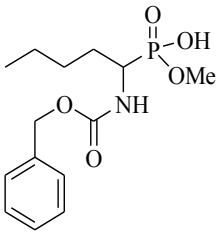

PI-2-87-1

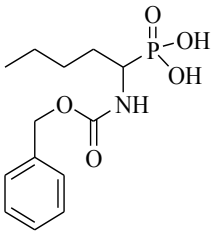

PI-2-56-2

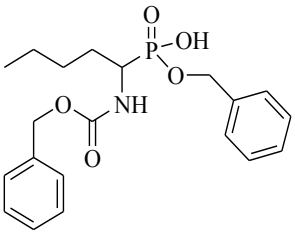

PI-3-67-1

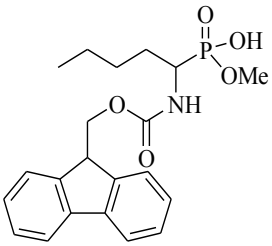

PI-2-15-1

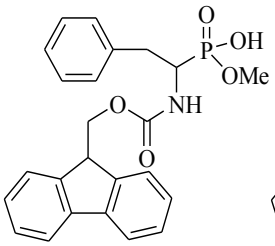

PI-2-25-1

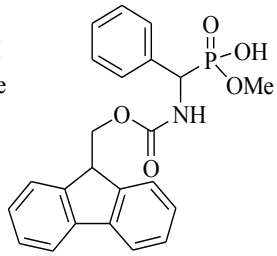

PI-2-4-3

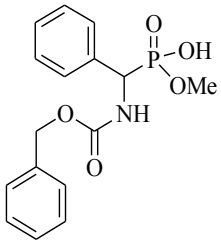

PI-1-89-1

Figure 3.6.: *N*-protected aminophosphonates.

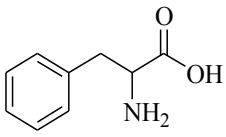

Phe

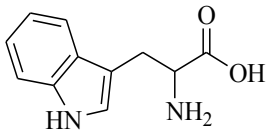

Trp

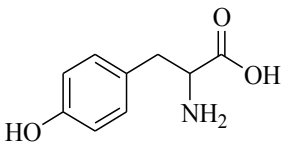

Tyr

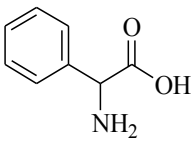

Phenyl-Gly

Figure 3.7.: Zwitterionic compounds.

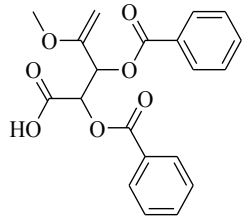

DBTAMME

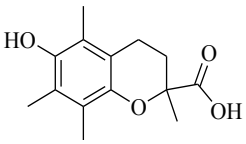

Trolox

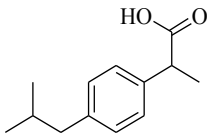

Ibuprofen

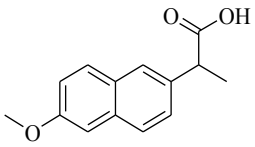

Naproxen

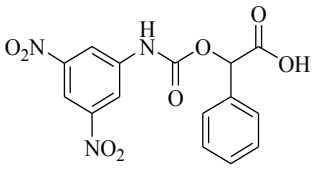

DNP-Mandelic acid

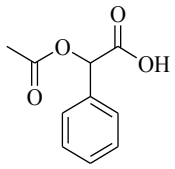

Acetylmandelic acid

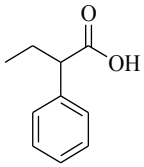

Phenylbutyric acid

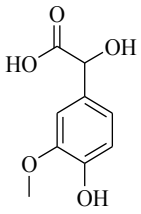

Vanillylmandelic acid

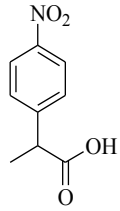

Nitrophenylpropionic acid

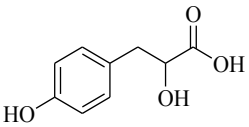

Hydroxyphenyllactic acid

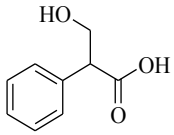

Tropic acid

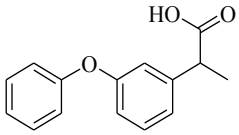

Fenoprofen

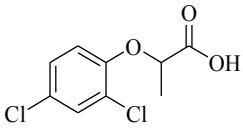

Dichlorprop

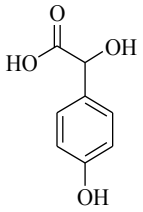

Hydroxymandelic acid

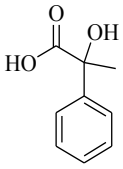

Atrolactic acid

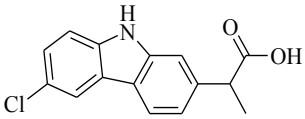

Carprofen

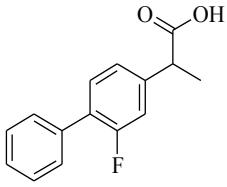

Flurbiprofen

Figure 3.8.: Carboxylic acids (including profens).

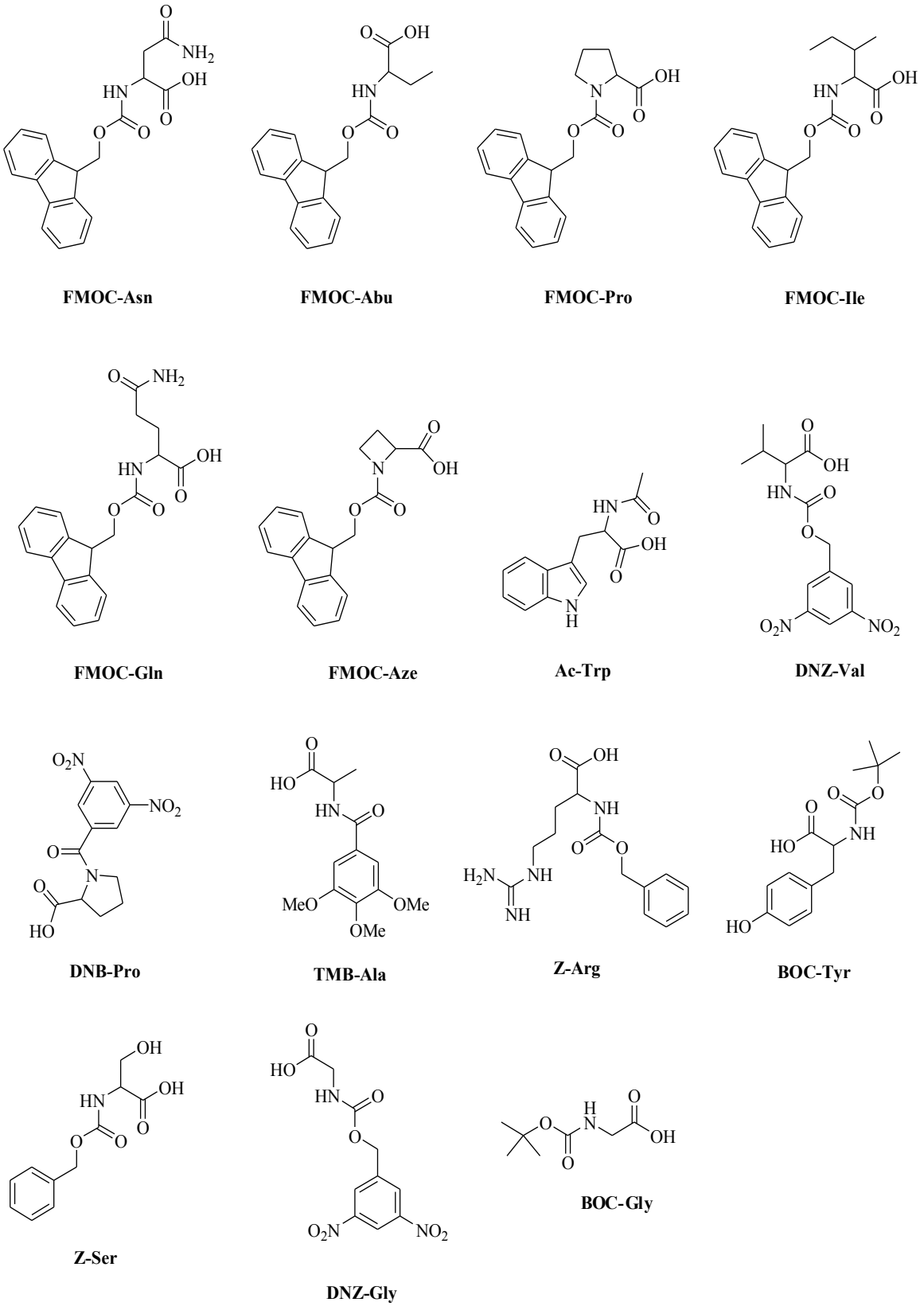

Figure 3.9.: *N*-protected amino acids.

3.3. Materials and Methods for Evaluation

The chromatographic screening of the columns was carried out on a 1290 series Infinity HPLC system from Agilent Technologies (Waldbronn, Germany) consisting of an automated sampler, solvent tray, a binary pump with two channels, a degasser, a thermostated column compartment for six columns and a diode array detector (DAD). All SAs were detected at a wavelength of 254 nm. The columns were thermostated at 25.0 ± 0.1°C. Data processing was carried out with a ChemStation chromatographic data software from Agilent Technologies and Excel spreadsheet software from Microsoft Corporation.

The loading studies were carried out on an 1100 series HPLC system from Hewlett Packard (Waldbronn, Germany) consisting of an automated sampler, solvent tray, a binary pump with two channels, a degasser, a thermostated column compartment and a multiple wavelength detector (MWD). The SAs were detected at a wavelength of 270 nm. The columns were thermostated at 25 ± 0.1°C. Racemic Ac-Phe (obtained from Sigma) was dissolved in pure MeOH at a sample concentration of 100 ± 0.1 mg/mL. The injection volume was 5 to 100 µL. Elution was performed in isocratic mode with a flow rate of 0.5 mL/min for 15 min. As a starting mobile phase the same composition as for screening was used (see below).

For screening purposes 5 µL of each SA-solution with a concentration of 1.0 ± 0.1 mg/mL in MeOH were injected. For determining the elution order in a racemic mixture a single enantiomer was – if available – measured as well. Elution was performed in isocratic mode with a flow rate of 1.0 mL/min at 25.0 ± 0.1°C. The composition of the mobile phase used for screening was MeOH/AcOH/NH_4OAc (99/1/0.25 v/v/w). The mobile phase was degassed by sonication prior to use. This mobile phase composition is a diluted version of a commonly and successfully used mobile phase in polar organic (PO) mode used e.g. by Kacprzak et al. [47].

The acetic acid in the mobile phase is necessary to provide weakly acidic conditions in the chromatographic system for protonation of the selector. The acidic additive and buffer salt also act as co- and counterion that determines the electrostatic interactions between SA and CSP [76]. Because buffer salts also act as competitors to the SAs and are therefore displacers for the SAs, the retention time is highly dependent on an ion strength and ion charge in the mobile phase.

3.4. Chromatographic Parameters

For evaluation of the different CSPs it is necessary to define the main chromatographic parameters:

- Retention Factor k_i:

$$k_i = \frac{t_i - t_0}{t_0} \quad \textbf{[3.1]}$$

The retention factor k_i reflects the binding strength between a SA or single enantiomer of the SA and the SO immobilized on the surface of a CSP. The larger the value of k_i, the stronger is the interaction. The retention factor is calculated by dividing the difference between the retention time and the void time by the void time.

- Selectivity coefficient α:

$$\alpha = \frac{k_2}{k_1} \quad \textbf{[3.2]}$$

The selectivity coefficient or separation factor α describes the ratio of the retention factors of two separated SAs or enantiomers. It is calculated by dividing the retention factor of the second eluted enantiomer (k_2) by the retention factor of the first eluted enantiomer (k_1). If separation takes place, the α-value is higher 1. For preparative purposes high selectivity is one important prerequisite.

- Resolution R:

$$R = \frac{\sqrt{N_{av}}}{4} \cdot \frac{\alpha - 1}{\alpha} \cdot \frac{k_2}{1 + k_{av}} \quad \textbf{[3.3]}$$

The resolution R indicates the quality of separation and consists of three terms (efficiency, selectivity and retention). The first term includes the average number of theoretical plates for separation N_{av} (see **equation [3.4]**). This term

describes the separation performance. The resolution is directly proportional to the square root of N_{av}. The higher the number of plates, the higher is the resolution. The second term includes the selectivity coefficient α. The retention factor of the second eluted enantiomer (k_2) and the average retention factor for both enantiomers are described in the third term.

- Number of theoretical plates N_i:

$$N_i = 5.54 \cdot \left(\frac{t_i}{w_{i_{1/2}}} \right) \qquad \textbf{[3.4]}$$

The number of theoretical plates N_i indicates the separation performance. N_i informs on the number of equilibrium settings of the SA between the mobile and stationary phase. It is dependent on the quality of packing of the column and the SO density on the surface of the silica material. N_i is calculated by dividing the retention time by the width of the peak at half maximum $w_{i1/2}$.
Please note that in the following discussion N_i always refers to the respective column length.

3.5. Influence of immobilization strategy

In **figures 3.10.** to **3.12.** one can see the influence of the immobilization strategy on the performance of the same selector. CSP2 (DHQD-type) in column 2 was prepared by the radical thiol-ene addition, while CSP9 (DHQD-type) in column 9 was immobilized by alkyne-azide click chemistry. This is the only structural difference between the two CSPs, because the remaining structures of the SOs are the same. SO loading of CSP2 was 144 µmol/g and for CSP9 150 µmol/g, so they both are comparable in terms of the SO density on the surface. The chromatographic conditions used were the same for both measurements.
The acidic compounds are at least partially separated; the elution order for amino acid derivatives is always *L* before *D*, except for DNB-Pro, which was observed for any other DHQD-type CSP as well. DNB-*N*-Me-Leu was not separated on the column 9, and the alpha-value on the column 2 was very low. Basic compounds like QN, QD, clenbuterol hydrochloride and zwitterionic compounds are neither retained

nor separated; they all had a *k*-value below 0.3. **Figure 3.10.** shows that the *k*-values are comparable for both columns. Column 9 exhibits an increased selectivity for the aminophosphonic compound PI-2-15-1 (α = 1.71) in comparison to column 2 (α = 1.16). The alpha-values for the other SAs are comparable (see **figure 3.11.**). These results demonstrate that both types of CSPs are capable of separating a variety of chiral acidic compounds, independently on structural variations and acidity.

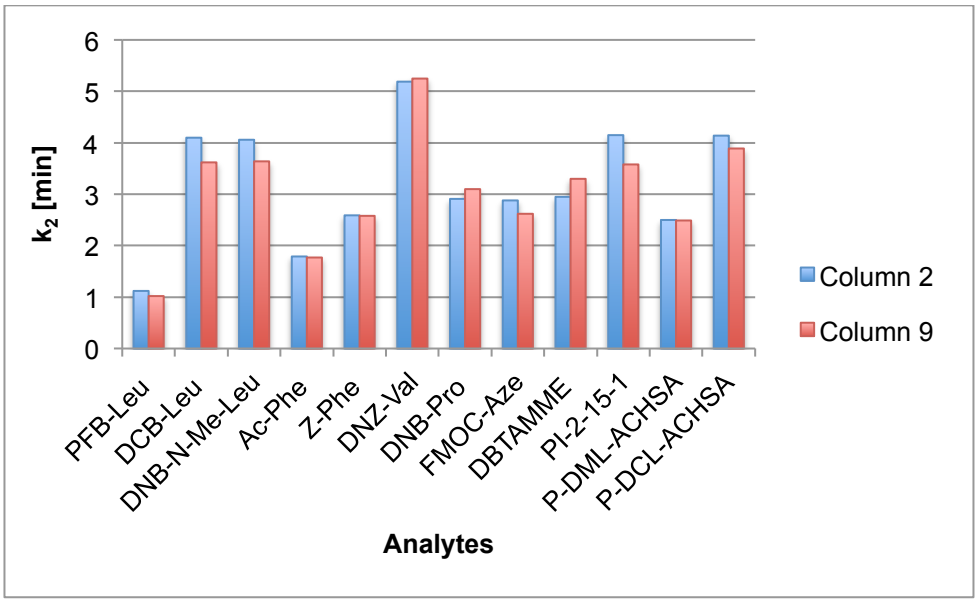

Figure 3.10.: Dependency of retention of the immobilization strategy; column 2: DHQD-type, 140 µmol/g; column 9: DHQD-type, 150 µmol/g.

In terms of resolution the behavior is different (see **figure 3.12.**). *R* is always higher for the radical thioether like CSP. One example is DCB-Leu: Resolution is about 13 for column 2 and 8 for column 9. This is based on the different number of theoretical plates for each column, because *k* and alpha-values are comparable.

For column 2 N_{av} is about 5300 (all measured samples), for column 9 the number of theoretical plates is a factor of 2.3 lower (N_{av} = 2300, all measured samples). One reason for different resolution-values could be a different packing density of the two columns, because packing also influences the number of plates and therefore the resolution.

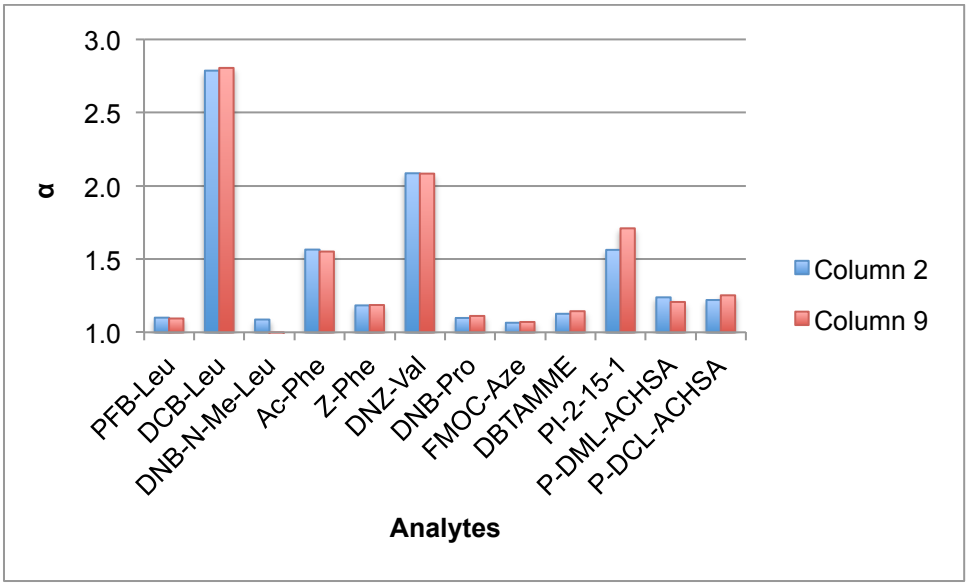

Figure 3.11.: Dependency of selectivity of the immobilization strategy; column 2: DHQD-type, 140 µmol/g; column 9: DHQD-type, 150 µmol/g.

The same results and trends were observed when comparing columns 1 and 5, the corresponding DHQN-type CSPs with 179 µmol/g and 214 µmol/g SO loading, respectively.

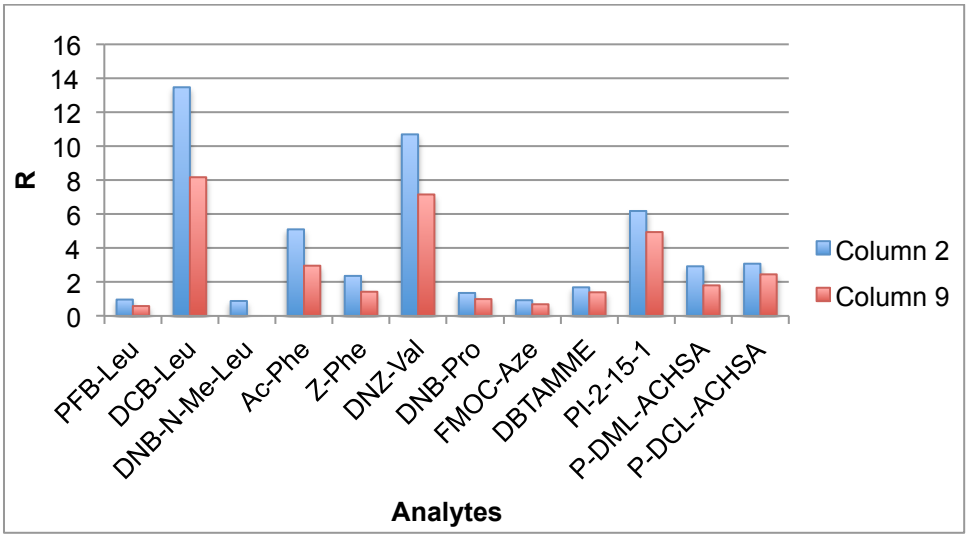

Figure 3.12.: Dependency of resolution of the immobilization strategy; column 2: DHQD-type, 140 µmol/g; column 9: DHQD-type, 150 µmol/g.

3.6. Influence of free Azide groups on Retention

The influence of free azide-groups on silica is shown in **figure 3.13**. The effect of free azide-groups could be important for low loaded CSPs, because there are free

azide groups not-clicked with an alkyne residue. The azide itself is highly polarized and therefore it can potentially interact with polarized groups of SAs. This study was performed with pure AzP-Silica as a non-chiral stationary phase (SP1, column 16).

The influence of pure AzP-Silica is low. There is – of course – no enantioselectivity and no retention as well, except a very low retention value for QN and QD. The other SAs used for this study eluted before t_0. The overall effect is quite limited and there is almost no contribution with regard to retention.

The average *k*-value is below zero (k_{av} = -0.1). Furthermore, Franco et al. carried out retention studies with pure MP-Silica as a reference material and they documented that there is also no substantial contribution of the carrier material with respect to retention [42]. They have observed average *k*-values below 0.1 for a variety of *N*-protected amino acids as well.

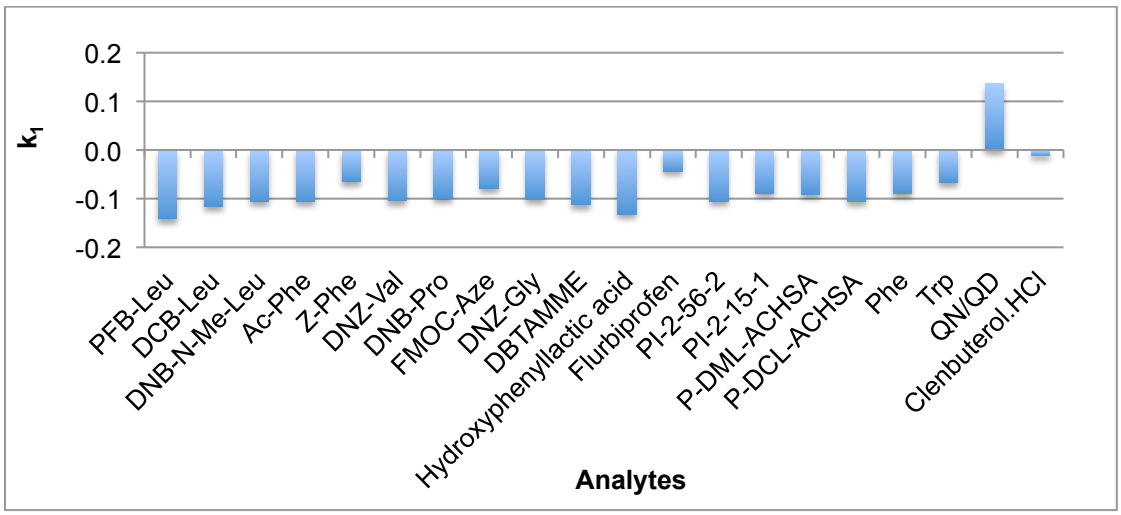

Figure 3.13.: Influence of free azide-groups on silica; column 16: AzP-type, 629 µmol/g.

3.7. Influence of Endcapping

In **figures 3.14.** and **3.15.** the influence of endcapping in terms of selectivity and resolution is shown. For this study CSP9 (DHQD-type) was used, part of which was endcapped with propargyl alcohol to give CSP10. SO loading is almost the same after endcapping (138 µmol/g for CSP10 in comparison to 150 µmol/g for CSP9), 12 µmol (8%) of SO per gram silica have been cleaved off during immobilization and the work-up procedure. The average number of theoretical plates for column 9 was N_{av} = 2324, for column 10 N_{av} = 3486 (factor of 1.5).

Even with this low amount of immobilized SO at least partial separation of the SAs was possible. Only hydroxyphenyllactic acid was not separated on column 10, on the other hand, partial separation on column 9 was achieved (α = 1.07).

The k_1- and k_2-values (not shown here, see **appendix**) were generally lower for the endcapped material. This can be explained by the slightly lower SO loading. The aminophosphonate derivative PI-2-15-1 exhibits, however, slightly higher retention on column 10.

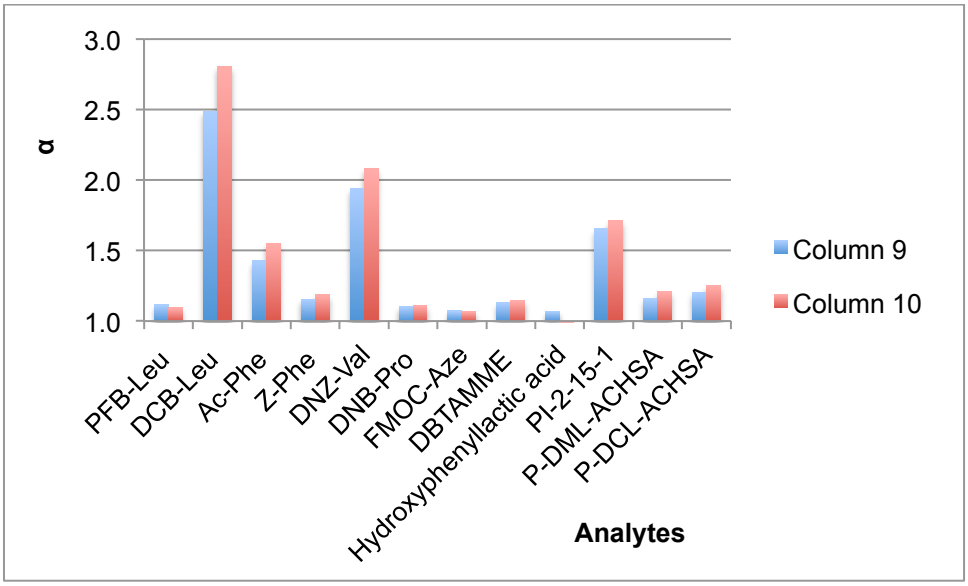

Figure 3.14.: Influence of endcapping in terms of selectivity; column 9: DHQD-type, 150 µmol/g; column 10: DHQD-type, 138 µmol/g (endcapped).

DCB-Leu and the two aminosulfonic acid derivatives P-DML-ACHSA and P-DCL-ACHSA do have higher k_2-values on column 10 compared to column 9.

There is a trend that alpha-values for *N*-protected amino acid derivatives are slightly increased for the encapped material, so selectivity is better. On the other hand, the resolution is lower. For the tested aminophosphonate and the aminosulfonic acid derivatives resolution is increased, which is in agreement with the trend observed for selectivity coefficient α.

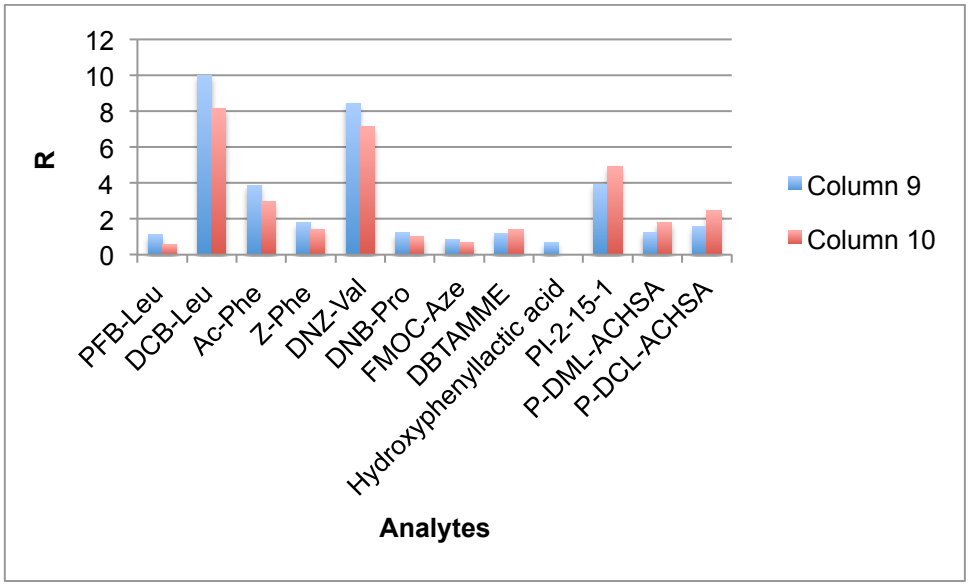

Figure 3.15.: Resolution-influence of endcapping;
column 9: DHQD-type, 150 µmol/g; column 10: DHQD-type, 138 µmol/g (endcapped).

3.8. Reversal of the Elution Order

Referring to the pseudoenantiomeric behavior of the building blocks DHQN (*8S*,*9R*) and DHQD (*8R,9S*; both of them *1S,2R,3S*) [13, 49, 67-69], reversal of the elution order was observed for every single separated racemic SA, without any exception. The DHQN and DHQD derived CSPs show exactly opposite behavior in terms of enantioselectivity as indicated in **figure 3.16.** for the separation of P-DCL-ACHSA (*S,S* > *R,R*) on column 1 (DHQN-type) and column 2 (DHQD-type). For the *N*-protected amino acid derivatives elution order was always *D* before *L* for DHQN-type CSPs except for DNB-Pro (*L* before *D*). The DHQD-type SOs behaved just the opposite way. This indicates an equal separation mechanism for all *N*-protected amino acid derivatives except for DNB-Pro.

Maier et al. reported that *"the absolute configuration of the C_9 stereogenic center in the cinchonan backbone determines the elution order of these analytes. SOs having (9R)-configuration, i.e., QN- […] derived CSPs, show stronger retention for N-acylated (S)-amino acids, whereas their (R)-enantiomers interact more strongly with QD- […] based selectors"* [67].

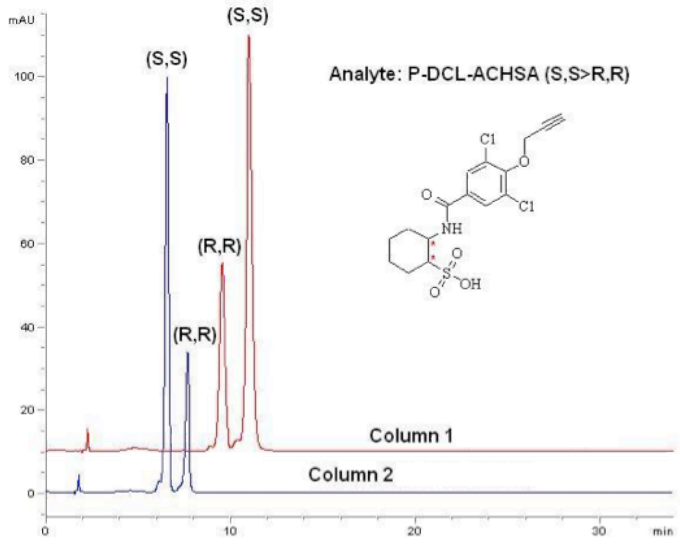

Figure 3.16.: Reversal of the elution order on changing from DHQN to DHQD-type CSPs; column 1: DHQN-type, 179 µmol/g, column 2: DHQD-type, 140 µmol/g.

3.9. Comparison of DHQN and DHQD-type CSPs

Column 5 (DHQN-type) and column 6 (DHQD-type) are well suited for the comparison of DHQN and DHQD-type CSPs because they have approximately the same amount of SO immobilized on the surface via Huisgen alkyne-azide click chemistry. CSP 5 in column 5 has a SO loading of 214 µmol/g in comparison to CSP6 in column 6 with a loading of 232 µmol/g silica.

In **figure 3.17.** the ratio of partial separation, baseline separation and no separation for 58 acidic chiral SAs for columns 5 and 6 is shown. In case of the DHQD-type CSP (column 6) 53% of the 58 acidic SAs were baseline separated and 19% were partially separated. All together separation was observed for 72% of the acidic SAs.

The percentage of baseline separated SAs for the DHQN-type CSP (column 5) is lower (50%), but all together 72% of the SAs were at least partially separated. The value for not separated compounds is equal for both columns (28%). The observed partial separation of Trp on the DHQN-type CSP5 (α = 1.14, R = 0.48) is not included in the calculation. This separation was not observed for CSP6. The other three zwitterionic compounds and the three basic compounds were not separated. For the DHQD-type CSP no zwitterionic and basic compound was separated.

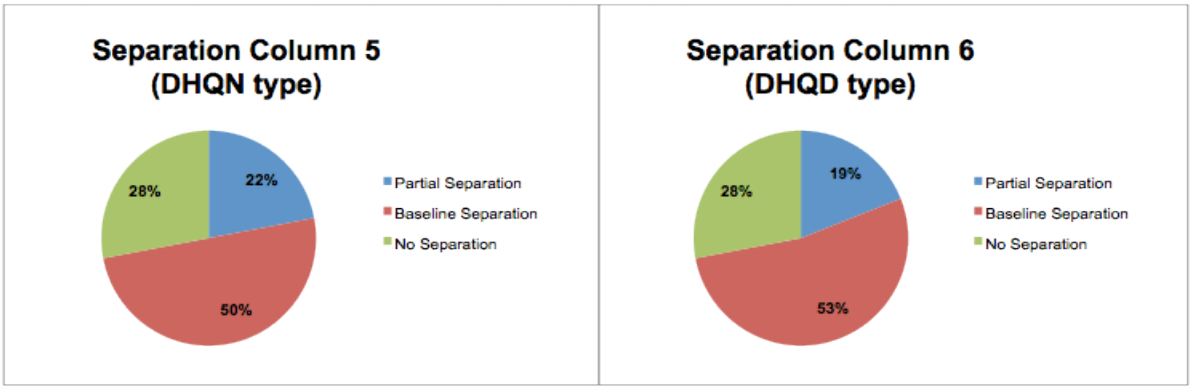

Figure 3.17.: Ratio of partial separated (0 < *R* < 1.5), baseline separated (*R* ≥ 1.5) and not separated acidic SAs (*R* = 0) observed for column 5 (DHQN-type, 214 µmol/g) and column 6 (DHQD-type, 232 µmol/g).

However, one should consider that these results were observed for just one mobile phase (polar organic mode, MeOH/AcOH/NH_4OAC 99/1/0.25 v/v/w). Variation of the mobile phase could of course alter the percentages for partial, baseline and no separation.

3.9.1. Selectivity

In **figure 3.18.** the average values of the selectivity coefficients for the different groups of acidic SAs are shown. A general trend for all the groups of SAs is that selectivity is increased for the DHQD-type CSP6. The *N*-protected phenylalanine derivatives represent an exception in two aspects:

1. Both for DHQN and for DHQD-type CSP the average alpha-value is the highest compared to the other groups of chiral acidic SAs.
2. The behavior, in terms of selectivity, is exactly the opposite in comparison to the other groups of acidic compounds – the DHQN-type CSP has an increased selectivity by a factor of 1.67. This is because the selectivity for DNZ-Phe is doubled in case of the DHQN-type CSP (21.4 for DHQN-type and 10.4 for DHQD-type CSP).

Alpha-values of other *N*-protected phenylalanine derivatives are increased for the DHQD-type CSP (column 6).

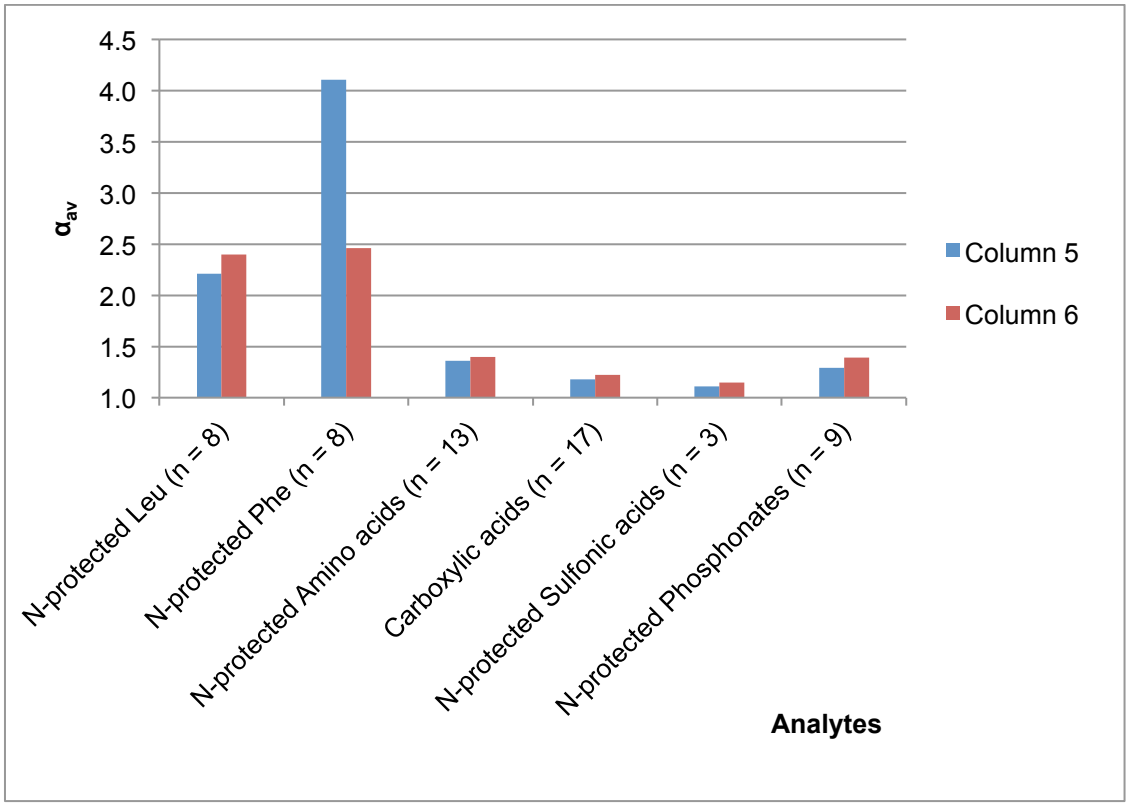

Figure 3.18.: Average *α*-values for the different groups of acidic SAs; column 5: DHQN-type, 214 µmol/g; column 6: DHQD-type, 232 µmol/g.

The carboxylic acid derivatives, in particular profens (representing aryl propionic acids) are hard to separate. In this regard Lämmerhofer et al. noticed that this type of carboxylic acids is not capable of forming additional dipole interaction or hydrogen bonding due to the absence of an additional polar unit between the aromatic group and the chiral center [49].

3.9.2. Resolution

A comparison between CSP5 and 6 in terms of average resolution shows a clear trend for higher resolution for the DHQD-type CSP. **Figure 3.19.** represents a graphical illustration of this behavior. Generally, the resolution is increased for every group of SA by a factor of 1.27. The resolution dependent average number of theoretical plates N_{av} is increased by a factor of 1.14 for the DHQD-type CSP as well.

In combination with the observed increase of selectivity (see **chapter 3.9.1.**), one can conclude that the DHQD-type SO is generally more suitable for the separation of chiral acids.

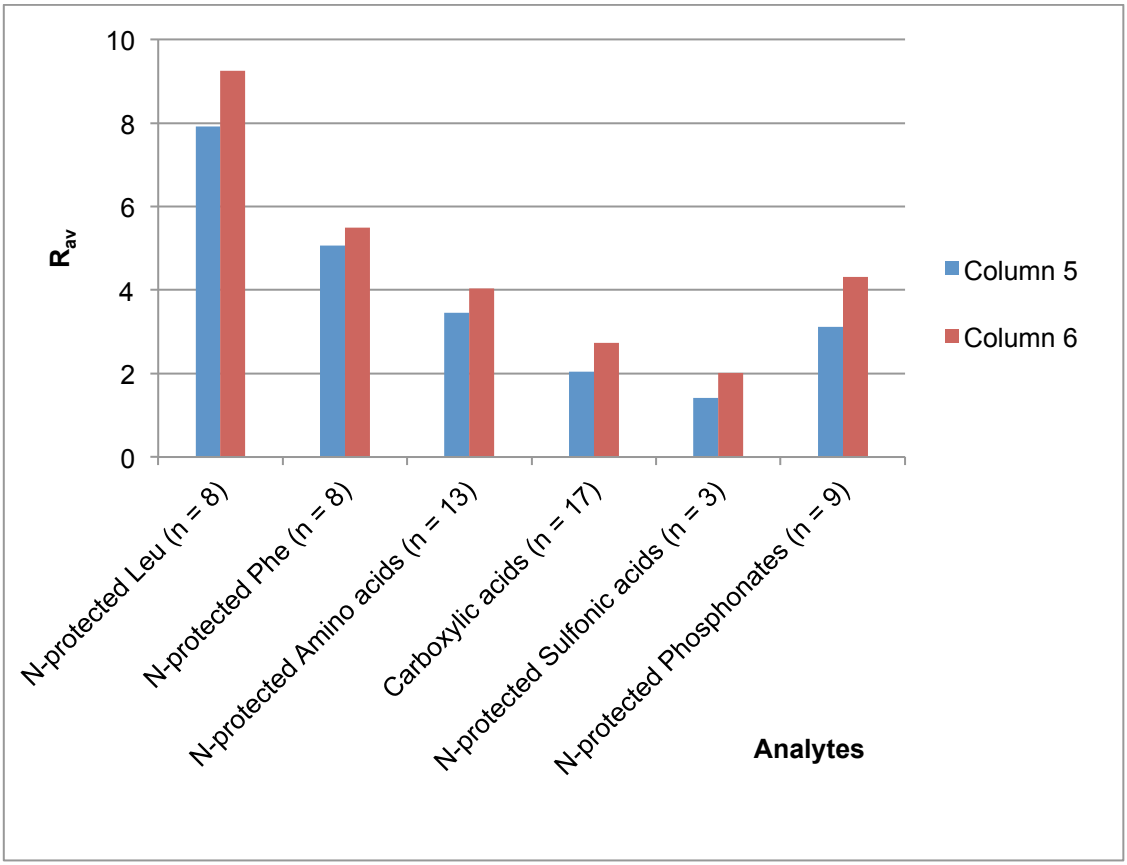

Figure 3.19.: Average resolution-values for the different groups of acidic SAs column 5: DHQN-type, 214 µmol/g; column 6: DHQD-type, 232 µmol/g.

3.10. Separation capability compared between Columns 1 to 6

For comparing structural influences on the separation behavior it is reasonable to do that with the results obtained for the column with the highest separation capability. In **table 3.2.** the results of the separation studies between columns 1 to 6 are summarized for the 58 chiral acidic SAs. Please note that BOC-Gly and DNZ-Gly are non-chiral acidic compounds and therefore are not included in the calculation below. Because all the CSPs represent weak anion exchange type CSPs, the set of non-acidic SAs is excluded from the considerations as well.

The results obtained for columns 7 to 12 are not included in this study because in this case a smaller set of samples was used for screening and therefore it is not possible to do systematic comparative studies on the structural influence of the SAs.

The largest part of baseline separated chiral acidic compounds was observed for column 2 (55%, DHQD-type CSPs). The smallest part of not separated compounds was observed for column 5 and 6 (both 28%).

Out of these results column 6 is the column with the highest separation capability and therefore the results observed for column 6 were used for comparing structural influences of the SAs on the separation behavior.

Table 3.2.: Overall separation capabilities of columns 1 to 6; partial separation 0 < *R* < 1.5; baseline separation *R* ≥ 1.5; no separation *R* = 0.

Column	CSP Type	SO loading [µmol/g]	Baseline Separation [%]	Partial Separation [%]	No Separation [%]
Column 1	DHQN	179	52	17	31
Column 2	DHQD	140	55	16	29
Column 3	DHQN	477	29	33	38
Column 4	DHQD	490	34	31	34
Column 5	DHQN	214	50	22	28
Column 6	DHQD	232	53	19	28

3.11. Influence of analyte structure on Separation

In **chapter 3.10.** the column with the highest separation capability turned out to be column 6. In this case the largest part of chiral acidic compounds was at least partially separated (72%). CSP6 in column 6 has got a SO loading of 232 µmol of SO4 (DHQD-type) per gram CSP.

3.11.1. *N*-protected leucine derivatives

DNB-*N*-Me-Leu was not separated on column 6 (see **figure 3.20.**). On the other side, the enantioselectivity is dramatically increased for the structurally related DNB-Leu, which shows the highest values of enantioselectivity and resolution for the *N*-protected leucines. The only difference between these two SAs is that the amido hydrogen of DNB-Leu is alkylated and replaced by a methyl group for DNB-*N*-Me-Leu. Evidently this amido hydrogen is essential for chiral recognition and enantioselectivity, respectively. Lämmerhofer et al. observed the same result when comparing these two SAs [49]. This behavior is also in agreement with the results previously found by Mandl et al. [50].

Without the capability of forming a hydrogen bond between the amido hydrogen as a donor and the carbonyl of the SO carbamate as an acceptor, enantioseparation is not possible for the DNB-Leu derivatives. The k_2-value for the methylated derivative

is 4.93 in comparison to 14.88 for the non-methylated compound, so there is much stronger interaction between the cinchona based carbamoylated SO and the non-methylated DNB-Leu due to hydrogen bonding. Since the amido hydrogen of DNB-Leu is close to the center of chirality, enantiodiscrimination between *L* and *D* is possible.

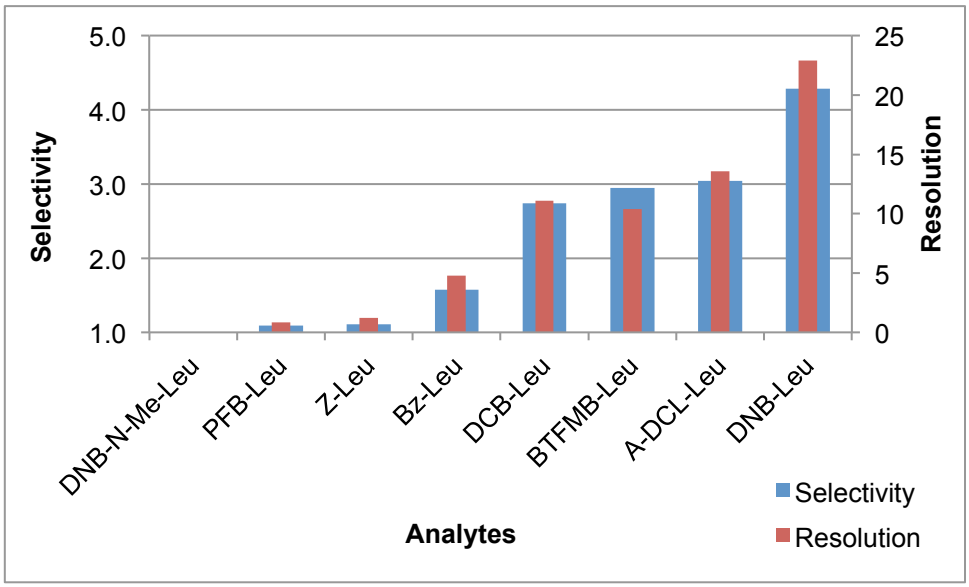

Figure 3.20.: Comparison of selectivity *α* and resolution *R* between *N*-protected leucine derivatives; column 6: DHQD-type, 232 µmol/g.

When comparing DCB-Leu and A-DCL-Leu, the structural difference is based on the *para*-allyloxy substitution at the protecting benzoyl group. Both of them are analogously *meta*-substituted with two chloro atoms at the benzoyl protecting group. The k_2-values are slightly increased for A-DCL-Leu (k_2 = 5.09) compared to DCL-Leu (k_2 = 4.67). The retention factors for the first eluted enantiomers are almost equal. Substitution with an allyloxy group also increases the enantioselectivity and resolution – this effect could be either due to the increased sterical demand of the rotating allyloxy group or due to different polarization of the aromatic system because of the introduction of an oxygen atom.

Complete substitution of all aromatic H-atoms with five fluorine atoms results in descending enantioselectivity and resolution. It has to be noted that fluoro-substitution generally results in special behavior. Of course no fluorophilic interaction with the SO can take place and therefore retention is low. The opposite result was observed e.g. by Kohout et al. when using trifluoromethyl substituted SOs based on

mefloquine as a basic module [77]. They observed that the trifluoromethyl groups of the SO are capable of promoting the recognition of PFB-Leu.

The separation parameters observed for Z-Leu are similar to those observed for PFB-Leu. Introducing an oxycarbonyl with a flexible CH_2 spacer instead of carbonyl for Bz-Leu results in decreased selectivity and resolution. One can conclude that the carbamate is less interacting with the SO in comparison to the amide.

For disubstituted Bz-Leu the selectivity coefficient decreases in the order DNB-Leu > BTFMB-Leu > DCB-Leu. In terms of resolution the behavior is slightly different, just BTFMB-Leu and DCB-Leu are exchanged in the order. Compared to the other leucine derivatives DNB-Leu shows extraordinary high values for α and R. The retention time of the stronger retained *D* enantiomer is approximately four times higher than for the corresponding *D* enantiomer of DCB-Leu. Due to the negative mesomeric effect of the nitro groups the aromatic ring is a stronger π-acid compared to DCB-Leu and the other benzoyl-substituted leucines. This of course leads to the stronger interaction with the π-basic SO.

3.11.2. *N*-protected phenylalanine derivatives

Concerning *N*-protected phenylalanine derivatives the selectivity coefficient and resolution-value are strikingly increased for DNZ-Phe (α = 10.43 and R = 20.01). The same result was observed for DNB-Leu (see **chapter 3.11.1.**). The average α-value for all the other *N*-protected phenylalanine derivatives is about 8 times lower (α_{av} = 1.32, n = 6).

In **figure 3.21.** the selectivity coefficients and resolution-values for the *N*-protected phenylalanine derivatives are shown with the exception of DNZ-Phe. The highest resolution was observed for Bz-Phe, followed by Ac-Phe. These two compounds are both baseline separated on column 6. In case of Ac-Phe - which is the smallest compound of the phenylalanine derivatives - no interaction with the SO is possible for the protecting group except hydrogen acceptation via the carbonyl group and of course hydrogen donation via the amido hydrogen. Switching from α-Phe to β-Phe derivatives resulted in a decrease in both selectivity and resolution.

Introducing benzyloxycarbonyl instead of benzoyl results in decreased selectivity and resolution. Hence the carbamate may be less interacting with the SO. The same result was observed for Bz-Leu and Z-Leu (see **chapter 3.11.1.**) This result indicates

that the distance between the center of chirality and the aromatic moiety of the *α*-amino acid derivative including flexibility and conformation are of great importance for optimal interaction. This conclusion was also drawn by Maier et al. [67].

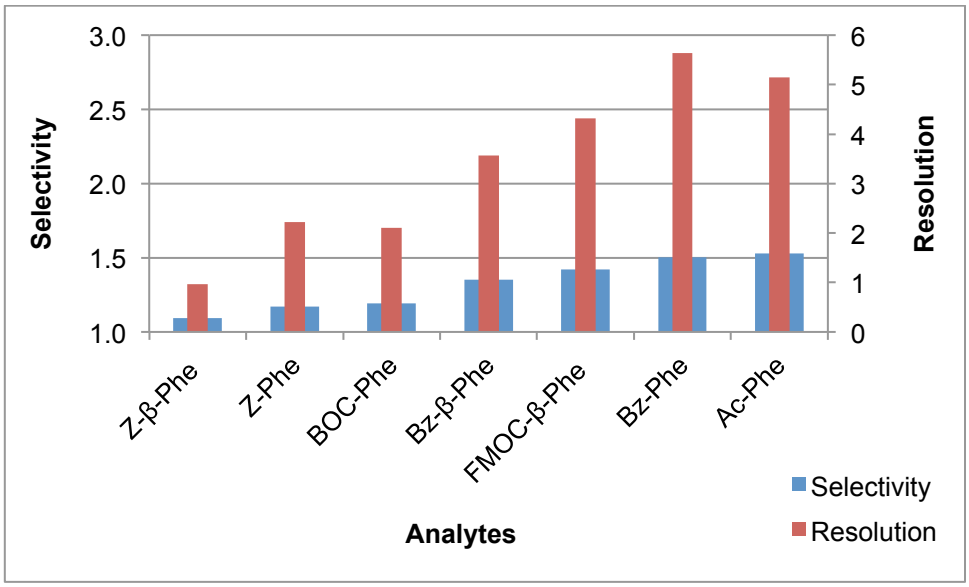

Figure 3.21.: Comparison of selectivity *α* and resolution *R* among *N*-protected phenylalanine derivatives; column 6: DHQD-type, 232 µmol/g.

3.11.3. *N*-protected amino sulfonic acids

In **figure 3.22.** the effect of substitution for three *N*-protected aminosulfonic acids is shown. All three of them are comparable according to selectivity ($1.10 \leq \alpha \leq 1.19$). The non-substituted Bz-ACHSA gives the lowest value for resolution ($R = 1.44$).
P-DML-ACHSA and P-DCL-ACHSA are sterically more demanding in comparison to Bz-ACHSA. In combination with the influence of the oxygen of the propargyloxy-substituent on the electron distribution this may result in a higher resolution for substituted Bz-ACHSA derivatives. Exchanging the methoxy-substituents by chlorine results in an increase of resolution.

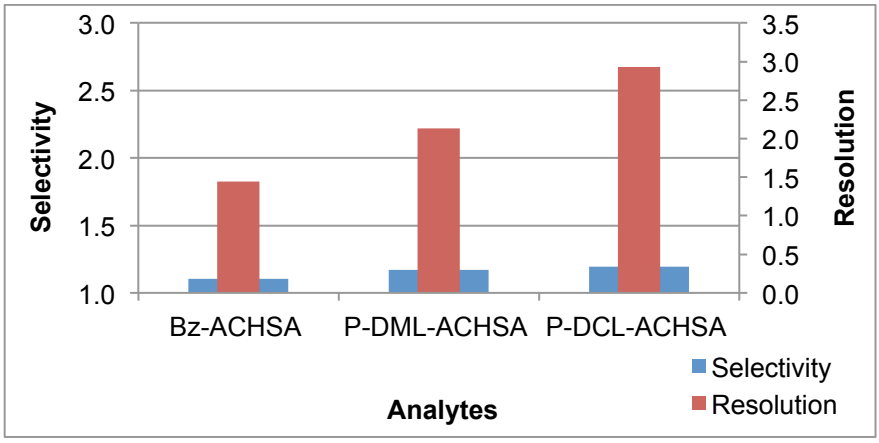

Figure 3.22.: Comparison of selectivity *α* and resolution *R* within the series of *N*-protected aminosulfonic acids; column 6: DHQD-type, 232 µmol/g.

3.11.4. *N*-protected aminophosphonates

For structure comparative studies a number of different aminophosphonate derivatives was also employed. In **figure 3.23.** the summarized results in terms of selectivity coefficients and resolution are shown for column 6 (DHQD-type, 232 µmol/g).

One can clearly see that PI-2-4-3 (*N*-FMOC-protected *α*-phenylphosphonic acid methyl ester) shows the largest value both for selectivity and resolution. Both values are slightly decreased when exchanging the *α*-phenyl by a butyl residue as it was observed for PI-2-15-1. Exchanging the *α*-phenyl by a benzyl residue results in a drop of the two chromatographic parameters.

The only structural difference between PI-2-15-1 and PI-2-87-1 is the protecting group (Z in case of PI-2-87-2 instead of FMOC). In this case the FMOC-protected aminophosphonate shows much higher resolution and a selectivity coefficient that is almost a factor of 1.4 higher in comparison to Z-protection. Exchanging the methyl ester by a benzyl ester in case of PI-2-87-1 and PI-3-67-1, respectively, slightly increases the resolution, wherein the *α*-values are almost equal. Hydrolysis of the ester results in compound PI-2-56-2. There was just a very slight separation observed for the free phosphonic acid derivative compared to the methyl ester. The shorter the backbone alkyl chain, the higher selectivity was observed, although there is almost no difference between ethyl and propyl side chain for compound PI-2-38-1 and PI-2-34-1.

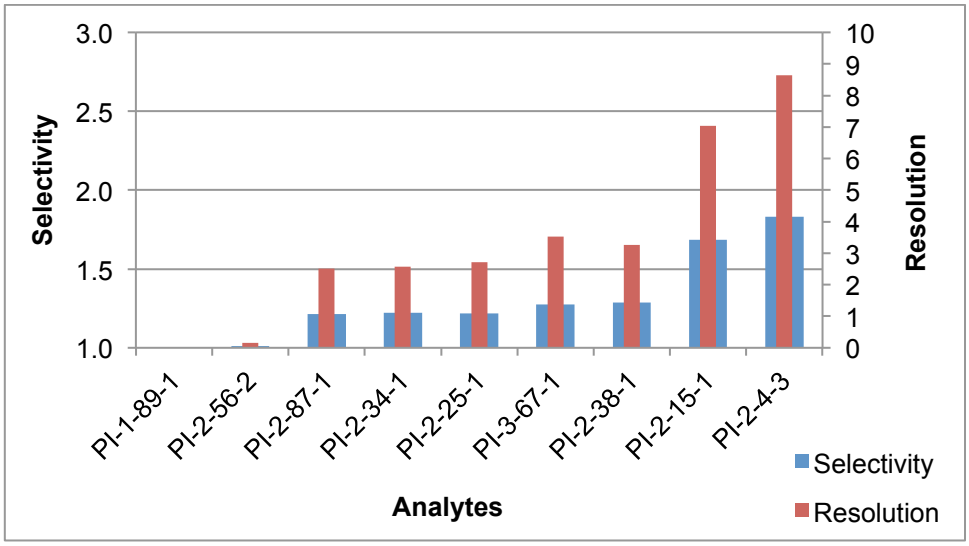

Figure 3.23.: Comparison of selectivity *α* and resolution *R* among *N*-protected aminophosphonates; column 6: DHQD-type, 232 µmol/g.

The aminophosphonate derivative PI-1-89-1 was not separated on column 6 (DHQD-type CSP). This compound could never be separated on DHQD-type CSPs (column 2, 4 and 6). Exactly the opposite was observed for DHQN-type CSPs (column 1, 3 and 5), where at least partial separation could be observed. On column 13 and 14, which are standard QN-AX and QD-AX CSPs for comparative purposes, compound PI-1-89-1 could be separated on both QN and QD type CSP.

3.11.5. FMOC-protected amino acids

Because of the larger number of FMOC-protected amino acids present in the set of SAs, it is also possible to compare them with respect to the amino acid residue. Lämmerhofer et al. observed that these aryloxycarbonyl as well as the alkyloxycarbonyl amino acid derivatives behave in a similar way to their amido congeners because they are also capable of hydrogen donation and acceptation [49]. Since the elution order is the same when comparing DHQN and DHQD-type CSPs, an analogous mechanism for chiral separation can be assumed.

No separation was observed for FMOC-Gln. The retention factor for the FMOC-Gln is k = 0.14, so almost no interaction with the SO was possible. Glutamine is an amino acid with a polar side chain, namely a primary amide. Hence a competitive hydrogen bonding of the primary amide group could be possible.

Separation could be possible with a different mobile phase composition, but this has not been investigated so far.

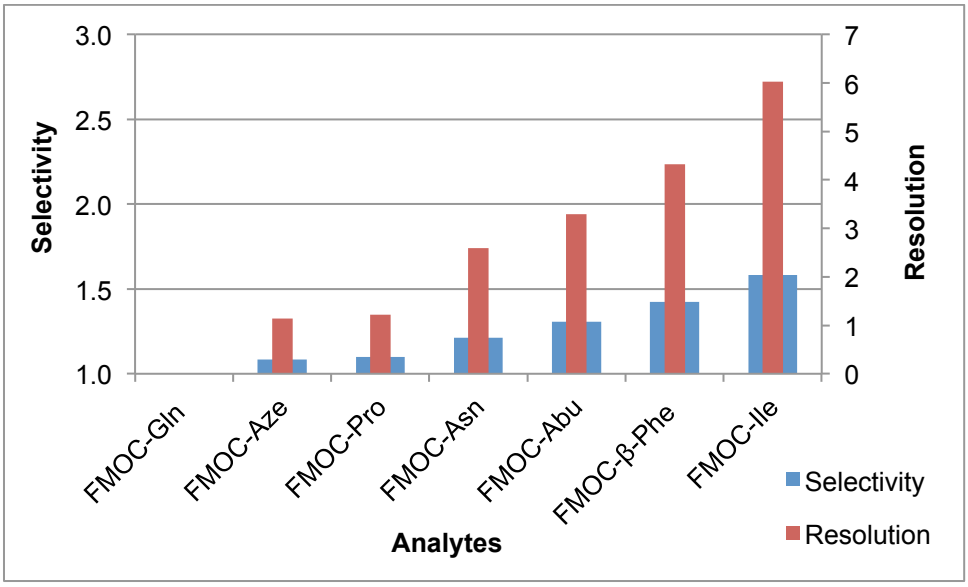

Figure 3.24.: Comparison of selectivity *α* and resolution *R* within the series of *N*-protected amino acids; column 6: DHQD-type, 232 µmol/g.

Interestingly, FMOC-Asn was partially separated on column 6. This observation cannot be explained without further experiments and mobile phase variations, because the behavior should be similar to FMOC-Gln (both amino acids contain a primary amide). When comparing FMOC-Aze and FMOC-Pro (both containing a heterocyclic ring consisting four or five atoms), one can observe no significant difference in terms of *α* and *R*.

3.12. Comparison of Columns with the same total amount of SO

Column 6, 7 and 12 do almost have the same total amount of immobilized SO per column (SO4, DHQD-type SO), but with different properties. The CSP in column 6 has a SO loading of 232 µmol/g (column dimensions: 150x4 mm ID), column 12 is a short 75x4 mm ID column with a SO loading of 490 µmol/g and column 7 is a homogenous physical mixture made prepared from the same material used for packing column 12 and pure AzP-Silica (column dimensions: 150x4 mm ID). All in all almost the same total amount of SO is in all three columns. In **figure 3.25.** a model for these three columns is shown.

When comparing all three columns with the same flow rate (1.0 mL/min), the retention times t_1 of the first eluted enantiomers are similar for most of the SAs, but retention time of column 6 is in most cases the longest (see **figure 3.26.**).

This result indicates that the overall retention is predominantly dependent on the total amount of SO per column.

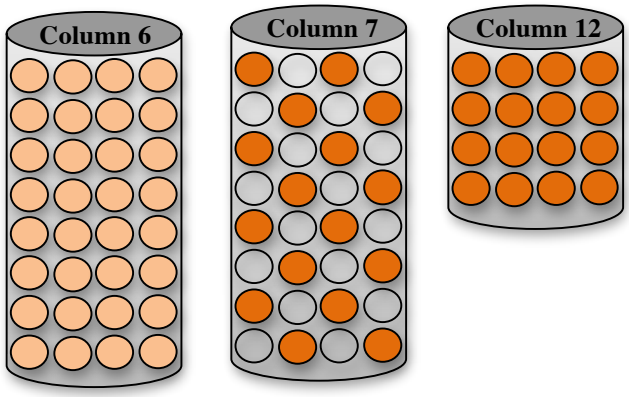

Figure 3.25.: Model for the compared columns in terms of SO density distribution and column dimensions; light orange: 232 µmol/g (DHQD-type SO4); dark orange: 490 µmol/g (DHQD-type SO4); colorless: AzP-Silica particles.

Column 7 and 12 behave more similar to each other compared to column 6, which behaves a bit different. For the aminosulfonic acids retention time t_1 is significantly higher, as well as for the aminophosphonates. The same results were observed for the retention times of the second eluted enantiomer (not shown here, for the data see **appendix**).

There was no separation observed for PFB-Leu and DNB-*N*-methyl leucine for columns 7 and 12. On the other hand, PFB-Leu was partially separated on column 6 (α = 1.09). The retention factors (see **figure 3.27.**) are comparable but slightly lower for most of the SAs for column 7 compared to column 6. This reflects the expectation. The CSP in column 7 is a physical mixture prepared from CSP4 and pure AzP-Silica to give an average SO density of 238 µmol/g. The distribution of the SO density is locally inhomogenous. **Figure 3.25.** can be seen as a model for the SO density distribution.

As one can imagine, the retention strength along the column is always the same for column 6 and 12 because of homogenous SO-concentration along the whole column.

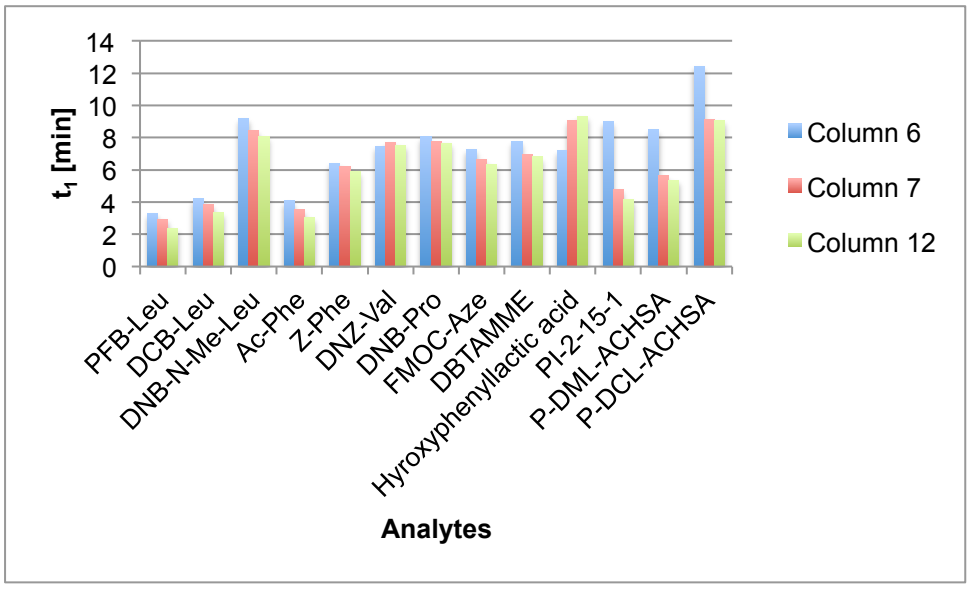

Figure 3.26.: Comparison of the retention times of the first eluted enantiomer; flow rate always 1.0 mL/min; column 6: DHQD-type, 232 µmol/g; column 7: DHQD-type, 238 µmol/g; column 12: DHQD-type, 490 µmol/g.

The different properties are also reflected in the selectivity coefficient alpha, the resolution *R* and the average number of theoretical separation plates N_{av}: For this comparative purpose the flow rates are different to ensure a fair comparison. The flow rate for the two 150 mm long columns is 1.0 mL/min in comparison to the half of the flow rate (0.5 mL/min) for the column with the half of the length (75 mm). The selectivity coefficients are comparable for the high loaded short column 12 and the physical mixture CSP in column 7 with the same total amount of SO (see **figure 3.28.**).

There was no separation observed for PFB-Leu and DNB-*N*-Me-Leu both for columns 7 and 12, as already mentioned above.

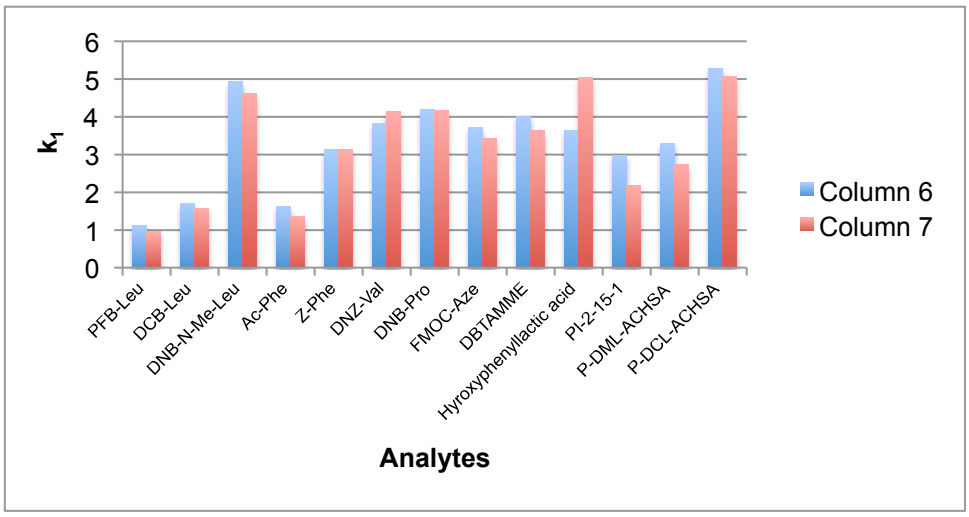

Figure 3.27.: Comparison of the retention factors k_1; flow rate for columns 6 and 7: 1.0 mL/min.; column 6: DHQD-type, 232 µmol/g; column 7: DHQD-type, 238 µmol/g.

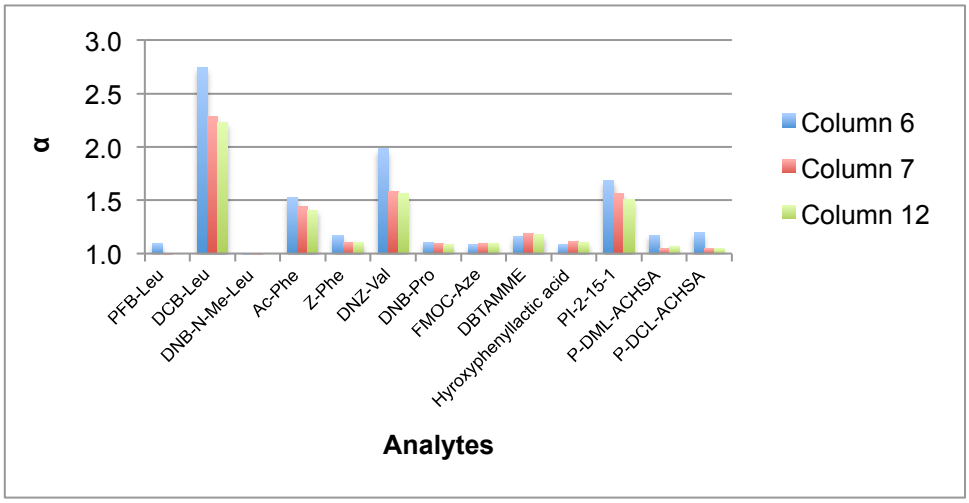

Figure 3.28.: Comparison of the selectivity coefficients; flow rate for columns 6 and 7 1.0 mL/min, for column 12 0.5 mL/min.; column 6: DHQD-type, 232 µmol/g; column 7: DHQD-type, 238 µmol/g; column 12: DHQD-type, 490 µmol/g.

The resolution *R* for column 6 is always higher compared to 7 and 12 (see **figure 3.29.**). Columns 7 and 12 are – in terms of resolution – more similar. This leads to the conclusion that a high-loaded CSP like in the case of the 75x4 mm ID column 12 (490 µmol/g) is not as efficient as a middle-loaded CSP like in the case of column 6 (150x4 mm ID, 232 µmol/g). They both include the same total amount of SO, but the average efficiency is almost doubled (factor of 1.9) for column 6 in comparison to column 12. The difference between column 6 and 7 is even higher (average factor of 2.3 in terms of resolution).

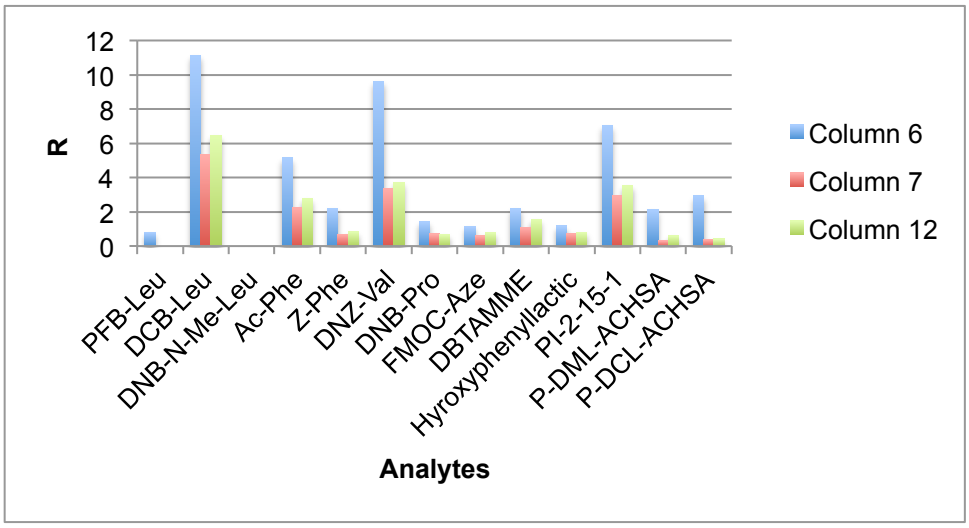

Figure 3.29.: Comparison of the resolution; flow rate for columns 6 and 7 1.0 mL/min, for column 12 0.5 mL/min.; column 6: DHQD-type, 232 µmol/g; column 7: DHQD-type, 238 µmol/g; column 12: DHQD-type, 490 µmol/g.

The average numbers of theoretical plates N_{av} are compared in **figure 3.30.**. One can clearly see that in the case of column 6 the number of theoretical plates is higher in comparison to the two other columns. Columns 7 and 12 do have almost the same number of theoretical plates (N_{av} = 1473 and 1443, n = 20, all measured compounds). Compared to column 6 N_{av} (4691, n = 67, all measured compounds) is decreased for both of them by an average factor of 3.2.

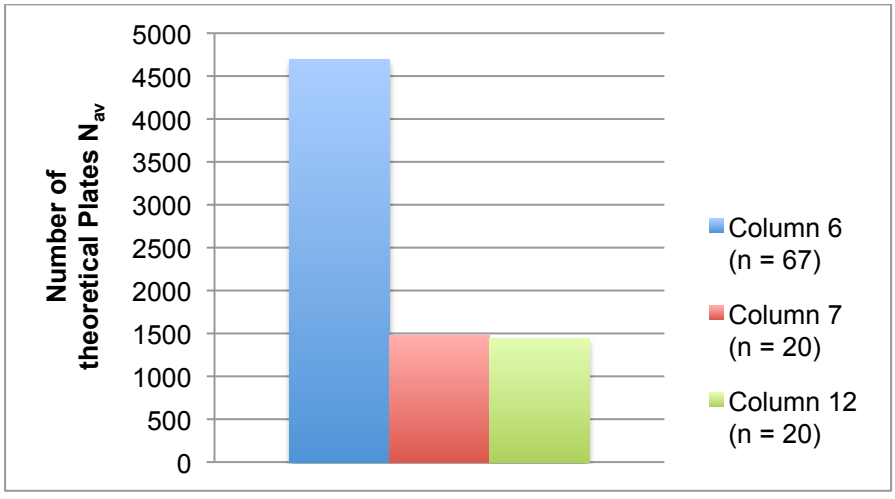

Figure 3.30.: Comparison of average number of theoretical plates N_{av}; flow rate for columns 6 and 7 1.0 mL/min, for column 12 0.5 mL/min.; column 6: DHQD-type, 232 µmol/g; column 7: DHQD-type, 238 µmol/g; column 12: DHQD-type, 490 µmol/g.

3.13. Effects of different SO loading

Because a large number of CSPs with different SO loading was prepared, it was possible to determine the effect of SO loading with regards to retention, selectivity, resolution and efficiency. The columns used for this study were all packed with DHQD-type CSPs based on the same SO (SO4), but with different SO density on the surface. In **table 3.3.** a summary of all used columns for determining the effects of different SO loading including their properties is given.

Table 3.3.: Summary of all used columns for determining the effects of different SO loading (all SOs DHQD-type).

Column Number	CSP Number	Type of SO	Dimensions of the columns	Dimensions of Silica	SO loading [µmol/g]
4	CSP4	SO4	150x4 mm ID	5 µm, 120 Å	490
8	CSP8				314
6	CSP6				232
9	CSP9				150

Of course retention time and *k*-values are increasing with higher SO loading as depicted in **figure 3.31.** (see below). An almost linear relationship for example was observed for the aminosulfonic acid derivative P-DML-ACHSA. CSP8 with 314 µmol/g slightly differs from the other CSPs in terms of *k*-values.

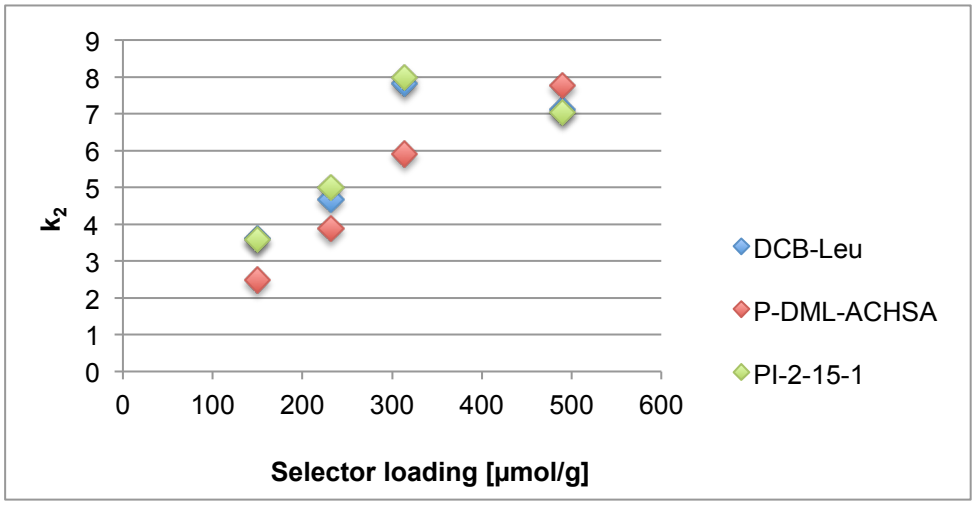

Figure 3.31.: Dependency of k_2 of the SO loading (DHQD-type).

In **figure 3.32.** a more detailed diagram of the k_2 dependency on the SO loading for *N*-protected amino acid derivatives is shown. The overall effect of increasing retention factors among higher SO loading was observed for every single acidic SA, including *N*-protected aminosulfonic acids, carboxylic acids and *N*-protected aminophosphonates.

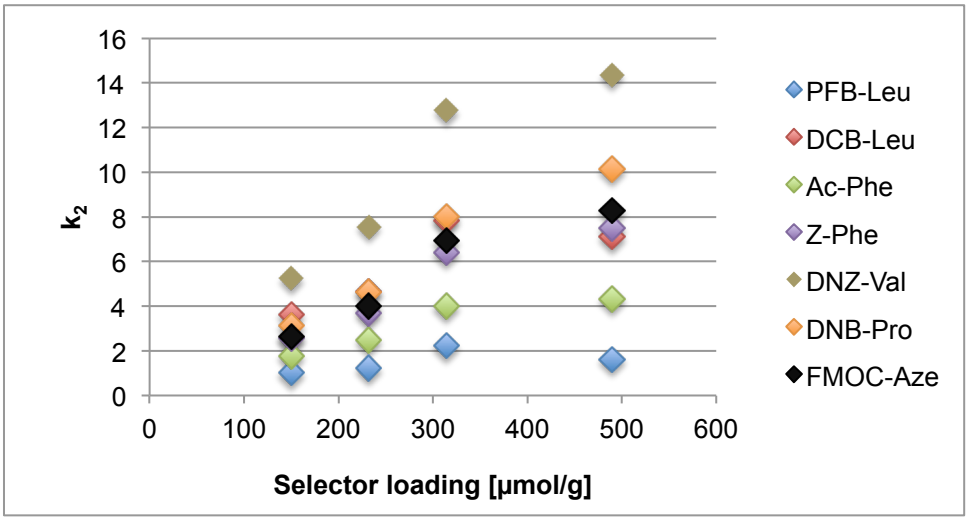

Figure 3.32.: Dependency of k_2 of the SO loading (DHQD-type) shown for a series of *N*-protected amino acid derivatives.

A different behavior was observed for the selectivity coefficient alpha. The selectivity drops with increasing SO loading for every single acidic SA. This trend is close to linear behavior.

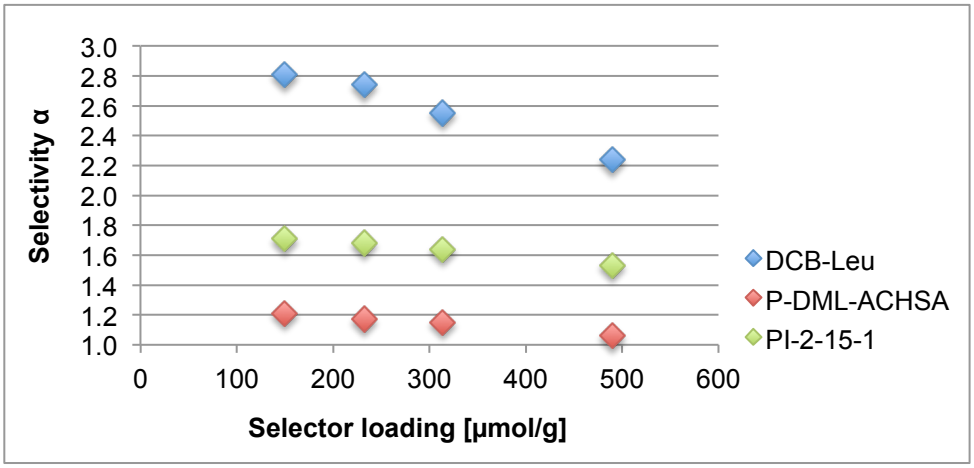

Figure 3.33.: Dependency of the selectivity of the SO loading (DHQD-type).

The corresponding resolution has a maximum value at a SO loading of 314 µmol/g, higher loading results in rapid loss of resolution. This result indicates a blockage of the silica pores due to high SO loading which leads to the limited conformational freedom of the immobilized SOs, and thus hindered interactions with SAs. Before this threshold of about 310 µmol/g the resolution-values increase with increasing SO loading. A SO concentration of about 310 µmol/g seems to be an optimal coverage.

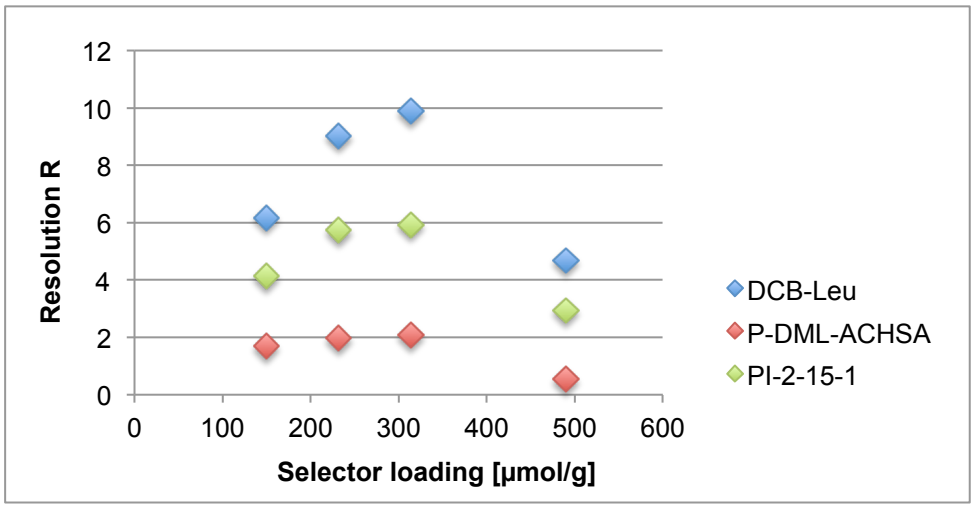

Figure 3.34.: Dependency of the resolution of the SO loading (DHQD-type).

Exactly the same behavior was observed for the resolution-dependent number of theoretical plates for separation. After exceeding the limit value at 314 µmol/g *N* drops rapidly and efficiency is actually decreased below the value obtained for a SO loading of 150 µmol/g.

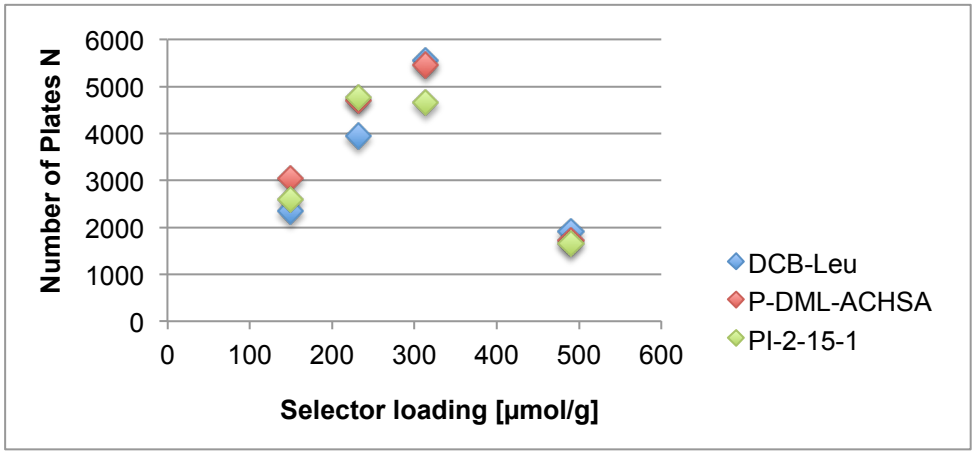

Figure 3.35.: Dependency of the number of theoretical plates of the SO loading (DHQD-type).

Since a lower loading also results in higher selectivity values and lower retention times, a quite low selector-loaded CSP (e.g. 150 µmol/g) has to be preferred relative to a CSP with saturated SO density, which of course is more economic as well.

3.14. Comparison of Column 8 to QD-AX

Regarding the effects of different SO loading column 8 is well suited for a comparison to the standard QD-AX CSP packed column 14. Both these columns are quinidine derived CSPs and contain a similar amount of immobilized SO per gram silica (column 8 314 µmol/g; column 14 app. 340 µmol/g). The QD-AX SO has been immobilized via radical thiol alkene addition using the vinyl residue at position 3 of the quinuclidine ring as immobilizing anchor. The two CSPs are therefore not only different in the structure of the SO, but also immobilized via different immobilization strategies at different positions, because CSP8 in column 8 has been immobilized via Huisgen alkyne-azide click chemistry with the propargyl moiety of the aromatic linker as an immobilizing anchor. For the structure of the CSP in column 14 see **figure 3.1.**, the structure of CSP8 is shown in the experimental part of the thesis.

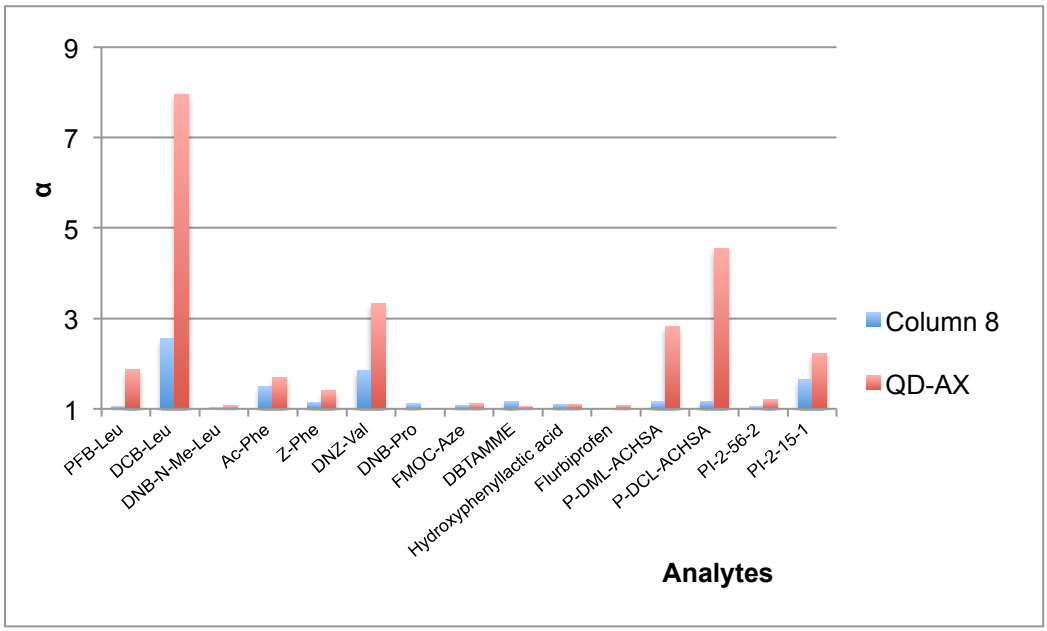

Figure 3.36.: Comparison of the selectivities of column 8 and column 14; column 8: DHQD-type, 314 µmol/g; column 14: QD-AX type, app. 340 µmol/g.

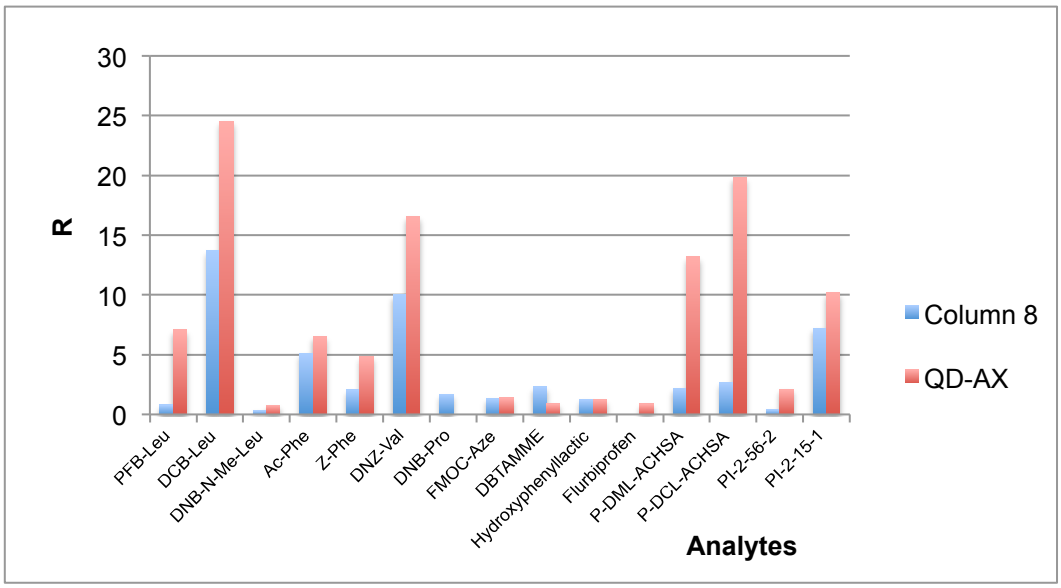

Figure 3.37.: Comparison of the resolution-values of column 8 and column 14; column 8: DHQD-type, 314 µmol/g; column 14: QD-AX type, app. 340 µmol/g.

First of all, the two columns differ in the general separation capability for chiral acidic compounds. DNB-Pro was not separated on QD-AX, whereas flurbiprofen was not separated on column 8 under the given mobile phase composition. All the other samples shown in **figure 3.36.** and **3.37.** were at least partially separated.
The alpha-values obtained with QD-AX are generally higher compared to column 8. The difference for example for DCB-Leu is striking, also for the two aminosulfonic acids P-DML-ACHSA and P-DCL-ACHSA. The same results were observed in terms of resolution. Solvophobic effects and different binding increments in terms of relative strength and position could make the difference in this case.
One exception is DBTAMME (dibenzoyltartaric acid monomethyl ester), where the behavior is exactly the opposite.

3.15. Loading Study

The loadability of the highest-loaded CSP in terms of a possible preparative application was another topic for the evaluation. Therefore an SA that meets several criteria has to be used:

- Solubility in methanol or mobile phase should be high.
- Retention time should be short.

- Selectivity coefficient and resolution-value should be reasonably large.
- The SA must be available in larger quantities than analytical amounts.

This loading study was performed with racemic Ac-Phe as an SA of choice. Ac-Phe was not the SA with the best prerequisites, but it was a compromise between all the criteria. In order to avoid long retention time a 75x4 mm ID column with 490 µmol/g SO loading (CSP4, column 12) and a SA solution with a concentration of 100 mg/mL in MeOH were used. Further chromatographic conditions that were used were 0.5 mL/min flow rate, 15 min run time and a detection wavelength of 270 nm.

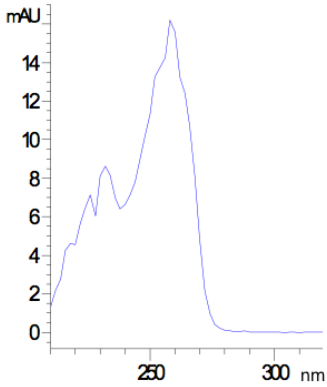

Figure 3.38.: Absorption spectra of Ac-Phe.

The wavelength was chosen higher than the usual 254 nm for screening, because sensitivity is lower and therefore the detector does not reach its limit at higher concentrations. In **figure 3.38.** an absorption spectrum of Ac-Phe from 210 to 310 nm is shown. As an initial mobile phase the same phase composition as used for screening was applied (MeOH/AcOH/NH_4OAc 99/1/0.25 v/v/w).

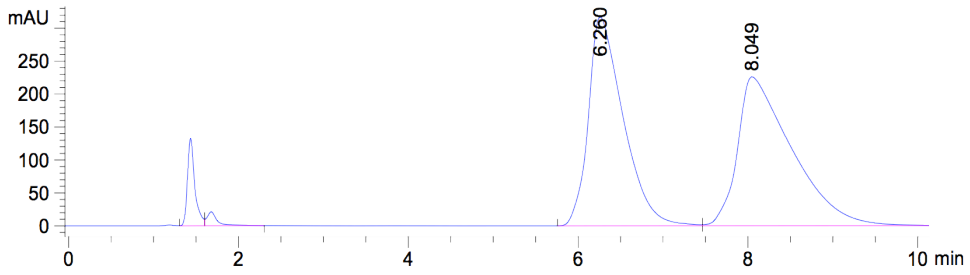

Figure 3.39.: Chromatogram for Ac-Phe (α = 1.37); column 12 (75x4 mm ID, 490 µmol/g, DHQD-type CSP); injection volume: 5 µL (= 0.5 mg); sample concentration: 100 mg/mL Ac-Phe in MeOH; flow rate: 0.5 mL/min; detection wavelength: 270 nm; mobile phase composition: MeOH/AcOH/NH_4OAc 99/1/0.25 (v/v/w); temperature: 25°C.

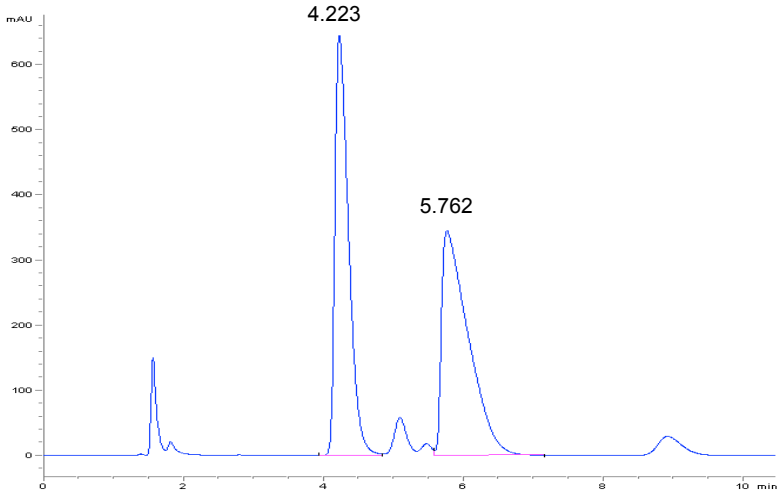

Figure 3.40.: Chromatogram for Ac-Phe (α = 1.58); column 15 (75x4 mm ID, app. 340 µmol/g, QD-AX type CSP); injection volume: 5 µL (= 0.5 mg); sample concentration: 100 mg/mL Ac-Phe in MeOH; flow rate: 0.5 mL/min; detection wavelength: 270 nm; mobile phase composition: MeOH/AcOH/NH_4OAc 99/1/0.25 (v/v/w); temperature: 25°C.

In **figure 3.39.** one chromatogram for a 5 µL injection volume (0.5 mg total amount of injected SA) is shown. Retention time is 6.26 min for the first eluted enantiomer (*L*) and 8.05 min for the second eluted enantiomer (*D*) at a void time of 1.46 min; selectivity coefficient of 1.37 and a resolution of 1.96. Both enantiomers are baseline separated according to the chromatogram.

For comparative purposes another loading study was carried out with a 75x4 mm ID standard QD-AX column (column 15). For a better comparison of the two columns, retention time for QD-AX had to be adjusted and therefore extended, because it was not the same as for column 12 (see **figure 3.40.**). It was easily possible to adjust the k_2-value via modification of the buffer concentration (counter-ion concentration) by diluting the standard mobile phase with pure MeOH [67]. This behavior follows the well-established stoichiometric displacement model [13, 78].

Alternative possibilities would be to vary the flow rate, pH-value, temperature and the content of organic modifier like ACN. In previous studies by Mandl et al. it has been shown that according to an anion-exchange mechanism the retention times are decreasing with increasing buffer salt concentration in the mobile phase [50]. However, enantioselectivity remains almost constant and therefore it is not significantly affected by the buffer concentration [13].

Table 3.4.: Adjustment of k_2 by variation of the buffer concentration.

k_2	log(k_2)	Bufferconc. [%]	log(1/Bufferconc.)
5.762	0.761	0.250	0.602
7.706	0.887	0.125	0.903
9.841	0.993	0.063	1.204
8.049	0.906	0.107	0.971

In **figure 3.41.** and **table 3.4.** the results for the adjustment of the buffer concentration are shown. Using the linear equation it was easily possible to adjust the k_2-value for column 15 (QD-AX type) without a significant loss of enantioselectivity. In reality the adjusted k_2-value was slightly higher than the calculated k_2-value, because the mobile phase was freshly prepared and not diluted from the concentrated version used for the mobile phase variation.

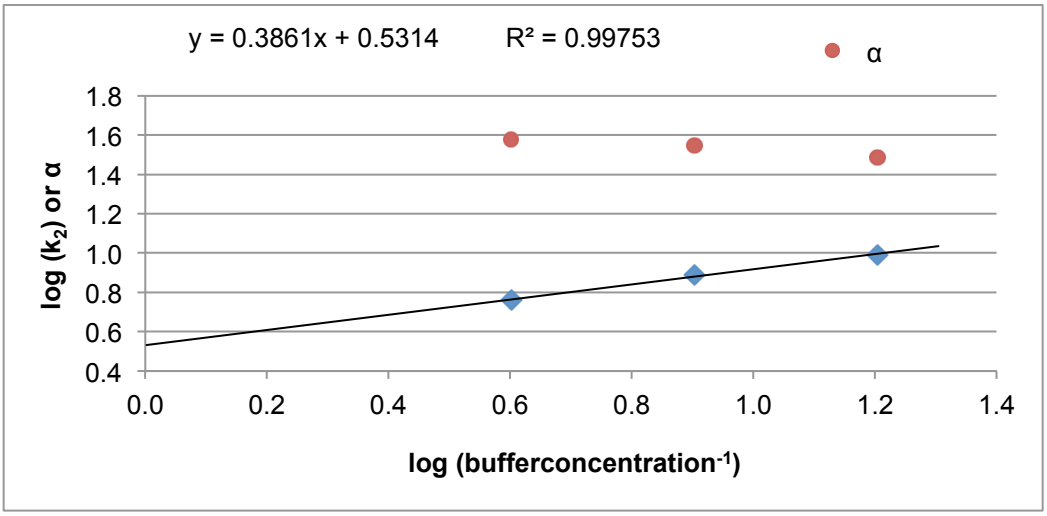

Figure 3.41.: Linear correlation between log(k_2) vs. log(bufferconcentration^{-1}); column 15: QD-AX type, app. 340 µmol/g.

In **figure 3.42.** one can see the overlaid chromatograms for column 12. The retention is shifted to lower retention times the higher the amount of injected sample is, because the higher retained enantiomer (Ac-*D*-Phe) acts as a displacer for the lower retained enantiomer (Ac-*L*-Phe). Furthermore, overloading-effects of the column are involved in the retention.

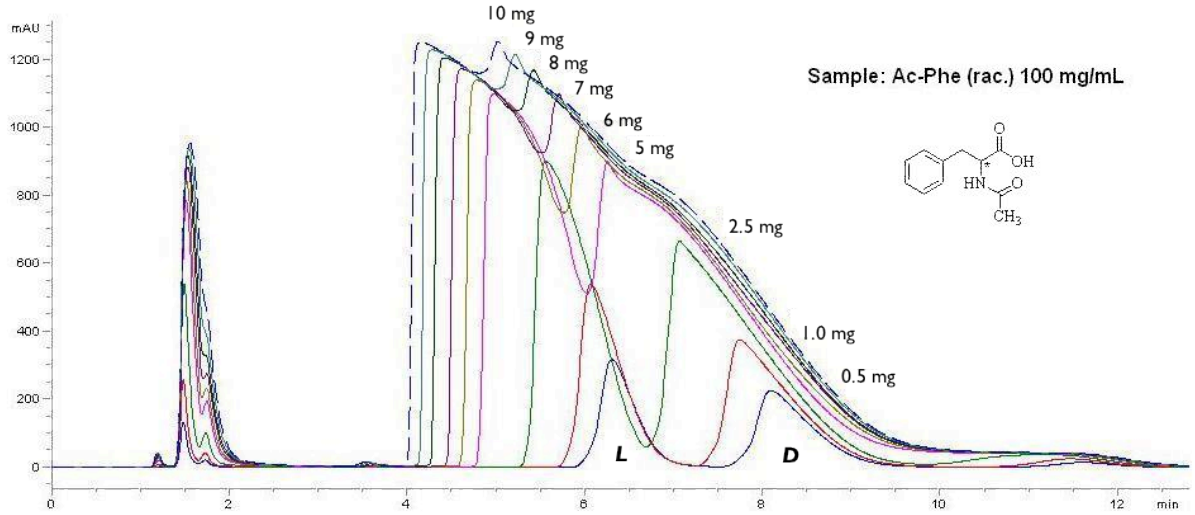

Figure 3.42.: Overlaid chromatograms for Ac-Phe; column 12 (75x4 mm ID, 490 µmol/g, DHQD-type CSP); injection volume: 5-100 µL (0.5-10 mg); sample concentration: 100 mg/mL Ac-Phe in MeOH; flow rate: 0.5 mL/min; detection wavelength: 270 nm; mobile phase composition: MeOH/AcOH/NH_4OAc 99/1/0.25 (v/v/w); temperature: 25°C.

The selectivity is almost constant (column 12 α_{av} = 1.36, n = 9; QD-AX α_{av} = 1.57, n = 12), as well as the end of the second peak at about 10 minutes. The resolution and plate numbers are of course decreasing rapidly with higher amount of injected sample (data not shown here, see **appendix**). In **figure 3.43.** the overlaid chromatograms for QD-AX column 15 are shown. One can clearly see that the sample contains impurities, which are retained exactly in between the two enantiomers of Ac-Phe. However, for a possible preparative purpose this would not be a problem because one can easily cut impurity-containing fractions out of the fractions with the pure enantiomer as the product.

With the assumption that approximately 0.7 g of CSP are packed in a 75x4 mm ID column, the calculated theoretical productivity for column 12 is about 0.4 kg pure enantiomer per kg CSP per day. For QD-AX the productivity is about 0.6 kg/kg/day, so 50% higher. Please note that the selectivity coefficient for the separation on QD-QX is higher in comparison to column 12 (see above), so therefore the productivity has to be better.

The calculated productivities are just approximate calculations for one mobile phase system. There are many parameters, which can be optimized to achieve higher productivities.

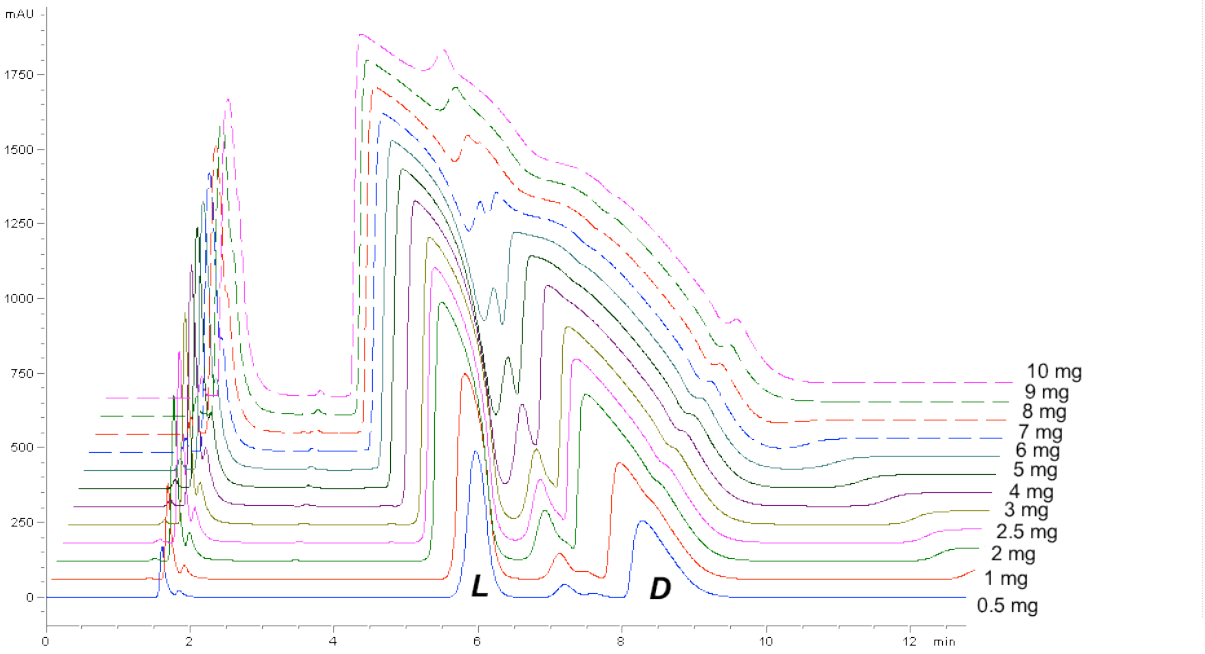

Figure 3.43.: Overlaid chromatograms for Ac-Phe; column 15 (75x4 mm ID, app. 340 µmol/g, QD-AX type CSP); injection volume: 5-100 µL (0.5-10 mg); sample concentration: 100 mg/mL Ac-Phe in MeOH; flow rate: 0.5 mL/min; detection wavelength: 270 nm; mobile phase composition: MeOH/AcOH/NH_4OAc 99.46/0.43/0.11 (v/v/w); temperature: 25°C.

4. Experimental Part

4.1. Materials and Methods

^{1}H-NMR and ^{13}C-NMR spectra were measured with a Bruker DRX 400 spectrometer (Karlsruhe, Germany) at 400 MHz and 100 MHz, respectively, at room temperature. Either $CDCl_3$ or CD_3OD (both 99.8%, Deutero GmbH, Kastellaun, Germany) were used as solvents and the solvent signals were used as reference signals. The raw data were processed with SpinWorks 2.5 software.

The IR-measurements were carried out on a Bruker Tensor 27 Diamond ATR FTIR spectrometer (Ettlingen, Germany) with Opus 4.2 software.

Mass spectrometric measurements of the selectors (SOs) were performed using a 4000 QqLIT mass spectrometer with an ESI ion source from Applied Biosystems (Foster City, USA). All mass spectrometric measurements were carried out in positive ionization mode. For data processing the software Analyst 1.5 was used. The mass spectrometer was coupled with a 1200 series HPLC system from Agilent Technologies (Santa Clara, USA). The chromatographic runs for LC/MS were done using reversed phase mode chromatography.

CHNS elemental analyses of the CSPs were operated on a EURO EA 3000 CHNS-O instrument from HEKAtech (Wegberg, Germany). Determination of the chlorine content of the CSPs was performed using potentiometric titration with a Mettler DL 21 titrator (Greifensee, Switzerland).

For thin layer chromatography TLC Silica gel 60 F_{254} from Merck was used. Flash column chromatography was carried out using Normasil 60 Silica Gel from VWR. Daisogel SP-120-5P from Daiso (Japan) was used as a basis for AzP-Silica and MP-Silica (both 5 µm, 120 Å). MP-Silica was prepared by modification and endcapping in house.

The solvents for synthesis were purchased from VWR, ROTH, DonauChem, Sigma-Aldrich, Merck and FLUKA. As reagents and catalysts the following chemicals were used: 3,5-dichloro-4-hydroxybenozic acid (97%, Sigma-Aldrich), allyl bromide (99%, Aldrich), propargyl bromide (80% in toluene, FLUKA), $(COCl)_2$ (98%, Aldrich), anhydrous DMF (99.8%, Sigma-Aldrich), NaN_3 (>99%, Aldrich), DHQN and DHQD.HCl (both >97%, Buchler), dibutyltin dilaurate (95%, Aldrich), AIBN (≥98%, Merck), p-toluenesulfonic acid monohydrate (98.5%, Sigma-Aldrich), 3-chloropropyl-

trimethoxysilane (97%, ABCR), tetrabutylammonium iodide (98%, Merck), diisopropylethylamine (98%, FLUKA), CuI (98%, Aldrich), EDTA disodium salt (99%, FLUKA) and propargyl alcohol (99%, AcrosOrganics).

As mobile phase compounds the following chemicals were used: MeOH (HPLC grade quality, 99.8%, VWR), AcOH (≥ 99%, Sigma-Aldrich) and NH_4OAc (≥ 97%, p.a., Fluka).

4.2. Synthesis of Linker 1

4-Allyloxy-3,5-dichlorobenzoic acid allyl ester (**2a**)

33.88 g of 3,5-dichloro-4-hydroxybenzoic acid **1** (158.8 mmol), 32 mL allyl bromide (369.8 mmol) and 64.85 g of potassium carbonate (447.5 mmol) were suspended in 300 mL of acetone and refluxed for 16 h. The orange suspension was cooled to room temperature and poured into 600 mL of water. After extraction with EtOAc (3x100 mL), the combined organic phases were washed with 100 mL of H_2O and 50 mL of saturated aqueous NaCl solution. The combined organic solution was dried with anhydrous $MgSO_4$, filtered and evaporated under reduced pressure. The obtained orange crude 4-allyloxy-3,5-dichlorobenzoic acid allyl ester was then purified by flash column chromatography on silica (250 g of silica, PE/EtOAc 20:1). The fractions with pure intermediate (control on TLC with the same mobile phase as used for flash column chromatography) were collected, filtered and evaporated under reduced pressure.

Yield: 40.55 g (141.2 mmol, 89%) of a colorless transparent oil.

^{1}H-NMR [CD_3OD]: δ = 7.87 (s, 2H), 6.03 (m, 1H), 5.94 (m, 1H), 5.32 (m, 2H), 5.19 (m, 2H), 4.72 (m, 2H), 4.54 (m, 2H).

^{13}C-NMR [CD_3OD]: δ = 172.6 (C=O), 154.1 (C_{ar}-O), 134.7 (C_{ar}Cl), 134.3 (C_{ar}H), 131.6 (CH), 131.6 (CH), 130.4 (C_{ar}), 120.7 (CH_2=), 120.4 (CH_2=), 76.3 (CH_2), 68.0 (CH_2).

IR: 3074 cm^{-1} (v=CH_2), 1719 cm^{-1} (vC=O).

4-Allyloxy-3,5-dichlorobenzoic acid (**3a**)

The 4-allyloxy-3,5-dichlorobenzoic acid allyl ester **2a** (40.55 g, 141.2 mmol) was diluted with 60 mL of EtOH and a solution of 12.15 g NaOH (303.8 mmol) in 60 mL H_2O was added. The reaction mixture was refluxed for 1 h. After cooling to 0°C the

orange-brown solution was diluted with 30 mL EtOH and 50 mL of H_2O. After acidification with concentrated HCl to pH~2 the 4-allyloxy-3,5-dichlorobenzoic acid **3a** immediately precipitated as a white solid. The suspension was filtered, the filtration cake was washed with cold H_2O (2x100 mL) and afterwards dried under reduced pressure at 60°C for 48 h.

Yield: 34.80 g (140.9 mmol, quantitative yield) of a white solid.

^{1}H-NMR [CD_3OD]: δ = 7.97 (s, 2H), 6.15 (m, 1H), 5.35 (dd, 2H), 4.89 (s, 1H), 4.64 (d, 2H).

^{13}C-NMR [CD_3OD]: δ = 167.7 (C=O), 156.5 (C_{ar}-O), 134.5 (C_{ar}H), 131.8 (CH), 131.3 (C_{ar}Cl), 130.0 (C_{ar}), 119.7 (CH_2=), 76.0 (CH_2).

IR: 3077 cm^{-1} (v=CH_2), 1690 cm^{-1} (vC=O).

4-Allyloxy-3,5-dichlorobenzoyl chloride (**4a**)

Dry 4-allyloxy-3,5-dichlorobenzoic acid **3a** (10.83 g, 43.8 mmol) was slowly suspended in 50 mL of $(COCl)_2$ and four drops of dry DMF as a catalyst were added slowly. The suspension was refluxed for 1 h while it turned into an orange clear solution with a small amount of brown precipitate. The main part of unreacted oxalyl chloride was distilled off and 70 mL of petroleum ether (PE) were added to the reaction mixture together with a spatula tip of activated carbon (app. 200 mg) for adsorption of side products and impurities. After refluxing for three min the still boiling reaction mixture was filtered and evaporated under reduced pressure. No further purification was carried out. Characterization of the product by NMR and IR spectroscopy was not carried out, because the product is not very stable and therefore it was directly converted into the corresponding acyl azide.

Yield: 11.04 g (41.6 mmol, 95%) of an orange-brown liquid acyl halide.

4-Allyloxy-3,5-dichlorobenzoyl azide (**5a**)

The acyl halide **4a** (11.04 g, 41.6 mmol) was dissolved in 70 mL of cold acetone and cooled to 0°C. A solution of 12.55 g NaN_3 (193.0 mmol) in 40 mL of H_2O was then added dropwise to the acyl halide solution under vigorous stirring during 1 h at 0°C. After a while a white precipitate appeared in the red-brown solution. The reaction mixture was then diluted with 100 mL of water and extracted with EtOAc (3x75 mL). The combined organic phases were washed with 30 mL of saturated aqueous NaCl

solution, dried with $MgSO_4$, filtered and evaporated under reduced pressure at room temperature. No further purification was carried out.

Yield: 9.83 g (36.1 mmol, 87%) of an orange-brown oil.

^{1}H-NMR [CD_3OD]: δ = 7.88 (d, 2H), 6.05 (m, 1H), 5.35 (d, 1H), 5.23 (d, 1H), 4.57 (d, 2H).

^{13}C-NMR [CD_3OD]: δ = 170.4 (C=O), 156.2 (C_{ar}-O), 132.8 (C_{ar}H), 130.6 (C_{ar}Cl), 130.4 (CH), 127.9 (C_{ar}), 119.9 (CH_2=), 75.1 (CH_2).

IR: 3073 cm^{-1} (v=CH_2), 2162 cm^{-1} (vN_3), 1686 cm^{-1} (vC=O).

4-Allyloxy-3,5-dichlorophenylisocyanate (**L1**)

The last step of the synthesis of **L1** was the formation of isocyanate via Curtius-rearrangement of the acyl azide. The acyl azide **5a** (9.83 g, 36.1 mmol) was dissolved in 100 mL of azeotropically dried toluene and refluxed for 3h. Emerging nitrogen indicated the successful rearrangement. After 3 h no nitrogen bubbles were visible in the bubble counter, so the reaction was completed. After evaporation of the solvent under reduced pressure, the transparent liquid isocyanate **L1** was obtained by vacuum distillation (boiling point: 99°C at 0.10 mbar). The purified liquid product was stored in the freezer with air-exclusion, because the isocyanate is highly water sensitive.

Yield: 7.22 g (29.6 mmol, 82%) of a colorless liquid **L1**.

^{1}H-NMR [$CDCl_3$]: δ = 6.90 (s, 2H), 5.97 (m, 1H), 5.20 (dd, 2H), 4.39 (d, 2H).

^{13}C-NMR [$CDCl_3$]: δ = 149.7 (C_{ar}-O), 133.0 (CH), 130.6 (C_{ar}Cl), 130.5 (C_{ar}), 125.4 (C_{ar}H), 119.6 (CH_2=), 74.9 (CH_2).

IR: 2250 cm^{-1} (vN=C=O).

4.3. Synthesis of Linker 2

3,5-Dichloro-4-propargyloxybenzoic acid propargyl ester (**2b**)

7.29 g of 3,5-dichloro-4-hydroxybenzoic acid **1** (34.2 mmol), 15.35 mL of propargyl bromide (80% in toluene, 118.7 mmol) and 8.35 g of potassium carbonate (60.4 mmol) were suspended in 40 mL of DMF and heated up to 60°C for 18 h. The orange-brown suspension was cooled to room temperature and poured into 150 mL of water. After extraction with EtOAc (3x75 mL), the combined organic phases were washed with 50 mL of H_2O and 30 mL of saturated aqueous NaCl solution. The

combined organic solution was dried with $MgSO_4$, filtered and evaporated under reduced pressure. The obtained orange-brown solid crude product was then purified by flash column chromatography on silica (150 g of silica, CH_2Cl_2 as a mobile phase for flash column chromatography and fraction control on TLC). The fractions with pure intermediate were collected, filtered and evaporated under reduced pressure.
Yield: 9.23 g (32.6 mmol, 95%) of a white solid.
^{1}H-NMR [$CDCl_3$]: δ = 8.02 (s, 2H), 4.89 (dd, 4H), 2.54 (t, 2H).
^{13}C-NMR [$CDCl_3$]: δ = 163.7 (C=O), 154.5 (C_{ar}-O), 130.8 (C_{ar}Cl), 130.7 (C_{ar}H), 127.5 (C_{ar}), 77.7 (C_4), 76.0 (CH), 61.0 (CH_2), 53.5 (CH_2).
IR: 3298 cm^{-1} (v≡CH), 3257 cm^{-1} (v≡CH), 2125 cm^{-1} (vC≡C), 1710 cm^{-1} (vC=O).

3,5-Dichloro-4-propargyloxybenzoic acid (**3b**)

The 3,5-dichloro-4-propargyloxybenzoic acid propargyl ester **2b** (9.23 g, 32.6 mmol) was dissolved in 70 mL of EtOH and a solution of 2.94 g NaOH (73.5 mmol) in 40 mL H_2O was added. The reaction mixture was refluxed for 1 h. The yellowish clear solution was diluted with 20 mL of EtOH and 20 mL of H_2O and cooled down to 0°C with an ice-bath. After acidification with concentrated HCl to pH~2, the 3,5-dichloro-4-propargyloxybenzoic acid immediately precipitated as a white solid. The suspension was filtered and the filtration cake was washed with 2x100 mL of cold H_2O and afterwards dried under reduced pressure at 60°C for 48 h.
Yield: 7.30 g (29.8 mmol, 91%) of a white solid.
^{1}H-NMR [CD_3OD+$CDCl_3$]: δ = 7.97 (s, 2H), 4.85 (d, 2H), 2.79 (t, 1H).
^{13}C-NMR [CD_3OD+$CDCl_3$]: δ = 166.2 (C=O), 153.9 (C_{ar}-O), 130.6 (C_{ar}H), 130.3 (C_{ar}Cl), 129.0 (C_{ar}), 78.2 (CH), 77.9 (C_4), 60.9 (CH_2).
IR: 3294 cm^{-1} (v≡CH), 2131cm^{-1} (vC≡C), 1698 cm^{-1} (vC=O).

3,5-Dichloro-4-propargyloxybenzoyl chloride (**4b**)

7.30 g of the acid **3b** (29.8 mmol) were slowly suspended in 50 mL of $(COCl)_2$ at 0°C and four drops of dry DMF as a catalyst were added slowly. The suspension was stirred at 0°C for 15 min and then heated up to 30°C for 45 min. The suspension turned into a yellowish clear solution with little brown drops. The bulk of unreacted oxalyl chloride was then distilled off and 120 mL of PE were added to the reaction mixture together with a spatula tip of activated carbon (app. 200 mg) for adsorption of side products and impurities. After refluxing for 3 min the still boiling reaction

mixture was filtered and evaporated under reduced pressure. No further purification was carried out. Characterization of the product by NMR and IR spectroscopy was not carried out, because the product is not very stable. The acyl chloride was then directly converted into acyl azide.
Yield: 7.16 g (27.2 mmol, 91%) of a slightly yellowish solid acyl halide.

3,5-Dichloro-4-propargyloxybenzoyl azide (**5b**)

7.16 g of the acyl chloride **4b** (27.2 mmol) were dissolved in 70 mL of cold acetone and cooled to 0°C with an ice-bath. A solution of 5.48 g NaN_3 (84.3 mmol) in 30 mL of H_2O was then added dropwise to the acyl halide solution under vigorous stirring during 1 h at 0°C. After a while a voluminous white precipitate appeared in the orange solution. The precipitate was filtered and washed with cold H_2O (2x50 mL). For an effective drying the filtration cake was dissolved in 150 mL of EtOAc and the organic solution was washed with 20 mL of H_2O, 20 mL of saturated aqueous NaCl solution and afterwards dried with anhydrous $MgSO_4$. Evaporation of the solvent and drying under vacuum at room temperature yielded a fully dry product.
Yield: 6.43 g (23.8 mmol, 88%) of a white solid.
^{1}H-NMR [$CDCl_3$]: δ = 7.91 (s, 2H), 4.81 (d, 2H), 2.47 (t, 1H).
^{13}C-NMR [$CDCl_3$]: δ = 170.3 (C=O), 155.2 (C_{ar}-O), 130.9 (C_{ar}Cl), 130.4 (C_{ar}H), 128.6 (C_{ar}), 77.7 (CH), 77.0 (C_4), 61.1 (CH_2).
IR: 3297 cm^{-1} (v≡CH), 2166 cm^{-1} (vN_3), 1686 cm^{-1} (vC=O).

3,5-Dichloro-4-propargyloxyphenylisocyanate (**L2**)

5.21 g of the acyl azide **5b** (19.3 mmol) were dissolved in 200 mL of azeotropically dried toluene and refluxed for 3 h. After evaporation of the solvent under reduced pressure a white solid was obtained by vacuum distillation, but implementation of the distillation was difficult and only 1.41 g of **L2** (5.8 mmol, 30%) could be isolated.
Therefore the formation of **L2** was carried out in azeotropically dried toluene as described above. The reaction solution was then cooled to room temperature and **L2** was directly used *in solution* without further purification, because isolation by vacuum distillation resulted in large losses of the product.
^{1}H-NMR [$CDCl_3$]: δ = 7.10 (s, 1H), 6.91 (s, 1H), 4.60 (dd, 2H), 2.37 (m, 1H).
^{13}C-NMR [$CDCl_3$]: δ = 125.4 (C_{ar}Cl), 119.2 (C_{ar}), 76.6 (C_4), 61.0 (CH), 53.1 (CH_2).
IR: 3294 cm^{-1} (v≡CH), 2263 cm^{-1} (vN=C=O).

4.4. Synthesis of Selector 1

9-(4-Allyloxy-3,5-dichlorophenylcarbamoyl)dihydroquinine (**SO1**)

1.84 g of commercially available DHQN (5.6 mmol) were dissolved in 100 mL of toluene. After flushing the apparatus with nitrogen, 50 mL of toluene were distilled off under nitrogen atmosphere. After finishing the drying process 1.51 g of **L1** (6.2 mmol) and 40 µL of DBTDL as a catalyst were added with nitrogen flushing of the apparatus. The reaction mixture was refluxed for 16 h. Due to several by-products visible on TLC the clear brownish solution was evaporated to dryness and the crude product was purified by flash column chromatography on silica (150 g of silica, CH_2Cl_2/MeOH 10:1). The fractions with pure product (monitored by TLC using the same eluent) were collected, filtered and evaporated under reduced pressure. The obtained solid was dried under vacuum at room temperature.

Yield: 2.85 g (5.0 mmol, 89%) of a white solid.

^{1}H-NMR [$CDCl_3$]: δ = 8.67 (d, 1H), 7.99 (d, 1H), 7.48 (d, 1H), 7.35 (d, 1H), 7.33 (s, 2H), 7.26 (d, 1H), 6.54 (d, 1H), 6.11 (m, 1H), 5.38 (dd, 1H), 5.25 (dd, 1H), 4.49 (d, 2H), 3.96 (s, 3H), 3.34 (q, 1H), 3.15-2.95 (broad, 2H), 2.63 (m, 1H), 2.36 (d, 1H), 1.89-1.78 (broad, 2H), 1.77-1.64 (broad, 1H), 1.59-1.39 (broad, 3H), 1.39-1.22 (broad, 2H), 0.86 (t, 3H).

^{13}C-NMR [$CDCl_3$]: δ =158.6 (C_{ar}-O), 152.4 (C=O), 147.3 (C_{ar}H), 144.7 (C_{ar}), 143.4 (C_{ar}), 134.4 (C_{ar}), 132.9 (CH=), 131.7 (C_{ar}H), 129.7 (C_{ar}), 127.2 (C_{ar}), 121.9 (C_{ar}H), 118.8 (CH_2=), 118.8 (C_{ar}H), 118.7 (C_{ar}H), 101.4 (C_{ar}H), 74.4 (CH), 74.4 (CH_2), 58.9 (CH), 58.0 (CH_2), 55.7 (CH_3-O), 42.6 (CH_2), 37.3 (CH), 28.3 (CH_2), 27.7 (CH_2), 25.2 (CH), 24.2 (CH_2), 12.1 (CH_3).

IR: 2930 cm^{-1}, 2865 cm^{-1}, 1730 cm^{-1} (νC=O).

MS [ESI, positive]: 570 $[M+H]^+$, 286 $[M+2H]^{2+}$.

4.5. Synthesis of Selector 2

DHQD free base

5.0 g of commercially available DHQD.HCl (13.8 mmol) were dissolved in 800 mL of H_2O and alkalized with $NaHCO_3$ to pH 8. The solution was stirred for 18 h at 50°C. DHQD as free base was extracted with CH_2Cl_2 (3x75 mL) and the combined organic phases were washed with 30 mL of H_2O and 30 mL of saturated aqueous NaCl

solution. After drying with $MgSO_4$ the solvent was evaporated. The obtained white crystals were dried under vacuum for 24 h.
Yield: 4.50 g (quantitative yield).

9-(4-Allyloxy-3,5-dichlorophenylcarbamoyl)dihydroquinidine (**SO2**)

1.88 g of DHQD free base (5.8 mmol) were suspended in 100 mL of toluene. After flushing the apparatus with nitrogen 50 mL of toluene were distilled off under nitrogen atmosphere. After finishing the drying process 1.61 g of **L1** (6.7 mmol) and 40 µL of DBTDL as a catalyst were added. The reaction mixture was then refluxed for 16 h. Due to several by-products visible on TLC the clear brownish solution was evaporated to dryness and the crude product was purified by flash column chromatography on silica (150 g of silica, CH_2Cl_2/MeOH 10:1). The fractions with pure product monitored by TLC were collected, filtered and evaporated under reduced pressure. The obtained crystals were dried under vacuum.
Yield: 2.12 g (3.7 mmol, 64%) of a white solid.
^{1}H-NMR [$CDCl_3$]: δ = 8.70 (d, 1H), 8.01 (d, 1H), 7.48 (d, 1H), 7.38 (s, 2H), 7.36 (d, 1H), 7.32 (d, 1H), 6.54 (d, 1H), 6.13 (m, 1H), 5.40 (dd, 1H), 5.27 (dd, 1H), 4.53 (d, 2H), 3.97 (s, 3H), 3.73 (q, 2H), 3.31 (q, 1H), 2.95-2.56 (broad, 3H), 1.77 (m, 1H), 1.65-1.41 (broad, 4H), 1.23 (t, 2H), 0.92 (t, 3H).
^{13}C-NMR [$CDCl_3$]: δ = 158.4 (C_{ar}-O), 153.0 (C=O), 147.7 (C_{ar}H), 145.1 (C_{ar}), 144.3 (C_{ar}), 134.9 (C_{ar}), 133.3 (CH=), 132.0 (C_{ar}H), 130.2 (C_{ar}), 127.8 (C_{ar}), 122.3 (C_{ar}H), 119.4 (CH_2=), 119.3 (C_{ar}H), 119.2 (C_{ar}H), 102.0 (C_{ar}H), 74.8 (CH), 74.2 (CH_2), 59.8 (CH), 58.8 (CH_2), 56.0(CH_3-O), 50.1 (CH_2), 37.7 (CH), 27.6 (CH_2), 26.3 (CH), 25.9 (CH_2), 24.4 (CH_2), 12.4 (CH_3).
IR: 2933 cm^{-1}, 2870 cm^{-1}, 1729 cm^{-1} (νC=O).
MS [ESI, positive]: 592 $[M+Na]^+$, 570 $[M+H]^+$, 286 $[M+2H]^{2+}$.

4.6. Synthesis of Selector 3

9-(3,5-Dichloro-4-propargyloxyphenylcarbamoyl)dihydroquinine (**SO3**)

1.85 g of commercially available DHQN (5.7 mmol) were dissolved in 100 mL of toluene. After flushing the apparatus with nitrogen 50 mL of toluene were distilled off under nitrogen atmosphere. After finishing the drying process 1.41 g of purified solid **L2** (5.8 mmol) and 30 µL of DBTDL as a catalyst were added. The reaction mixture

was refluxed for 18 h. The clear dark green solution was then evaporated to dryness and because of several by-products visible on TLC the crude product was purified by flash column chromatography on silica (150 g silica, CH_2Cl_2/MeOH 10:1). The fractions with product were collected, filtered and evaporated under reduced pressure. The pre-purified not fully dry greenish solid was then coated onto 7.50 g of silica and further purified by flash column chromatography on silica (150 g silica, CH_2Cl_2/MeOH 10:1). The fractions with the pure product monitored by TLC were collected, filtered, evaporated and the obtained solid product was dried under reduced pressure.

Yield: 2.10 g (3.7 mmol, 65%) of a slightly greenish solid.

^{1}H-NMR [$CDCl_3$]: δ = 8.60 (d, 1H), 7.91 (d, 1H), 7.41 (d, 1H), 7.30 (d, 1H), 7.20 (s, 2H), 7.19 (d, 1H), 6.46 (d, 1H), 4.64 (d, 2H), 3.89 (s, 3H), 3.27 (q, 1H), 3.08-2.89 (broad, 2H), 2.56 (m, 1H), 2.43 (t, 1H), 2.29(d, 1H), 1.83-1.71 (broad, 2H), 1.69-1.59 (broad, 1H), 1.51-1.32 (broad, 3H), 1.32-1.21 (broad, 2H), 0.80 (t, 3H).

^{13}C-NMR [$CDCl_3$]: δ = 158.6 (C_{ar}-O), 152.8 (C=O), 147.7 (C_{ar}H), 146.4 (C_{ar}), 145.2 (C_{ar}), 143.7 (C_{ar}), 135.4 (C_{ar}), 132.1 (C_{ar}H), 130.4 (C_{ar}Cl), 127.6 (C_{ar}), 122.4 (C_{ar}H), 119.2 (C_{ar}H), 101.8 (C_{ar}H), 78.3 (CH≡), 76.6 (C_4), 60.9 (CH_2), 59.3 (CH), 58.5 (CH_2), 56.2 (CH_3-O), 43.0 (CH_2), 37.7 (CH), 28.7 (CH_2), 28.1 (CH_2), 25.6 (CH), 24.7 (CH_2), 12.5 (CH_3).

IR: 3298 cm^{-1} (v≡CH), 2930 cm^{-1}, 2868cm^{-1}, 1730 cm^{-1} (vC=O).

MS [ESI, positive]: 1158 $[2M+Na]^+$, 568 $[M+H]^+$, 284 $[M+2H]^{2+}$.

4.7. Synthesis of Selector 4

3,5-Dichloro-4-propargyloxyphenylisocyanate (**L2**)

80 mL of toluene were dried via azeotropic distillation (30 mL of the solvent were removed). After addition of 2.38 g of dry acyl azide **5b** (8.8 mmol), the yellowish solution was refluxed for 3 h to get the isocyanate **L2** via Curtius-rearrangement. Then the solution was cooled to room temperature. An infrared spectrum of the solution confirmed the successful quantitative acyl azide conversion to isocyanate.

IR: 2261 cm^{-1} (vN=C=O).

9-(3,5-Dichloro-4-propargyloxyphenylcarbamoyl)dihydroquinidine (**SO4**)

2.10 g of DHQD (6.4 mmol) were suspended in 80 mL of toluene. After flushing the apparatus with nitrogen 40 mL of toluene were distilled off under nitrogen atmosphere. The suspension was cooled below the boiling point of toluene and then the previously prepared solution of **L2** in dry toluene was added under nitrogen. Additional 30 mL of solvent were distilled off before adding 40 µL of DBTDL as a catalyst. The reaction mixture was then refluxed for 18 h. The initially white suspension became gradually turbid yellowish and a slightly brownish precipitate was formed at the bottom of the flask.

After 18 h the reaction mixture was evaporated to dryness. The crude product was coated onto 15 g of silica and purified by flash column chromatography (200 g silica, CH_2Cl_2/MeOH 10:1). The fractions with pure product monitored by TLC were collected, filtered and evaporated to dryness.

Yield: 2.07 g (3.6 mmol, 56%) of slightly brownish crystals.

^{1}H-NMR [$CDCl_3$]: δ = 8.68 (d, 1H), 7.99 (d, 1H), 7.45 (d, 1H), 7.37 (s, 2H), 7.34 (d, 1H), 7.30 (d, 1H), 6.53 (d, 1H), 4.71 (d, 2H), 3.95 (s, 3H), 3.28 (q, 1H), 2.93-2.85 (broad, 1H), 2.82-2.54 (broad, 3H), 2.50 (t, 1H), 1.80-1.72 (broad, 2H), 1.61-1.53 (broad, 2H), 1.50-1.38 (broad, 2H), 1.27-1.21 (broad, 2H), 0.90 (t, 3H).

^{13}C-NMR [$CDCl_3$]: δ =158.5 (C_{ar}-O), 152.9 (C=O), 147.7 (C_{ar}H), 146.4 (C_{ar}), 145.1 (C_{ar}), 144.2 (C_{ar}), 135.5 (C_{ar}), 132.1 (C_{ar}H), 130.4 (C_{ar}Cl), 127.8 (C_{ar}), 122.3 (C_{ar}H), 119.2 (C_{ar}H), 101.9 (C_{ar}H), 78.2 (CH≡), 76.6 (C_4), 74.2 (CH), 60.9 (CH_2), 59.8 (CH), 56.0 (CH_3-O), 51.2 (CH_2), 37.7 (CH), 27.6 (CH_2), 26.3 (CH), 25.9 (CH_2), 24.4 (CH_2), 12.4 (CH_3).

IR: 3296 cm^{-1} (v≡CH), 2932 cm^{-1}, 2870 cm^{-1}, 1728 cm^{-1} (vC=O).

MS [ESI, positive]: 568 $[M+H]^+$, 284 $[M+2H]^{2+}$.

4.8. Immobilization of SO1 onto MP-Silica = CSP1

2.57 g of mercaptopropyl-modified silica (5 µm, 120 Å, endcapped with hexamethyl-disilazane, 650 µmol thiol-groups per gram modified silica, corresponding to 1.67 mmol thiol-groups), 1.76 g of **SO1** (3.09 mmol) and 228 mg of AIBN as a radical starter were suspended in 25 mL of MeOH under nitrogen atmosphere. The suspension was mechanically stirred and heated under reflux. After 18 h the reaction mixture was cooled to room temperature and the modified silica was filtered with a

frit and washed with MeOH and CH_2Cl_2 (each 3x50 mL). After drying under vacuum at 60°C SO loading was determined by elemental analysis (EA).
Yield: 2.56 g.
EA: C: 10.93 w-%; H: 1.75 w-%; N: 0.749 w-%; S: 1.94 w-%; Cl: 0.960 w-%.
SO loading calculated according to the nitrogen content: 179 µmol/g.

4.9. Immobilization of SO2 onto MP-Silica = CSP2

2.49 g of **MP-Silica** (5 µm, 120 Å, endcapped with hexamethyl-disilazane, 660 µmol thiol-groups per gram modified silica, corresponding to 1.64 mmol thiol-groups), 1.76 g **SO2** (3.10 mmol) and 212 mg of AIBN as a radical starter were suspended in 30 mL of MeOH under nitrogen atmosphere. The suspension was mechanically stirred and heated under reflux. After 18 h the reaction mixture was cooled to room temperature and the silica was filtered with a frit and washed with MeOH and CH_2Cl_2 (each 3x50 mL). After drying under vacuum at 60°C SO loading was determined by elemental analysis.
Yield: 2.64 g.
EA: C: 9.41 w-%; H: 1.64 w-%; N: 0.59 w-%; S: 1.92 w-%; Cl: 0.91 w-%.
SO loading calculated according to the nitrogen content: 144 µmol/g.

4.10. Synthesis of AzP-Silica

Chloropropyl-modified silica (**CP-Silica**)

15.78 g of silica (Daisogel for HPLC; Grade SP-120-5P, 5 µm, 120 Å) were suspended in 200 mL toluene and dried via azeotropic distillation. During the distillation 20 mg of p-toluenesulfonic acid were added to the suspension and also dried together with toluene and silica. After distilling off 100 mL of the solvent, the descending condenser was replaced by a dry reflux condenser and 4.6 mL of 3-chloropropyltrimethoxysilane (25 mmol) were added to the suspension. The reaction mixture was mechanically stirred and heated under reflux for 18 h. The suspension was then cooled to room temperature, filtered with a frit, washed with toluene and methanol (each 2x100 mL) and resuspended in 100 mL toluene again. This suspension was mechanically stirred for 0.5 h and heated under reflux.

Afterwards the suspension was filtered and washed the same way as before. **CP-Silica** was then dried under vacuum at 60°C and chloropropyl-loading was determined by elemental analysis.
Yield: 17.19 g.
EA: C: 3.61 w-%; H: 1.01 w-%; N: < 0.03 w-%; S: < 0.01 w-%; Cl: 2.63 w-%.
Chloropropyl-loading calculated according to the chlorine content: 742 µmol/g.

Azidopropyl-modified silica (**AzP-Silica**)
17.19 g of **CP-Silica** were suspended in 110 mL 0.5 M NaN_3 in warm DMSO (55 mmol) and 60 mg of tetrabutylammonium iodide as a catalyst were added. This reaction mixture was then mechanically stirred for 72 h at 80°C. **AzP-Silica** was then filtered with a frit, washed with 500 mL H_2O and 250 mL MeOH and dried under vacuum. Azide-loading was determined by elemental analysis.
Yield: 16.07 g.
EA: C: 3.64 w-%; H: 0.92 w-%; N: 2.64 w-%; S: < 0.01 w-%; Cl: 0.18 w-%.
Azidopropyl-loading calculated according to the nitrogen content: 629 µmol/g (85% conversion from chloropropyl to azidopropyl).

4.11. Immobilization of SO3 onto AzP-Silica = CSP3

3.00 g of **AzP-Silica** (corresponding to 1.89 mmol $-N_3$) and 1.78 g **SO3** (3.13 mmol) were suspended in 60 mL of ACN in a glass bottle. 1.06 mL (6.25 mmol) of *N,N*-diisopropylethylamine were added and the suspension was sealed with a septum and degassed by flushing with N_2 through a syringe needle for 10 min. 25 mg of CuI (0.13 mmol, 6.9 mol% according to $-N_3$) as a catalyst were added under nitrogen flushing and the glass bottle was closed and sealed with Parafilm®. The sealed glass bottle was shaken for 72 h on an overhead shaker at room temperature. After 48 h additional 22 mg of catalyst (0.12 mmol, 6.3 mol%) were added under nitrogen flushing, the glass bottle was closed and the reaction continued under given conditions. After 72 h the ocher reaction mixture was filtered with a frit and washed with ACN, MeOH, 2 w-% EDTA in H_2O, MeOH/H_2O 1:1 v/v, 10 v-% AcOH in MeOH and pure MeOH (each 150 mL). **CSP3** was then dried under vacuum at 60°C for 72 h. SO loading was determined by elemental analysis.

Yield: 4.07 g.

EA: C: 19.20 w-%; H: 2.16 w-%; N: 4.24 w-%; S: < 0.02 w-%; Cl: 3.38 w-%.

SO loading calculated according to the chlorine content: 477 µmol/g (76% conversion of azido-groups).

4.12. Immobilization of SO4 onto AzP-Silica = CSP4

3.00 g of **AzP-Silica** (corresponding to 1.89 mmol $-N_3$) and 1.73 g of **SO4** (3.04 mmol) were suspended in 60 mL of ACN in a glass bottle. 1.06 mL of DIPEA (6.25 mmol) were added and the suspension was degassed for 10 min as described above. 25 mg of CuI (0.13 mmol, 6.9 mol% according to $-N_3$) as a catalyst were added under nitrogen flushing and the glass bottle was closed and sealed with Parafilm®. The sealed glass bottle was shaken for 72 h on an overhead shaker. After 48 h additional 21 mg of catalyst (0.11 mmol, 5.8 mol%) were added under nitrogen flushing and the reaction continued under given conditions. After additional 24 h the ocher reaction mixture was filtered with a frit and washed with ACN, MeOH, 2 w-% EDTA in H_2O, MeOH/H_2O 1:1 v/v, 10 v-% AcOH in MeOH and pure MeOH (each 150 mL). **CSP4** was then dried under vacuum at 60°C for 72 h. SO loading was determined by elemental analysis.

Yield: 4.13 g.

EA: C: 19.04 w-%; H: 2.19 w-%; N: 4.18 w-%; S: < 0.02 w-%; Cl: 3.48 w-%.

SO loading calculated according to the chlorine content: 490 µmol/g (78% conversion of azido-groups).

4.13. Immobilization of SO3 onto AzP-Silica = CSP5

3.50 g of **AzP-Silica** (corresponds to 2.20 mmol $-N_3$) and 458 mg of **SO3** (0.81 mmol) were suspended in 60 mL of ACN in a glass bottle. 1.24 mL of DIPEA (7.31 mmol) were added and the suspension was degassed by flushing with N_2 for 10 min as described above. 28 mg of CuI (0.15 mmol, 7.4 mol% according to $-N_3$) as a catalyst were added under nitrogen flushing and the glass bottle was closed and sealed with Parafilm®. The sealed glass bottle was shaken for 72 h on an overhead shaker. After 48 h additional 25 mg of catalyst (0.13 mmol, 6.0 mol%) were added under nitrogen flushing and the reaction continued under given conditions. After

additional 24 h the greenish reaction suspension was filtered with a frit and washed with ACN, MeOH, 2 w-% EDTA in H_2O, MeOH/H_2O 1:1 v/v, 10 v-% AcOH in MeOH and pure MeOH (each 150 mL). **CSP5** was then dried under vacuum at 60°C for three days. SO loading was determined by elemental analysis.
Yield: 3.90 g.
EA: C: 10.04 w-%; H: 1.41 w-%; N: 3.42 w-%; S: < 0.02 w-%; Cl: 1.52 w-%.
SO loading calculated according to the chlorine content: 214 µmol/g (93% of **SO3** immobilized).

4.14. Immobilization of SO4 onto AzP-Silica = CSP6

2.40 g of **AzP-Silica** (corresponding to 1.51 mmol -N_3) and 341 mg of **SO4** (250 µmol/g silica) were suspended in 50 mL of ACN in a glass bottle. 886 µL of DIPEA were added (5.21 mmol) and the suspension was degassed by flushing with N_2 for 10 min. 36 mg of CuI (189 µmol, 12.5 mol% according to -N_3) as a catalyst were added under nitrogen flushing and the glass bottle was closed and sealed with Parafilm®. The sealed glass bottle was shaken for 72 h on an overhead shaker. The ocher suspension was filtered with a frit and washed with ACN, MeOH, 2 w-% EDTA in H_2O, MeOH/H_2O 1:1 v/v, 10 v-% AcOH in MeOH and pure MeOH (each 150 mL). CSP6 was then dried under vacuum at 60°C for 24 h. SO loading was determined by elemental analysis.
Yield: 2.68 g.
EA: C: 9.90 w-%; H: 1.38 w-%; N: 3.11 w-%; S: < 0.02 w-%; Cl: 1.83 w-%.
SO loading calculated according to the chlorine content: 232 µmol/g (93% of **SO4** immobilized).

4.15. Preparation of CSP7

1.23 g of **CSP4** (490 µmol **SO4** per gram silica) were combined with 1.28 g of **AzP-Silica** (azidopropyl-loading of 629 µmol/g) and suspended in 250 mL of MeOH to result in a calculated final selector-concentration of 240 µmol/g. This suspension was mechanically stirred at room temperature for 4 h. Afterwards the homogenously mixed silica material was filtered and washed with 50 mL of MeOH. **CSP7** was dried under vacuum at 60°C for 24 h. SO loading was determined by elemental analysis.

Yield: 2.50 g.

EA: C: 11.14 w-%; H: 1.54 w-%; N: 3.34 w-%; S: < 0.02 w-%; Cl: 1.69 w-%.

SO loading calculated according to the chlorine content: 238 µmol/g (99% of the expected value).

4.16. Immobilization of SO4 onto AzP-Silica = CSP8

2.50 g of **AzP-Silica** (corresponding to 1.57 mmol $-N_3$) and 512 mg of **SO4** (0.90 mmol) were suspended in 60 mL of ACN in a glass bottle. 1.0 mL of DIPEA was added (5.88 mmol) and the suspension was degassed by flushing with N_2 for 10 min. 50 mg of CuI (263 µmol, 17 mol% according to $-N_3$) as a catalyst were added under nitrogen flushing and the glass bottle was closed and sealed with Parafilm®. The sealed glass bottle was shaken for 72 h on an overhead shaker. The yellow suspension was filtered with a frit and washed with ACN, MeOH, 2 w-% EDTA in H_2O, MeOH/H_2O 1:1 v/v, 10 v-% AcOH in MeOH and pure MeOH (each 150 mL). **CSP8** was then dried under vacuum at 60°C for 24 h. SO loading was determined by elemental analysis.

Yield: 2.79 g.

EA: C: 12.96 w-%; H: 1.65 w-%; N: 3.28 w-%; S: < 0.02 w-%; Cl: 2.23 w-%.

SO loading calculated according to the chlorine content: 314 µmol/g (87% of **SO4** immobilized).

4.17. Immobilization of SO4 onto AzP-Silica = CSP9

10.0 g of **AzP-Silica** (corresponding to 6.29 mmol $-N_3$) and 853 mg of **SO4** (1.50 mmol) were suspended in 200 mL of ACN in a glass bottle. 10 mL of DIPEA were added (58.8 mmol) and the suspension was degassed by flushing with N_2 for 15 min. 200 mg of CuI (1.05 mmol, app. 17 mol% according to $-N_3$) as a catalyst were added under nitrogen flushing and the glass bottle was closed and sealed with Parafilm®. The sealed glass bottle was shaken for 72 h on an overhead shaker. The yellow suspension was filtered with a frit and washed with ACN, MeOH, 2x2 w-% EDTA in H_2O, MeOH/H_2O 1:1 v/v, 10 v-% AcOH in MeOH and pure MeOH (each 300 mL). **CSP9** was then dried under vacuum at 60°C for 24 h. SO loading was determined by elemental analysis.

Yield: 10.46 g.
EA: C: 7.75 w-%; H: 1.24 w-%; N: 2.82 w-%; S: < 0.02 w-%; Cl: 1.24 w-%.
SO loading calculated according to the chlorine content: 150 µmol/g (**SO4** quantitatively immobilized).

4.18. Endcapping of CSP9 resulting in CSP10

2.5 g of **CSP9** (**SO4** loading of 150 µmol/g) were suspended in 60 mL of ACN in a glass bottle. 1.0 mL of DIPEA was added (5.88 mmol) and the suspension was degassed by flushing with N_2 for 10 min. 50 mg of CuI (0.26 mmol, app. 22 mol% according to free -N_3) as a catalyst and 100 µL of propargyl alcohol (1.73 mmol) were added under nitrogen flushing and the glass bottle was closed and sealed with Parafilm®. The sealed glass bottle was shaken for 72 h on an overhead shaker. The yellow suspension was filtered with a frit and washed with ACN, MeOH, 2 w-% EDTA in H_2O, MeOH/H_2O 1:1 v/v, 10 v-% AcOH in MeOH and pure MeOH (each 150 mL). **CSP10** was then dried under vacuum at 60°C for 24 h. SO loading was determined by elemental analysis.
Yield: 2.49 g of a slightly yellowish modified silica.
EA: C: 8.98 w-%; H: 1.33 w-%; N: 2.72 w-%; S: < 0.02 w-%; Cl: 1.16 w-%.
SO loading calculated according to the chlorine content: 138 µmol/g (92% of **CSP9**, 8% of **SO4** have been splitted off during endcapping and the work-up process).

4.19. Column-packing

Column-packing was carried out in the same way for every single CSP and the AzP-Silica-Column using standard slurry-method. The modified silica was sieved through a 40 µm sieve and 2.30 g of it were suspended in 20 mL of iPrOH and 1.0 mL AcOH.
The suspension was homogenized in an ultrasonic bath for 20 min and the silica material was packed *in house* under high pressure (app. 650 bar) into a 150x4 mm ID Bischoff stainless steel HPLC column followed by rinsing with methanol (**columns 1** to **10**, **13**, **14** and **16**).

When packing 75x4 mm ID columns only 1.80 g of CSP were used for packing (**columns 11**, **12** and **15**). Before using the packed columns they were rinsed with 100 mL 1.0 w-% aqueous EDTA solution (except **columns 1**, **2** and **13** to **16**), 50 mL bidistilled H_2O and 100 mL of MeOH.

II. List of Abbreviations

///	no value, no data	MeOH	methanol
α_i	selectivity coefficient	min	minute
ACHSA	aminocyclohexanesulfonic acid	MP-Silica	mercaptopropyl-modified silica
ACN	acetonitrile	MS	mass spectrometry
AcOH	acetic acid	MWD	multiple wavelength detector
AIBN	2,2'-azobis(2-methylpropionitrile)	n	number
AzP-Silica	azidopropyl-modified silica	N_i	number of theoretical plates
ATR	attenuated total reflection	NMR	nuclear magnetic resonance spectroscopy
av	average	NP	normale phase
CD	circular dichroism	Φ	phase ratio
CDA	chiral derivatizing agent	PE	petroleum ether
CE	capillary electrophoresis	PI	photoinitiator
CP-Silica	chloropropyl-modified silica	PO	polar organic mode
CSP	chiral stationary phase	QD	quinidine
DAD	diode array detector	QN	quinine
DBTDL	dibutyltin dilaurate	QqLIT	hybrid quadrupole linear ion trap
DEA	diethylamine	R	residue
DHQD	dihydroquinidine	R_i	resolution
DHQN	dihydroquinine	RP	reversed phase
DIPEA	diisopropylethylamine, Hünig base	RT	room temperature
DMF	*N,N*-dimethylformamide	SA	selectand
DMSO	dimethylsulfoxide	SCX	strong cation exchange
DNA	deoxyribonucleic acid	SFC	supercritical fluid chromatography
DOPA	3,4-dihydroxyphenylalanine	SMB	simulated moving bed technology
e.g.	exempla gratia, for example	SO	selector
EA	elemental analysis	T	temperature
EDTA	ethylenediaminetetraacetic acid	*t*Butyl	*tert*-butyl
EO	elution order, first eluted enantiomer	THF	tetrahydrofuran
ESI	electrospray ionization	t_i	retention time
et al.	et alii, and others	TLC	thin layer chromatography
EtOAc	ethyl acetate	tren	tris(2-aminoethyl)amine
EtOH	ethanol	UV	ultraviolet
FTIR	fourier transform infrared spectroscopy	v-%	volume percent
GC	gas chromatography	v/v	volume to volume ratio
h	hour	v/v/w	volume to volume to mass ratio
HPLC	high performance liquid chromatography	V65	2,2'-azobis(2,4-dimethyl valeronitrile)
ID	internal diameter	VCD	vibrational circular dichroism
iPrOH	isopropanol	w-%	mass percent
IR	infrared spectroscopy	WAX	weak anion exchange
k_i	retention factor	WCX	weak cation exchange
L	linker	w_i	peak width at half maximum
LC	liquid chromatography	ZWIX	zwitterionic exchange type

III. Abbreviations of the Analytes

A-DCL-Leu	*N*-4-allyloxy-3,5-dichlorobenzoyl leucine
Ac-Phe	*N*-acetyl phenylalanine
Ac-Trp	*N*-acetyl tryptophane
Acetylmandelic acid	*O*-acetylmandelic acid
Atrolactic acid	2-phenyl-2-hydroxypropionic acid
BOC-Gly	*N*-*tert*-butyloxycarbonyl glycine
BOC-Phe	*N*-*tert*-butyloxycarbonyl phenylalanine
BOC-Tyr	*N*-*tert*-butyloxycarbonyl tyrosine
BTFMB-Leu	*N*-3,5-bis-(trifluoromethyl)benzoyl leucine
Bz-ACHSA	*N*-benzoyl-2-aminocyclohexanesulfonic acid
Bz-Leu	*N*-benzoyl leucine
Bz-Phe	*N*-benzoyl phenylalanine
Bz-*β*-Phe	*N*-benzoyl β-phenylalanine
Carprofen	2-(6-chloro-9*H*-carbazol-2-yl)propanoic acid
Clenbuterol	1-(4-amino-3,5-dichlorophenyl)-2-(*tert*-butylamino)ethanol
DBTAMME	dibenzoyltartaric acid monomethyl ester
DCB-Leu	*N*-3,5-dichlorobenzoyl leucine
Dichlorprop	2-(2,4-dichlorophenoxy)propanoic acid
DNB-Leu	*N*-3,5-dinitrobenzoyl leucine
DNB-*N*-Me-Leu	*N*-3,5-dinitrobenzoyl-*N*-methyl leucine
DNB-Pro	*N*-3,5-dinitrobenzoyl proline
DNP-Mandelic acid	*O*-(3,5-dinitrophenylcarbamoyl)mandelic acid
DNZ-Gly	*N*-3,5-dinitrobenzoyloxycarbonyl glycine
DNZ-Phe	*N*-3,5-dinitrobenzoyloxycarbonyl phenylalanine
DNZ-Val	*N*-3,5-dinitrobenzoyloxycarbonyl valine
Fenoprofen	2-(3-phenoxyphenyl)propanoic acid
Flurbiprofen	2-(2-fluorobiphenyl-4-yl)propanoic acid
FMOC-Abu	*N*-fluorenylmethoxycarbonyl-*α*-aminobutyric acid
FMOC-Asn	*N*-fluorenylmethoxycarbonyl asparagine
FMOC-Aze	*N*-fluorenylmethoxycarbonyl azetidine
FMOC-Gln	*N*-fluorenylmethoxycarbonyl glutamine
FMOC-Ile	*N*-fluorenylmethoxycarbonyl isoleucine
FMOC-Pro	*N*-fluorenylmethoxycarbonyl proline
FMOC-*β*-Phe	*N*-fluorenylmethoxycarbonyl *β*-phenylalanine
Hydroxymandelic acid	4-hydroxymandelic acid
Hydroxyphenyllactic acid	3-(4-hydroxyphenyl)lactic acid
Ibuprofen	2-(4-(2-methylpropyl)phenyl)propanoic acid
MFQ.HCl	mefloquine hydrochloride

Naproxen	2-(6-methoxynaphthalen-2-yl)propanoic acid
Nitrophenylpropionic acid	2-(4-nitrophenyl)propionic acid
P-DCL-ACHSA	*N*-(3,5-dichloro-4-propargyloxybenzoyl)-2-aminocyclohexanesulfonic acid
P-DML-ACHSA	*N*-3,5-dimethoxy-4-propargyloxybenzoyl-2-aminocyclohexanesulfonic acid
PFB-Leu	*N*-2,3,4,5,6-pentafluorobenzoyl leucine
Phe	phenylalanine
Phenyl-Gly	*α*-phenylglycine
Phenylbutyric acid	2-phenylbutyric acid
QD	quinidine
QN	quinine
TMB-Ala	*N*-3,4,5-trimethoxybenzoyl alanine
Trolox	6-hydroxy-2,5,7,8-tetramethylchroman-2-carboxylic acid
Tropic acid	3-hydroxy-2-phenylpropanoic acid
Trp	tryptophane
Tyr	tyrosine
Vanillylmandelic acid	4-hydroxy-3-methoxymandelic acid
Z-Arg	*N*-benzoyloxycarbonyl arginine
Z-Leu	*N*-benzoyloxycarbonyl leucine
Z-Phe	*N*-benzoyloxycarbonyl phenylalanine
Z-Ser	*N*-benzoyloxycarbonyl serine
Z-*β*-Phe	*N*-benzoyloxycarbonyl *β*-phenylalanine

IV. Conclusion and Outlook

The focus of the present master thesis was the synthesis and evaluation of novel arylcarbamoylated cinchona-based weak anion exchange type chiral stationary phases for liquid chromatography.

Commercially available dihydroquinine and corresponding pseudoenantiomeric dihydroquinidine as the building blocks were carbamoylated with two different linkers. In total four different selectors were successfully synthesized, wherein each two of them are pseudoenantiomers. Due to the protonation of the quinuclidine ring of the building blocks under weakly acidic mobile phase conditions anion exchange takes place.

On the basis of two differently substituted linkers (one allylated and one propargylated) it was possible to use two different immobilization strategies – radical mediated thiol-ene addition or Cu(I) and base catalyzed Huisgen alkyne-azide click chemistry. The radical addition onto mercaptopropyl-modified silica yielded low immobilization efficiencies; on the other hand, it was possible to control the amount of immobilized selector via alkyne-azide click chemistry, which yielded saturated selector densities in case the selector was offered in excess. Altogether ten CSPs with different selector loadings were synthesized through immobilization of the four selectors.

All CSPs were then evaluated in terms of their capability for enantioseparation with a set of 67 analytes; most of them were chiral acidic compounds. For comparative purposes two commercially available CSPs (QN-AX and QD-AX) were used as well.

As a trend it was observed that the immobilization via radical thiol-ene addition results in higher resolution values (taking into account that the selector densities are equal), but this behavior could also be caused by packing phenomena. Free azido groups on modified silica show no contribution to retention. Endcapping of the free azido groups results in higher selectivity and lower resolution. A 1:1 physical mixture prepared from a high loaded CSP and pure azidopropyl-modified silica behaves similarly to a half-length column containing the high loaded material. The elution order changes from DHQN to DHQD type CSPs, whereas DHQD type CSPs exhibit higher selectivity and resolution. The higher the selector loading, the higher the retention. The maximum resolution and selectivity were observed at a selector density of app. 310 µmol/g.

All CSPs are well suitable for the separation of *N*-protected aminophosphonates, which is an advantage in comparison to the commercially available QN-AX and QD-AX anion exchangers.

A loading study confirmed an ion exchange mechanism for the retention of acidic analytes under polar organic mode mobile phase conditions. The stoichiometric displacement model was proved to be valid as well.

In summary the synthesis of novel weak anion exchange type CSPs based on carbamoylated cinchona alkaloids was carried out successfully. New findings were achieved employing different immobilization strategies and selector densities. By the usage of the present synthesis protocols and immobilization strategies in combination with a derivatization of the substituted linker it is possible to perform further investigations in the field of enantioseparation in the future.

V. Zusammenfassung

Der Schwerpunkt der vorliegenden Masterarbeit war die Synthese und Evaluierung neuartiger Chinin-basierter chiraler Anionenaustauschermaterialien für die Trennung chiraler organischer Säuren mittels Hochleistungs-Flüssigkeitschromatographie.
Kommerziell erhältliches Dihydrochinin und das entsprechende pseudoenantiomere Dihydrochinidin wurden als chirale Grundbausteine mit zwei verschiedenen Isocyanaten carbamoyliert. Insgesamt konnten vier verschiedene Selektoren erfolgreich synthetisiert werden, wobei jeweils zwei davon als pseudoenantiomere Paare angesehen werden können. Durch Protonierung des Chinuclidinrings der Selektoren unter leicht sauren Bedingungen ist in weiterer Folge Anionenaustausch möglich.
Aufgrund von zwei unterschiedlich substituierten Isocyanaten als Linker (allyliert und propargyliert) war es möglich, zwei verschiedene Strategien für die Immobilisierung der Selektoren zu verwenden - radikale Thiol-En Addition oder Cu(I) und basenkatalysierte Huisgen Alkin-Azid Klick-Chemie. Die radikalische Immobilisierung auf Mercaptopropyl-modifiziertem Kieselgel ergab einerseits eine niedrige Immobilisierungseffizienz, andererseits war es möglich, die Menge an immobilisiertem Selektor über Alkin-Azid Klick-Chemie zu steuern. Zusammenfassend konnten zehn CSP mit unterschiedlicher Selektorbeladung synthetisiert werden.
Alle CSP wurden bezüglich ihrer Fähigkeit zur Trennung von Enantiomeren mit einem Set von 67 Analyten untersucht, wobei die meisten davon chirale saure Verbindungen waren. Zu Vergleichszwecken wurden zwei kommerziell erhältliche CSP (QN-AX und QD-AX) verwendet.
Als Trend wurde beobachtet, dass die Immobilisierung über radikalische Thiol-En-Addition bei gleicher Selektordichte höhere Auflösungen ergibt, was allerdings auch auf Packungsphänomene zurückzuführen sein könnte. Freie Azidogruppen auf modifiziertem Kieselgel liefern keinen Beitrag zur Retention der Analyten. Endcapping der freien Azidogruppen führt einerseits zu höherer Selektivität, andererseits zu geringerer Auflösung. Eine 1:1 physikalische Mischung hergestellt aus einer hoch belegten CSP und Azidopropyl-modifiziertem Kieselgel verhält sich ähnlich wie eine Säule, welche mit hoch belegtem Material gepackt wurde und nur die halbe Länge aufweist.

Eine Umkehr der Elutionsreihenfolge von DHQN zu DHQD Typ CSP konnte bei allen Analyten beobachtet werden, wobei die DHQD Typ CSP generell eine höhere Selektivität und Auflösung zeigten. Je höher die Selektordichte, desto größer war die Retention, jedoch begleitet von einer Abnahme der Selektivität. Das Maximum an Auflösung und Selektivität wurde bei einer Selektordichte von zirka 310 µmol/g beobachtet.

Die synthetisierten chiralen stationären Phasen waren sehr gut für die Trennung von *N*-geschützten Aminophosphonaten geeignet, was ein Vorteil im Vergleich zu den im Handel erhältlichen QN-AX und QD-AX Anionenaustauschermaterialien ist.

Eine Beladungsstudie bestätigte einen Ionenaustausch-Mechanismus für die Retention von sauren Analyten. Die Gültigkeit des stöchiometrischen Verdrängungs-Modells konnte ebenfalls erwiesen werden.

Zusammenfassend konnte die Synthese neuer Anionenaustauscherphasen für Hochleistungsflüssigkeitschromatographie auf der Basis von arylcarbamoylierten Chinin-Derivaten erfolgreich durchgeführt werden. Neue Erkenntnisse konnten durch den Einsatz unterschiedlicher Immobilisierungs-Strategien und Selektordichten auf der Kieselgeloberfläche gewonnen werden. Durch diese Erkenntnisse und die Verwendung der vorliegenden Syntheseprotokolle und Immobilisierungsstrategien in Kombination mit einer Derivatisierung des substituierten Linkers ist es möglich, weitere Untersuchungen auf dem Gebiet der Enantiomerentrennung durchzuführen.

VI. Curriculum Vitae

Name:	Hubert Hettegger
Geburtsdatum:	29.09.1988 (Schwarzach im Pongau)
Staatsbürgerschaft:	Österreich
Adresse:	Höritzergasse 4/7
	1140 Wien

Schulbildung:

1994-1998	Volksschule St. Veit im Pongau
1998-2006	Privatgymnasium der Herz Jesu Missionare in Salzburg/Liefering
2006	Matura

Studium:

2006 bis 2010	Bachelorstudium Chemie an der Universität Wien
2010 bis 1012	Masterstudium Chemie an der Universität Wien
2011 bis 2012	Masterarbeit

Mitgliedschaften in wissenschaftlichen Gesellschaften:

seit 2012	GÖCH - Gesellschaft Österreichischer Chemiker
seit 2012	ASAC - Austrian Society of Analytical Chemistry

VII. References

[1] Li, S., et al., *Direct chiral separations by capillary electrophoresis using capillaries packed with an α_1-acid glycoprotein chiral stationary phase.* Anal. Chem., 1993. **65**(24): p. 3684-3690.

[2] Li, S., et al., *Packed-capillary electrochromatographic separation of the enantiomers of neutral and anionic compounds using β-cyclodextrin as a chiral selector. Effect of operating parameters and comparison with free-solution capillary electrophoresis.* J. Chromatogr., A, 1994. **666**(1-2): p. 321-335.

[3] Lloyd, D.K., et al., *Protein chiral selectors in free-solution capillary electrophoresis and packed-capillary electrochromatography.* J. Chromatogr., A, 1995. **694**(1): p. 285-296.

[4] Lelievre, F., et al., *Capillary electrochromatography: operating characteristics and enantiomeric separations.* J. Chromatogr., A, 1996. **723**(1): p. 145-156.

[5] Wolf, C., et al., *Enantioseparations by electrochromatography with packed capillaries.* J. Chromatogr., A, 1997. **782**(2): p. 175-179.

[6] Wistuba, D., et al., *Enantiomer separation by pressure-supported electrochromatography using capillaries packed with a permethyl-β-cyclodextrin stationary phase.* J. Chromatogr., A, 1998. **815**(2): p. 183-188.

[7] Smith, N.W., et al., *The analysis of pharmaceutical compounds using electrochromatography.* Chromatographia, 1994. **38**(9-10): p. 649-657.

[8] Smith, N.W., et al., *Capillary zone electrophoresis in pharmaceutical and biomedical analysis.* J. Pharm. Biomed. Anal., 1994. **12**(5): p. 579-611.

[9] Smith, N.W., et al., *The efficient analysis of neutral and highly polar pharmaceutical compounds using reversed-phase and ion-exchange electrochromatography.* Chromatographia, 1995. **41**(3/4): p. 197-203.

[10] Euerby, M.R., et al., *Capillary electrochromatography in the pharmaceutical industry. Practical reality or fantasy?* Anal. Commun., 1996. **33**(11): p. 403-405.

[11] Lämmerhofer, M., et al., *High-efficiency chiral separations of N-derivatized amino acids by packed-capillary electrochromatography with a quinine-based chiral anion-exchange type stationary phase.* J. Chromatogr., A, 1998. **829**(1+2): p. 115-125.

[12] Maier, N.M., et al., *Separation of enantiomers: needs, challenges, perspectives.* J. Chromatogr., A, 2001. **906**(1-2): p. 3-33.

[13] Maier, N.M., *The Pursuit of Chiral Anion Exchange-Type Selectors: From Concept to Application.* Chromatography Today, 2009: p. 3-9.

[14] Lämmerhofer, M., *Stereoselective liquid chromatography*, Chromedia. A web Infotope for the Practicing Chromatography Community.

[15] Francotte, E.R., et al., *Preparative chromatographic separation of enantiomers.* J. Chromatogr., Biomed. Appl., 1992. **576**(1): p. 1-45.

[16] Francotte, E.R., *Contribution of preparative chromatographic resolution to the investigation of chiral phenomena.* J. Chromatogr., A, 1994. **666**(1-2): p. 565-601.

[17] Francotte, E.R., *Enantioselective chromatography as a powerful alternative for the preparation of drug enantiomers.* J. Chromatogr., A, 2001. **906**(1-2): p. 379-397.

[18] Bicchi, C., et al., *Cyclodextrin derivatives as chiral selectors for direct gas chromatographic separation of enantiomers in the essential oil, aroma and flavor fields.* J. Chromatogr., A, 1999. **843**(1+2): p. 99-121.

[19] Betts, T.J., *Chemical characterization of the different types of volatile oil constituents by various solute retention ratios with the use of conventional and novel commercial gas chromatographic stationary phases.* J. Chromatogr., A, 2001. **936**(1-2): p. 33-46.

[20] Ahmed, F.E., *Analysis of polychlorinated biphenyls in food products.* Trends Anal. Chem., 2003. **22**(3): p. 170-185.

[21] Vetter, W., et al., *Enantioselective determination of chiral organochlorine compounds in biota by gas chromatography on modified cyclodextrins.* J. Chromatogr., A, 1997. **774**(1+2): p. 143-175.

[22] Cochran, J.W., et al., *Recent developments in the high-resolution gas chromatography of polychlorinated biphenyls.* J. Chromatogr., A, 1999. **843**(1+2): p. 323-368.

[23] Bester, K., *Chiral analysis for environmental applications.* Anal. Bioanal. Chem., 2003. **376**(3): p. 302-304.

[24] He, L., et al., *Applications of enantiomeric gas chromatography: A review.* J. Liq. Chromatogr. Relat. Technol., 2005. **28**(7-8): p. 1075-1114.

[25] Ribeiro, A.E., et al., *Chiral separation of ketoprofen enantiomers by preparative and simulated moving bed chromatography.* Sep. Sci. Technol., 2011. **46**(11): p. 1726-1739.

[26] Burke, D., et al., *Chirality: a blueprint for the future.* British Journal of Anaesthesia, 2002. **88**(4): p. 563-576.

[27] Lorenz, H., et al., *Crystallization of enantiomers.* Chem. Eng. Process., 2006. **45**(10): p. 863-873.

[28] Vollhardt, K.P.C., et al., *Organische Chemie*. 4 ed. 2007, Weinheim, Germany: Wiley-VCH Verlag.

[29] Mortimer, C.E., et al., *Das Basiswissen der Chemie*. Vol. 8. 2003, Stuttgart, Germany: Georg Thieme Verlag.

[30] Davankov, V.A., *Analytical chiral separation methods.* Pure & Appl. Chem., 1997. **69**(7): p. 1469-1474.

[31] Liang, C., et al., *Topological chirality of iron-sulfur proteins.* Biopolymers, 1997. **42**(4): p. 411-414.

[32] Agranat, I., et al., *Putting chirality to work: the strategy of chiral switches.* Nat. Rev. Drug Discovery, 2002. **1**(10): p. 753-768.

[33] Pell, F.R., *Development and evaluation of zwitterionic chiral stationary phases*. Diploma Thesis, University of Vienna, Department of Chemistry, 2008.

[34] Reist, M., et al., *Chiral Inversion and Hydrolysis of Thalidomide: Mechanisms and Catalysis by Bases and Serum Albumin, and Chiral Stability of Teratogenic Metabolites.* Chem. Res. Toxicol., 1998. **11**(12): p. 1521-1528.

[35] Eriksson, T., et al., *Enantiomers of thalidomide: blood distribution and the influence of serum albumin on chiral inversion and hydrolysis.* Chirality, 1998. **10**(3): p. 223-228.

[36] Lämmerhofer, M., et al., *Recent developments in liquid chromatographic enantioseparation*, in *Handbook of Analytical Separations*, K. Valko, Editor. 2002, Elsevier Science B.V.: Amsterdam.

[37] Davankov, V.A., *The Nature of Chiral Recognition: Is it a Three-Point Interaction?* Chirality, 1997. **9**: p. 99-102.

[38] Dalgliesh, C.E., *The optical resolution of aromatic amino-acids on paper chromatograms.* J. Chem. Soc., 1952. **132**(0): p. 3940-3942.

[39] Mesecar, A.D., et al., *Structural biology: A new model for protein stereospecificity.* Nature (London), 2000. **403**(6770): p. 614-615.

[40] Lämmerhofer, M., *Chiral recognition by enantioselective liquid chromatography: Mechanisms and modern chiral stationary phases.* J. Chromatogr., A, 2010. **1217**(6): p. 814-856.

[41] Pirkle, W.H., et al., *Considerations of Chiral Recognition Relevant to the Liquid Chromatographic Separation of Enantiomers.* Chem. Rev., 1989. **89**: p. 347-362.

[42] Oberleitner, W.R., et al., *Enantioseparation of various amino acid derivatives on a quinine based chiral anion-exchange selector at variable temperature conditions. Influence of structural parameters of the analytes on the apparent retention and enantioseparation characteristics.* J. Chromatogr., A, 2002. **960**(1-2): p. 97-108.

[43] Lämmerhofer, M., et al., *Recent developments in liquid chromatographic enantioseparation*, in *Handbook of Analytical Separations*, K. Valko, Editor. 2002, Elsevier Science B.V.: Amsterdam.

[44] Hoffmann, C.V., et al., *Novel strong cation-exchange type chiral stationary phase for the enantiomer separation of chiral amines by high-performance liquid chromatography.* J. Chromatogr., A, 2007. **1161**(1-2): p. 242-251.

[45] Hoffmann, C.V., et al., *Synergistic effects on enantioselectivity of zwitterionic chiral stationary phases for separations of chiral acids, bases, and amino acids by HPLC.* Anal Chem, 2008. **80**(22): p. 8780-8789.

[46] Hoffmann, C.V., et al., *Stationary phase-related investigations of quinine-based zwitterionic chiral stationary phases operated in anion-, cation-, and zwitterion-exchange modes.* J. Chromatogr., A, 2009. **1216**(7): p. 1147-1156.

[47] Kacprzak K.M., et al., *Triazolo-linked cinchona alkaloid carbamate anion exchange-type chiral stationary phases: Synthesis by click chemistry and evaluation.* J. Chromatogr., A, 2011. **1218**(11): p. 1452-1460.

[48] Reischl, R.J., et al., *Chemoselective and enantioselective analysis of proteinogenic amino acids utilizing N-derivatization and 1-D enantioselective anion-exchange chromatography in combination with tandem mass spectrometric detection.* J. Chromatogr., A, 2011. **1218**(46): p. 8379-8387.

[49] Lämmerhofer, M., et al., *Quinine and quinidine derivatives as chiral selectors. I. Brush type chiral stationary phases for high-performance liquid chromatography based on cinchonan carbamates and their application as chiral anion exchangers.* J. Chromatogr., A, 1996. **741**(1): p. 33-48.

[50] Mandl, A., et al., *Quinine versus carbamoylated quinine-based chiral anion exchangers. A comparison regarding enantioselectivity for N-protected amino acids and other chiral acids.* J. Chromatogr., A, 1999. **858**(1): p. 1-11.

[51] Lämmerhofer, M., et al., *Liquid Chromatographic Enantiomer Separation and Chiral Recognition by Cinchona Alkaloid-Derived Enantioselective Separation Materials*, in *Advances in Chromatography*, E. Grushka and N. Grinberg, Editors. 2008, CRC Press: Florida. p. 1-107.

[52] Kolb, H.C., et al., *Click chemistry: diverse chemical function from a few good reactions.* Angew. Chem., Int. Ed., 2001. **40**(11): p. 2004-2021.

[53] Lowe, A.B., *Thiol-ene "click" reactions and recent applications in polymer and materials synthesis.* Polym. Chem. **1**(1): p. 17-36.

[54] Krishnaveni, N.S., et al., *Study of the Michael addition of β-cyclodextrin-thiol complexes to conjugated alkenes in water.* Chem. Commun. (Cambridge, U. K.), **2005**(5): p. 669-671.

[55] Rissing, C., et al., *Application of Thiol-Ene Chemistry to the Preparation of Carbosilane-Thioether Dendrimers.* Organometallics, 2009. **28**(11): p. 3167-3172.

[56] Killops, K.L., et al., *Robust, Efficient, and Orthogonal Synthesis of Dendrimers via Thiol-ene "Click" Chemistry.* J. Am. Chem. Soc., 2008. **130**(15): p. 5062-5064.

[57] Rostovtsev, V.V., et al., *Copper-catalyzed cycloaddition of azides and acetylenes.* Abstracts of Papers, 224th ACS National Meeting, Boston, MA, United States, August 18-22, 2002, 2002: p. ORGN-458.

[58] Tornœ, C.W., et al., *Peptidotriazoles on Solid Phase: [1,2,3]-Triazoles by Regiospecific Copper(I)-Catalyzed 1,3-Dipolar Cycloadditions of Terminal Alkynes to Azides.* J. Org. Chem., 2002. **67**(9): p. 3057-3064.

[59] Boren, B.C., et al., *Ruthenium-Catalyzed Azide-Alkyne Cycloaddition: Scope and Mechanism.* J. Am. Chem. Soc., 2008. **130**(28): p. 8923-8930.

[60] Harmand, L., et al., *Huisgen click cycloadditions from a copper(II)-tren precatalyst without external sacrificial reductant.* Tetrahedron Lett. **53**(11): p. 1417-1420.

[61] Liang, L., et al., *The copper(I)-catalyzed alkyne-azide cycloaddition (CuAAC) "click" reaction and its applications. An overview.* Coord. Chem. Rev. **255**(23-24): p. 2933-2945.

[62] Kacprzak, K.M., et al., *Highly efficient immobilization of Cinchona alkaloid derivatives to silica gel via click chemistry.* Tetrahedron Lett., 2006. **47**(49): p. 8721-8726.

[63] Katritzky A.R., et al., *Comprehensive Organic Functional Group Transformations*, ed. J. Moody Christopher. Vol. 5. 1995, Cambridge: Pergamon. 11.

[64] Maier, N.M., et al., *Elucidation of the Chiral Recognition Mechanism of Cinchona Alkaloid Carbamate-type Receptors for 3,5-Dinitrobenzoyl Amino Acids.* J. Am. Chem. Soc., 2002. **124**(29): p. 8611-8629.

[65] Kacprzak, K.M., et al., *Novel Pirkle-type quinine 3,5-dinitrophenylcarbamate chiral stationary phase implementing click chemistry.* J. Sep. Sci., 2011. **34**(18): p. 2391-2396.

[66] Li, G.-X., et al., *Dichloro-4-quinolinol-3-carboxylic acid: Synthesis and antioxidant abilities to scavenge radicals and to protect methyl linoleate and DNA.* Eur. J. Med. Chem., 2010. **45**(5): p. 1821-1827.

[67] Maier, N.M., et al., *Enantioselective anion exchangers based on cinchona alkaloid-derived carbamates: influence of C8/C9 stereochemistry on chiral recognition.* Chirality, 1999. **11**(7): p. 522-528.

[68] Dijkstra, G.D.H., et al., *Conformational study of cinchona alkaloids. A combined NMR, molecular mechanics and x-ray approach.* J. Am. Chem. Soc., 1989. **111**(21): p. 8069-8076.

[69] Czerwenka, C., et al., *Direct high-performance liquid chromatographic separation of peptide enantiomers: Study on chiral recognition by systematic evaluation of the influence of structural features of the chiral selectors on enantioselectivity.* Anal. Chem., 2002. **74**(21): p. 5658-5666.

[70] Lämmerhofer, M., et al., *High-efficiency chiral separations of N-derivatized amino acids by packed-capillary electrochromatography with a quinine-based chiral anion-exchange type stationary phase.* J. Chromatogr., A, 1998. **829**(1+2): p. 115-125.

[71] Marshall, M.A., et al., *Silane isomer effect on the capacity of silica-immobilized 8-quinolinol.* Anal. Chem., 1985. **57**(1): p. 375-376.

[72] Lämmerhofer, M., et al., *Computerized optimization of the high-performance liquid chromatographic enantioseparation of a mixture of 4-dinitrophenyl amino acids on a quinine carbamate-type chiral stationary phase using DRYLAB.* J. Chromatogr., B: Biomed. Appl., 1997. **689**(1): p. 123-135.

[73] Piette, V., et al., *High-performance liquid chromatographic enantioseparation of N-protected α-amino acids using nonporous silica modified by a quinine carbamate as chiral stationary phase.* Chirality, 1997. **9**(2): p. 157-161.

[74] Hudson, H.R. and Kukhar, V.P., eds. *Aminophosphonic and aminophosphinic acids: chemistry and biological activity*. 2000, Wiley. 634.

[75] Gavioli, E., et al., *Analyte Templating: Enhancing the Enantioselectivity of Chiral Selectors upon Incorporation into Organic Polymer Environments.* Anal. Chem., 2005. **77**(15): p. 5009-5018.

[76] Hoffmann, C.V., et al., *Synergistic effects on enantioselectivity of zwitterionic chiral stationary phases for separations of chiral acids, bases, and amino acids by HPLC.* Anal Chem, 2008. **80**(22): p. 8780-8789.

[77] Kohout, M., et al., *Novel Chiral Selector Based on Mefloquine - A Comparative NMR Study to Elucidate Intermolecular Interactions with Acidic Chiral Selectands.* Chirality, 2012 (in press).

[78] Stahlberg, J., *Retention models for ions in chromatography.* J. Chromatogr., A, 1999. **855**(1): p. 3-55.

VIII. Appendix

Table I: Column 1 (150x4 mm ID, 179 µmol/g, DHQN-type CSP; injection volume: 5 µL; sample concentration: 1 mg/mL MeOH; flow rate: 1.0 mL/min; detection wavelength: 254 nm; mobile phase composition: MeOH/AcOH/NH_4OAc 99/1/0.25 (v/v/w); temperature: 25°C): different t_0-values derive from different positions of the column in the column compartment.

Analyte	t_0 [min.]	t_{r1} [min.]	t_{r2} [min.]	EO	k_1	k_2	α	R	N_1	N_2
Bz-Leu (L>D)	1.441	3.612	4.440	D	1.51	2.08	1.38	3.53	4671	4771
PFB-Leu (rac.)	1.441	3.512	3.512	///	1.44	1.44	1.00	0.00	2273	2273
A-DCL-Leu (rac.)	1.441	4.729	9.698	D	2.28	5.73	2.51	11.39	4421	4330
DNB-Leu (rac.)	1.441	6.098	17.473	D	3.23	11.13	3.44	16.34	4645	4522
DCB-Leu (rac.)	1.441	4.547	8.540	D	2.16	4.93	2.29	10.34	4659	4529
BTFMB-Leu (rac.)	1.441	2.928	5.117	D	1.03	2.55	2.47	9.04	4451	4374
DNB-N-Me-Leu (rac.)	1.441	6.907	7.434	D	3.79	4.16	1.10	1.10	3874	3352
Ac-Phe (rac.)	1.441	3.707	4.579	D	1.57	2.18	1.38	3.70	4999	4898
Z-Phe (rac.)	1.441	6.148	6.553	D	3.27	3.55	1.09	1.03	4049	4297
Phe (rac.)	1.441	1.640	1.640	///	0.14	0.14	1.00	0.00	2034	2034
DNZ-Phe (D>L)	1.441	10.395	17.845	D	6.21	11.38	1.83	9.16	4782	4873
BOC-Phe (rac.)	1.441	4.136	4.517	D	1.87	2.13	1.14	1.55	4991	4867
FMOC-β-Phe (rac.)	1.441	5.103	5.730	D	2.54	2.98	1.17	1.94	4472	4475
Z-β-Phe (rac.)	1.441	3.575	3.575	///	1.48	1.48	1.00	0.00	4432	4432
Bz-Phe (D>L)	1.441	5.299	6.855	D	2.68	3.76	1.40	4.49	4937	4883
Phenyl-Gly (rac.)	1.441	1.649	1.649	///	0.14	0.14	1.00	0.00	907	907
DNZ-Val (D>L)	1.441	6.828	10.742	D	3.74	6.45	1.73	7.61	4766	4578
BOC-Tyr (rac.)	1.441	3.996	4.233	D	1.77	1.94	1.09	0.98	4645	4526
Ac-Trp (rac.)	1.441	4.841	5.819	D	2.36	3.04	1.29	3.13	4746	4552
FMOC-Asn (rac.)	1.441	7.120	7.990	D	3.94	4.54	1.15	1.92	4465	4447
DNB-Pro (rac.)	1.441	6.382	6.382	///	3.43	3.43	1.00	0.00	1739	1739
FMOC-Ile (L>D)	1.441	5.573	7.170	D	2.87	3.98	1.39	3.16	4581	501
FMOC-Gln (rac.)	1.441	1.686	1.686	///	0.17	0.17	1.00	0.00	3004	3004
Z-Ser (rac.)	1.441	4.494	4.494	///	2.12	2.12	1.00	0.00	4522	4522
FMOC-Pro (L>D)	1.441	5.960	5.960	///	3.14	3.14	1.00	0.00	2836	2836
FMOC-Aze (rac.)	1.441	6.743	7.090	D	3.68	3.92	1.07	0.87	4927	4779
DBTAMME (rac.)	1.441	6.951	7.805	S,S	3.82	4.42	1.15	2.00	4741	4839
Trolox (rac.)	1.441	3.738	4.062	S	1.59	1.82	1.14	1.42	4695	4644
Ibuprofen (rac)	1.441	2.623	2.623	///	0.82	0.82	1.00	0.00	2608	2608
Naproxen (rac.)	1.441	3.497	3.497	///	1.43	1.43	1.00	0.00	3936	3936
DNP-Mandelic acid (rac.)	1.775	29.004	39.736	R	15.34	21.39	1.39	5.10	4202	4325
Acetylmandelic acid (rac.)	1.441	4.924	5.286	S	2.42	2.67	1.10	1.26	5293	4880
Phenylbutyric acid (rac.)	1.441	2.370	2.370	///	0.64	0.64	1.00	0.00	4550	4550
TMB-Ala (rac.)	1.441	3.893	5.209	///	1.70	2.61	1.54	4.98	4775	4713
Bz-ACHSA (rac.)	1.441	5.289	5.678	///	2.67	2.94	1.10	1.27	5107	5224
MFQ.HCl (rac.)	1.441	1.401	1.401	///	-0.03	-0.03	1.00	0.00	1792	1792
BOC-Gly	1.441	3.999	///	///	1.78	///	///	///	254	///
DNZ-Gly	1.441	8.081	///	///	4.61	///	///	///	5041	///
Vanillylmandelic acid (rac.)	1.441	5.583	5.583	///	2.87	2.87	1.00	0.00	2105	2105
Nitrophenylpropionic acid (rac.)	1.441	3.894	3.952	///	1.70	1.74	1.02	0.32	7324	7672
Hydroxyphenyllactic acid (rac.)	1.441	5.269	5.829	///	2.66	3.05	1.15	1.73	4742	4618
Tropic acid (rac.)	1.441	2.766	2.766	///	0.92	0.92	1.00	0.00	4943	4943
Fenoprofen (rac.)	1.441	3.187	3.187	///	1.21	1.21	1.00	0.00	4000	4000
Dichlorprop (rac.)	1.441	6.718	6.718	///	3.66	3.66	1.00	0.00	4224	4224
Hydroxymandelic acid (rac.)	1.441	5.494	5.494	///	2.81	2.81	1.00	0.00	3455	3455
Atrolactic acid (rac.)	1.441	4.875	4.875	///	2.38	2.38	1.00	0.00	3243	3243
Carprofen (rac.)	1.441	4.034	4.149	///	1.80	1.88	1.04	0.54	6356	5591
FMOC-Abu (rac.)	1.441	5.474	6.250	///	2.80	3.34	1.19	2.07	3133	4656
Flurbiprofen (rac.)	1.441	3.622	3.622	///	1.51	1.51	1.00	0.00	2709	2709
Bz-β-Phe (rac.)	1.441	3.682	4.138	///	1.56	1.87	1.20	1.91	4246	4319
Z-Leu (rac.)	1.441	3.867	3.867	///	1.68	1.68	1.00	0.00	4627	4627
Z-Arg (L>D)	1.441	2.053	2.053	///	0.42	0.42	1.00	0.00	2335	2335
Trp (rac.)	1.441	1.840	1.840	///	0.28	0.28	1.00	0.00	1187	1187
Tyr (rac.)	1.441	1.654	1.654	///	0.15	0.15	1.00	0.00	2153	2153
QN/QD (2:1)	1.441	1.585	1.585	///	0.10	0.10	1.00	0.00	1578	1578
Clenbuterol.HCl (rac.)	1.441	1.281	1.281	///	-0.11	-0.11	1.00	0.00	2025	2025
PI-2-56-2	1.441	7.971	11.040	///	4.53	6.66	1.47	4.54	3408	2912
PI-2-4-3	1.441	11.452	11.596	///	6.95	7.05	1.01	0.19	4375	2714
PI-2-25-1	1.441	8.206	9.050	///	4.69	5.28	1.12	1.59	4363	4104
PI-2-34-1	1.441	4.369	5.477	///	2.03	2.80	1.38	3.44	3851	3622
PI-3-67-1	1.441	7.032	9.853	///	3.88	5.84	1.50	5.68	4601	4631
PI-1-89-1	1.441	7.342	8.181	///	4.10	4.68	1.14	1.84	4673	4613
PI-2-15-1	1.441	6.827	7.708	///	3.74	4.35	1.16	2.00	4330	4340
PI-2-38-1	1.441	4.165	5.314	///	1.89	2.69	1.42	4.14	4753	4576
PI-2-87-1	1.441	4.599	5.845	///	2.19	3.06	1.39	4.06	4748	4517
P-DML-ACHSA (S,S>R,R)	1.775	6.812	7.427	R,R	2.84	3.18	1.12	1.59	5480	5381
P-DCL-ACHSA (S,S>R,R)	1.775	9.517	10.991	R,R	4.36	5.19	1.19	2.70	5692	5571

Table II: Column 2 (150x4 mm ID, 144 µmol/g, DHQD-type CSP; injection volume: 5 µL; sample concentration: 1 mg/mL MeOH; flow rate: 1.0 mL/min; detection wavelength: 254 nm; mobile phase composition: MeOH/AcOH/NH_4OAc 99/1/0.25 (v/v/w); temperature: 25°C): different t_0-values derive from different positions of the column in the column compartment.

Analyte	t_0 [min.]	t_{r1} [min.]	t_{r2} [min.]	EO	k_1	k_2	α	R	N_1	N_2
Bz-Leu (L>D)	1.441	3.612	4.440	D	1.51	2.08	1.38	3.53	4671	4771
PFB-Leu (rac.)	1.441	3.512	3.512	///	1.44	1.44	1.00	0.00	2273	2273
A-DCL-Leu (rac.)	1.441	4.729	9.698	D	2.28	5.73	2.51	11.39	4421	4330
DNB-Leu (rac.)	1.441	6.098	17.473	D	3.23	11.13	3.44	16.34	4645	4522
DCB-Leu (rac.)	1.441	4.547	8.540	D	2.16	4.93	2.29	10.34	4659	4529
BTFMB-Leu (rac.)	1.441	2.928	5.117	D	1.03	2.55	2.47	9.04	4451	4374
DNB-N-Me-Leu (rac.)	1.441	6.907	7.434	D	3.79	4.16	1.10	1.10	3874	3352
Ac-Phe (rac.)	1.441	3.707	4.579	D	1.57	2.18	1.38	3.70	4999	4898
Z-Phe (rac.)	1.441	6.148	6.553	D	3.27	3.55	1.09	1.03	4049	4297
Phe (rac.)	1.441	1.640	1.640	///	0.14	0.14	1.00	0.00	2034	2034
DNZ-Phe (D>L)	1.441	10.395	17.845	D	6.21	11.38	1.83	9.16	4782	4873
BOC-Phe (rac.)	1.441	4.136	4.517	D	1.87	2.13	1.14	1.55	4991	4867
FMOC-β-Phe (rac.)	1.441	5.103	5.730	D	2.54	2.98	1.17	1.94	4472	4475
Z-β-Phe (rac.)	1.441	3.575	3.575	///	1.48	1.48	1.00	0.00	4432	4432
Bz-Phe (D>L)	1.441	5.299	6.855	D	2.68	3.76	1.40	4.49	4937	4883
Phenyl-Gly (rac.)	1.441	1.649	1.649	///	0.14	0.14	1.00	0.00	907	907
DNZ-Val (D>L)	1.441	6.828	10.742	D	3.74	6.45	1.73	7.61	4766	4578
BOC-Tyr (rac.)	1.441	3.996	4.233	D	1.77	1.94	1.09	0.98	4645	4526
Ac-Trp (rac.)	1.441	4.841	5.819	D	2.36	3.04	1.29	3.13	4746	4552
FMOC-Asn (rac.)	1.441	7.120	7.990	D	3.94	4.54	1.15	1.92	4465	4447
DNB-Pro (rac.)	1.441	6.382	6.382	///	3.43	3.43	1.00	0.00	1739	1739
FMOC-Ile (L>D)	1.441	5.573	7.170	D	2.87	3.98	1.39	3.16	4581	501
FMOC-Gln (rac.)	1.441	1.686	1.686	///	0.17	0.17	1.00	0.00	3004	3004
Z-Ser (rac.)	1.441	4.494	4.494	///	2.12	2.12	1.00	0.00	4522	4522
FMOC-Pro (L>D)	1.441	5.960	5.960	///	3.14	3.14	1.00	0.00	2836	2836
FMOC-Aze (rac.)	1.441	6.743	7.090	D	3.68	3.92	1.07	0.87	4927	4779
DBTAMME (rac.)	1.441	6.951	7.805	S,S	3.82	4.42	1.15	2.00	4741	4839
Trolox (rac.)	1.441	3.738	4.062	S	1.59	1.82	1.14	1.42	4695	4644
Ibuprofen (rac)	1.441	2.623	2.623	///	0.82	0.82	1.00	0.00	2608	2608
Naproxen (rac.)	1.441	3.497	3.497	///	1.43	1.43	1.00	0.00	3936	3936
DNP-Mandelic acid (rac.)	1.775	29.004	39.736	R	15.34	21.39	1.39	5.10	4202	4325
Acetylmandelic acid (rac.)	1.441	4.924	5.286	S	2.42	2.67	1.10	1.26	5293	4880
Phenylbutyric acid (rac.)	1.441	2.370	2.370	///	0.64	0.64	1.00	0.00	4550	4550
TMB-Ala (rac.)	1.441	3.893	5.209	///	1.70	2.61	1.54	4.98	4775	4713
Bz-ACHSA (rac.)	1.441	5.289	5.678	///	2.67	2.94	1.10	1.27	5107	5224
MFQ.HCl (rac.)	1.441	1.401	1.401	///	-0.03	-0.03	1.00	0.00	1792	1792
BOC-Gly	1.441	3.999	///	///	1.78	///	///	///	254	///
DNZ-Gly	1.441	8.081	///	///	4.61	///	///	///	5041	///
Vanillylmandelic acid (rac.)	1.441	5.583	5.583	///	2.87	2.87	1.00	0.00	2105	2105
Nitrophenylpropionic acid (rac.)	1.441	3.894	3.952	///	1.70	1.74	1.02	0.32	7324	7672
Hydroxyphenyllactic acid (rac.)	1.441	5.269	5.829	///	2.66	3.05	1.15	1.73	4742	4618
Tropic acid (rac.)	1.441	2.766	2.766	///	0.92	0.92	1.00	0.00	4943	4943
Fenoprofen (rac.)	1.441	3.187	3.187	///	1.21	1.21	1.00	0.00	4000	4000
Dichlorprop (rac.)	1.441	6.718	6.718	///	3.66	3.66	1.00	0.00	4224	4224
Hydroxymandelic acid (rac.)	1.441	5.494	5.494	///	2.81	2.81	1.00	0.00	3455	3455
Atrolactic acid (rac.)	1.441	4.875	4.875	///	2.38	2.38	1.00	0.00	3243	3243
Carprofen (rac.)	1.441	4.034	4.149	///	1.80	1.88	1.04	0.54	6356	5591
FMOC-Abu (rac.)	1.441	5.474	6.250	///	2.80	3.34	1.19	2.07	3133	4656
Flurbiprofen (rac.)	1.441	3.622	3.622	///	1.51	1.51	1.00	0.00	2709	2709
Bz-β-Phe (rac.)	1.441	3.682	4.138	///	1.56	1.87	1.20	1.91	4246	4319
Z-Leu (rac.)	1.441	3.867	3.867	///	1.68	1.68	1.00	0.00	4627	4627
Z-Arg (L>D)	1.441	2.053	2.053	///	0.42	0.42	1.00	0.00	2335	2335
Trp (rac.)	1.441	1.840	1.840	///	0.28	0.28	1.00	0.00	1187	1187
Tyr (rac.)	1.441	1.654	1.654	///	0.15	0.15	1.00	0.00	2153	2153
QN/QD (2:1)	1.441	1.585	1.585	///	0.10	0.10	1.00	0.00	1578	1578
Clenbuterol.HCl (rac.)	1.441	1.281	1.281	///	-0.11	-0.11	1.00	0.00	2025	2025
PI-2-56-2	1.441	7.971	11.040	///	4.53	6.66	1.47	4.54	3408	2912
PI-2-4-3	1.441	11.452	11.596	///	6.95	7.05	1.01	0.19	4375	2714
PI-2-25-1	1.441	8.206	9.050	///	4.69	5.28	1.12	1.59	4363	4104
PI-2-34-1	1.441	4.369	5.477	///	2.03	2.80	1.38	3.44	3851	3622
PI-3-67-1	1.441	7.032	9.853	///	3.88	5.84	1.50	5.68	4601	4631
PI-1-89-1	1.441	7.342	8.181	///	4.10	4.68	1.14	1.84	4673	4613
PI-2-15-1	1.441	6.827	7.708	///	3.74	4.35	1.16	2.00	4330	4340
PI-2-38-1	1.441	4.165	5.314	///	1.89	2.69	1.42	4.14	4753	4576
PI-2-87-1	1.441	4.599	5.845	///	2.19	3.06	1.39	4.06	4748	4517
P-DML-ACHSA (S,S>R,R)	1.775	6.812	7.427	R,R	2.84	3.18	1.12	1.59	5480	5381
P-DCL-ACHSA (S,S>R,R)	1.775	9.517	10.991	R,R	4.36	5.19	1.19	2.70	5692	5571

Table III: Column 3 (150x4 mm ID, 477 µmol/g, DHQN-type CSP; injection volume: 5 µL; sample concentration: 1 mg/mL MeOH; flow rate: 1.0 mL/min; detection wavelength: 254 nm; mobile phase composition: MeOH/AcOH/NH_4OAc 99/1/0.25 (v/v/w); temperature: 25°C): different t_0-values derive from different positions of the column in the column compartment.

Analyte	t_0 [min.]	t_{r1} [min.]	t_{r2} [min.]	EO	k_1	k_2	α	R	N_1	N_2
Bz-Leu (L>D)	1.334	3.643	4.186	D	1.73	2.14	1.24	1.23	1464	1072
PFB-Leu (rac.)	1.334	3.397	3.397	///	1.55	1.55	1.00	0.00	1492	1492
A-DCL-Leu (rac.)	1.334	5.227	8.658	D	2.92	5.49	1.88	4.64	1709	1112
DNB-Leu (rac.)	1.469	13.792	33.706	D	8.39	21.94	2.62	6.68	1291	739
DCB-Leu (rac.)	1.334	5.890	9.718	D	3.42	6.28	1.84	4.89	1893	1288
BTFMB-Leu (rac.)	1.334	2.947	4.030	D	1.21	2.02	1.67	3.63	2575	1811
DNB-N-Me-Leu (rac.)	1.334	10.705	10.705	///	7.02	7.02	1.00	0.00	692	692
Ac-Phe (rac.)	1.334	5.433	6.567	D	3.07	3.92	1.28	1.69	1377	1195
Z-Phe (rac.)	1.469	14.216	14.216	///	8.68	8.68	1.00	0.00	1196	1196
Phe (rac.)	1.469	1.500	1.500	///	0.02	0.02	1.00	0.00	1738	1738
DNZ-Phe (D>L)	1.469	2.133	2.407	D	0.45	0.64	1.41	1.64	2811	3061
BOC-Phe (rac.)	1.469	7.311	7.716	D	3.98	4.25	1.07	0.61	2162	1936
FMOC-β-Phe (rac.)	1.334	8.939	9.541	D	5.70	6.15	1.08	0.66	1981	1322
Z-β-Phe (rac.)	1.334	5.908	5.908	///	3.43	3.43	1.00	0.00	785	785
Bz-Phe (D>L)	1.334	10.036	12.081	D	6.52	8.06	1.24	1.96	1855	1749
Phenyl-Gly (rac.)	1.469	1.504	1.504	///	0.02	0.02	1.00	0.00	2222	2222
DNZ-Val (D>L)	1.469	17.772	23.674	D	11.10	15.12	1.36	2.46	1302	1089
BOC-Tyr (rac.)	1.469	10.197	10.614	D	5.94	6.23	1.05	0.57	2752	3809
Ac-Trp (rac.)	1.334	11.893	14.227	D	7.92	9.66	1.22	1.83	1618	1734
FMOC-Asn (rac.)	1.469	17.534	18.099	D	10.94	11.32	1.04	0.36	2446	1626
DNB-Pro (rac.)	1.469	16.237	16.237	///	10.05	10.05	1.00	0.00	760	760
FMOC-Ile (L>D)	1.334	9.265	10.844	D	5.95	7.13	1.20	1.58	1727	1500
FMOC-Gln (rac.)	1.469	1.533	1.533	///	0.04	0.04	1.00	0.00	2518	2518
Z-Ser (rac.)	1.334	10.699	10.699	///	7.02	7.02	1.00	0.00	944	944
FMOC-Pro (L>D)	1.334	9.895	9.895	///	6.42	6.42	1.00	0.00	931	931
FMOC-Aze (rac.)	1.334	12.908	13.492	D	8.68	9.11	1.05	0.50	2585	1514
DBTAMME (rac.)	1.469	17.555	20.878	S,S	10.95	13.21	1.21	1.48	1183	1168
Trolox (rac.)	1.334	8.815	11.411	S	5.61	7.55	1.35	1.75	816	672
Ibuprofen (rac)	1.334	3.576	3.576	///	1.68	1.68	1.00	0.00	1871	1871
Naproxen (rac.)	1.334	7.103	7.103	///	4.32	4.32	1.00	0.00	1267	1267
DNP-Mandelic acid (rac.)	1.469	97.687	109.533	R	65.50	73.56	1.12	0.85	947	824
Acetylmandelic acid (rac.)	1.334	10.063	11.157	S	6.54	7.36	1.13	1.01	1612	1477
Phenylbutyric acid (rac.)	1.334	3.464	3.464	///	1.60	1.60	1.00	0.00	2610	2610
TMB-Ala (rac.)	1.334	6.689	8.361	///	4.01	5.27	1.31	2.05	1490	1227
Bz-ACHSA (rac.)	1.334	12.861	12.861	///	8.64	8.64	1.00	0.00	594	594
MFQ.HCl (rac.)	1.334	1.143	1.143	///	-0.14	-0.14	1.00	0.00	1637	1637
BOC-Gly	1.469	4.263	///	///	1.90	///	///	///	217	///
DNZ-Gly	1.469	31.486	///	///	20.43	///	///	///	1335	///
Vanillylmandelic acid (rac.)	1.334	11.763	11.763	///	7.82	7.82	1.00	0.00	274	274
Nitrophenylpropionic acid (rac.)	1.334	9.590	9.590	///	6.19	6.19	1.00	0.00	956	956
Hydroxyphenyllactic acid (rac.)	1.469	24.526	33.506	///	15.70	21.81	1.39	2.82	1380	1277
Tropic acid (rac.)	1.334	6.119	13.920	///	3.59	9.43	2.63	4.63	339	794
Fenoprofen (rac.)	1.334	5.316	5.407	///	2.99	3.05	1.02	0.25	3279	3440
Dichlorprop (rac.)	1.469	18.216	24.548	///	11.40	15.71	1.38	2.62	1661	836
Hydroxymandelic acid (rac.)	1.469	30.397	30.397	///	19.69	19.69	1.00	0.00	2943	2943
Atrolactic acid (rac.)	1.334	11.194	13.432	///	7.39	9.07	1.23	1.30	255	1377
Carprofen (rac.)	1.334	11.100	11.100	///	7.32	7.32	1.00	0.00	801	801
FMOC-Abu (rac.)	1.334	10.524	11.521	///	6.89	7.64	1.11	0.96	1914	1673
Flurbiprofen (rac.)	1.334	6.809	7.072	///	4.10	4.30	1.05	0.50	3234	2367
Bz-β-Phe (rac.)	1.334	7.073	7.546	///	4.30	4.66	1.08	0.70	2127	1584
Z-Leu (rac.)	1.334	5.987	5.987	///	3.49	3.49	1.00	0.00	1462	1462
Z-Arg (L>D)	1.334	1.958	1.958	///	0.47	0.47	1.00	0.00	1873	1873
Trp (rac.)	1.334	1.935	1.935	///	0.45	0.45	1.00	0.00	1030	1030
Tyr (rac.)	1.334	1.738	1.738	///	0.30	0.30	1.00	0.00	1964	1964
QN/QD (2:1)	1.334	1.239	1.239	///	-0.07	-0.07	1.00	0.00	1726	1726
Clenbuterol.HCl (rac.)	1.334	1.089	1.089	///	-0.18	-0.18	1.00	0.00	2118	2118
PI-2-56-2	1.334	4.374	4.374	///	2.28	2.28	1.00	0.00	4552	4552
PI-2-4-3	1.469	21.847	28.416	///	13.87	18.34	1.32	2.01	1053	842
PI-2-25-1	1.469	13.764	13.764	///	8.37	8.37	1.00	0.00	676	676
PI-2-34-1	1.334	6.064	6.896	///	3.55	4.17	1.18	1.16	1478	1118
PI-3-67-1	1.334	9.989	11.607	///	6.49	7.70	1.19	1.42	1471	1385
PI-1-89-1	1.334	12.756	13.866	///	8.56	9.39	1.10	0.75	1286	1286
PI-2-15-1	1.334	8.402	10.120	///	5.30	6.59	1.24	1.75	1496	1354
PI-2-38-1	1.334	6.138	7.244	///	3.60	4.43	1.23	1.42	1377	989
PI-2-87-1	1.334	6.134	7.024	///	3.60	4.27	1.19	1.22	1463	1132
P-DML-ACHSA (S,S>R,R)	1.469	11.684	11.684	///	6.95	6.95	1.00	0.00	651	651
P-DCL-ACHSA (S,S>R,R)	1.469	20.879	20.879	///	13.21	13.21	1.00	0.00	1077	1077

Table IV: Column 4 (150x4 mm ID, 490 µmol/g, DHQD-type CSP; injection volume: 5 µL; sample concentration: 1 mg/mL MeOH; flow rate: 1.0 mL/min; detection wavelength: 254 nm; mobile phase composition: MeOH/AcOH/NH_4OAc 99/1/0.25 (v/v/w); temperature: 25°C): different t_0-values derive from different positions of the column in the column compartment.

Analyte	t_0 [min.]	t_{r1} [min.]	t_{r2} [min.]	EO	k_1	k_2	α	R	N_1	N_2
Bz-Leu (L>D)	1.287	3.294	4.105	L	1.56	2.19	1.40	2.04	1636	1143
PFB-Leu (rac.)	1.287	3.354	3.354	///	1.61	1.61	1.00	0.00	1487	1487
A-DCL-Leu (rac.)	1.287	4.727	9.456	L	2.67	6.35	2.37	6.92	2147	1302
DNB-Leu (rac.)	1.314	10.808	31.665	L	7.23	23.10	3.20	8.89	1621	999
DCB-Leu (rac.)	1.287	5.380	10.439	L	3.18	7.11	2.24	6.99	2325	1495
BTFMB-Leu (rac.)	1.287	2.706	4.331	L	1.10	2.37	2.15	5.74	3051	1891
DNB-N-Me-Leu (rac.)	1.287	13.335	13.335	///	9.36	9.36	1.00	0.00	671	671
Ac-Phe (rac.)	1.287	5.209	6.842	L	3.05	4.32	1.42	3.12	2149	2081
Z-Phe (rac.)	1.287	10.003	10.951	L	6.77	7.51	1.11	0.93	1773	1603
Phe (rac.)	1.314	1.490	1.490	///	0.13	0.13	1.00	0.00	1981	1981
DNZ-Phe (D>L)	1.314	2.028	2.266	L	0.54	0.72	1.33	1.49	2819	2950
BOC-Phe (rac.)	1.287	5.373	5.901	L	3.17	3.59	1.13	1.01	1954	1789
FMOC-β-Phe (rac.)	1.287	7.774	9.615	L	5.04	6.47	1.28	2.08	1711	1390
Z-β-Phe (rac.)	1.287	5.149	5.149	///	3.00	3.00	1.00	0.00	1099	1099
Bz-Phe (D>L)	1.287	9.044	11.589	L	6.03	8.00	1.33	2.29	1526	1233
Phenyl-Gly (rac.)	1.314	1.492	1.492	///	0.14	0.14	1.00	0.00	2258	2258
DNZ-Val (D>L)	1.287	13.089	19.781	L	9.17	14.37	1.57	4.06	1842	1342
BOC-Tyr (rac.)	1.287	7.192	8.014	L	4.59	5.23	1.14	1.07	1605	1503
Ac-Trp (rac.)	1.287	9.793	12.633	L	6.61	8.82	1.33	2.22	1290	1169
FMOC-Asn (rac.)	1.287	12.682	14.290	L	8.85	10.10	1.14	1.19	1713	1469
DNB-Pro (rac.)	1.287	13.354	14.336	D	9.38	10.14	1.08	0.72	1823	1429
FMOC-Ile (L>D)	1.287	7.743	10.233	L	5.02	6.95	1.39	2.93	1928	1654
FMOC-Gln (rac.)	1.314	1.530	1.530	///	0.16	0.16	1.00	0.00	2312	2312
Z-Ser (rac.)	1.287	8.682	8.682	///	5.75	5.75	1.00	0.00	1075	1075
FMOC-Pro (L>D)	1.287	8.495	9.183	L	5.60	6.14	1.10	0.81	1732	1713
FMOC-Aze (rac.)	1.287	10.985	11.933	L	7.54	8.27	1.10	0.86	1813	1612
DBTAMME (rac.)	1.287	11.516	13.338	R,R	7.95	9.36	1.18	1.39	1444	1432
Trolox (rac.)	1.287	6.373	7.519	R	3.95	4.84	1.23	1.54	1619	1162
Ibuprofen (rac)	1.287	2.983	2.983	///	1.32	1.32	1.00	0.00	1897	1897
Naproxen (rac.)	1.287	5.784	5.784	///	3.49	3.49	1.00	0.00	1788	1788
DNP-Mandelic acid (rac.)	1.314	59.366	75.860	S	44.18	56.73	1.28	2.13	1268	1163
Acetylmandelic acid (rac.)	1.314	9.256	9.256	///	6.04	6.04	1.00	0.00	1152	1152
Phenylbutyric acid (rac.)	1.287	2.992	2.992	///	1.32	1.32	1.00	0.00	3257	3257
TMB-Ala (rac.)	1.287	5.680	8.502	///	3.41	5.61	1.64	3.81	1517	1421
Bz-ACHSA (rac.)	1.314	13.464	13.464	///	9.25	9.25	1.00	0.00	1220	1220
MFQ.HCl (rac.)	1.287	1.142	1.142	///	-0.11	-0.11	1.00	0.00	1674	1674
BOC-Gly	1.287	3.792	///	///	1.95	///	///	///	1251	///
DNZ-Gly	1.314	26.203	///	///	18.94	///	///	///	1722	///
Vanillylmandelic acid (rac.)	1.287	17.937	17.937	///	12.94	12.94	1.00	0.00	1722	1722
Nitrophenylpropionic acid (rac.)	1.287	8.584	8.584	///	5.67	5.67	1.00	0.00	2387	2387
Hydroxyphenyllactic acid (rac.)	1.287	16.140	17.668	///	11.54	12.73	1.10	0.84	1478	1295
Tropic acid (rac.)	1.287	4.695	4.695	///	2.65	2.65	1.00	0.00	1955	1955
Fenoprofen (rac.)	1.287	5.516	5.516	///	3.29	3.29	1.00	0.00	4295	4295
Dichlorprop (rac.)	1.287	13.331	15.489	///	9.36	11.03	1.18	1.42	1876	1009
Hydroxymandelic acid (rac.)	1.287	19.727	20.058	///	14.33	14.59	1.02	0.20	2971	1584
Atrolactic acid (rac.)	1.287	10.682	10.682	///	7.30	7.30	1.00	0.00	1388	1388
Carprofen (rac.)	1.287	8.464	8.464	///	5.58	5.58	1.00	0.00	1395	1395
FMOC-Abu (rac.)	1.287	8.938	10.578	///	5.94	7.22	1.21	1.84	2040	1787
Flurbiprofen (rac.)	1.287	5.994	5.994	///	3.66	3.66	1.00	0.00	1938	1938
Bz-β-Phe (rac.)	1.287	5.879	7.140	///	3.57	4.55	1.27	1.97	1773	1520
Z-Leu (rac.)	1.287	4.846	5.131	///	2.77	2.99	1.08	0.76	2833	2796
Z-Arg (L>D)	1.287	1.826	1.826	///	0.42	0.42	1.00	0.00	2435	2435
Trp (rac.)	1.287	1.911	1.911	///	0.48	0.48	1.00	0.00	1651	1651
Tyr (rac.)	1.287	1.701	1.701	///	0.32	0.32	1.00	0.00	2208	2208
QN/QD (2:1)	1.287	1.215	1.215	///	-0.06	-0.06	1.00	0.00	1348	1348
Clenbuterol.HCl (rac.)	1.287	1.050	1.050	///	-0.18	-0.18	1.00	0.00	2126	2126
PI-2-56-2	1.287	12.833	13.793	///	8.97	9.72	1.08	0.58	1286	780
PI-2-4-3	1.314	20.062	32.418	///	14.27	23.67	1.66	4.12	1372	1081
PI-2-25-1	1.287	10.308	11.624	///	7.01	8.03	1.15	0.99	1135	1028
PI-2-34-1	1.287	5.312	6.143	///	3.13	3.77	1.21	1.40	1637	1331
PI-3-67-1	1.287	8.503	10.140	///	5.61	6.88	1.23	1.65	1491	1322
PI-1-89-1	1.287	11.596	11.596	///	8.01	8.01	1.00	0.00	1123	1123
PI-2-15-1	1.287	7.213	10.331	///	4.60	7.03	1.53	3.62	1797	1513
PI-2-38-1	1.287	5.260	6.323	///	3.09	3.91	1.27	1.70	1590	1145
PI-2-87-1	1.287	5.393	6.215	///	3.19	3.83	1.20	1.37	1650	1324
P-DML-ACHSA (S,S>R,R)	1.314	10.899	11.517	S,S	7.29	7.76	1.06	0.57	1697	1757
P-DCL-ACHSA (S,S>R,R)	1.314	18.773	18.773	///	13.29	13.29	1.00	0.00	736	736

Table V: Column 5 (150x4 mm ID, 214 µmol/g, DHQN-type CSP; injection volume: 5 µL; sample concentration: 1 mg/mL MeOH; flow rate: 1.0 mL/min; detection wavelength: 254 nm; mobile phase composition: MeOH/AcOH/NH_4OAc 99/1/0.25 (v/v/w); temperature: 25°C): different t_0-values derive from different positions of the column in the column compartment.

Analyte	t_0 [min.]	t_{r1} [min.]	t_{r2} [min.]	EO	k_1	k_2	α	R	N_1	N_2
Bz-Leu (L>D)	1.499	3.190	3.850	D	1.13	1.57	1.39	3.26	4878	4785
PFB-Leu (rac.)	1.499	3.082	3.082	///	1.06	1.06	1.00	0.00	2432	2432
A-DCL-Leu (rac.)	1.499	4.137	8.065	D	1.76	4.38	2.49	10.47	4497	3967
DNB-Leu (rac.)	1.499	5.768	16.912	D	2.85	10.28	3.61	15.45	4339	3570
DCB-Leu (rac.)	1.499	4.114	7.481	D	1.74	3.99	2.29	9.77	4811	4247
BTFMB-Leu (rac.)	1.499	2.643	4.244	D	0.76	1.83	2.40	7.85	4725	4405
DNB-N-Me-Leu (rac.)	1.499	6.522	6.836	D	3.35	3.56	1.06	0.74	3568	4421
Ac-Phe (rac.)	1.499	3.871	4.789	D	1.58	2.19	1.39	3.72	4935	4908
Z-Phe (rac.)	1.499	6.161	6.593	D	3.11	3.40	1.09	1.03	3455	3944
Phe (rac.)	1.498	1.658	1.658	///	0.11	0.11	1.00	0.00	2569	2569
DNZ-Phe (D>L)	1.499	1.936	10.853	D	0.29	6.24	21.41	21.36	3457	4052
BOC-Phe (rac.)	1.499	4.028	4.398	D	1.69	1.93	1.15	1.52	4734	4801
FMOC-β-Phe (rac.)	1.499	4.969	5.569	D	2.31	2.72	1.17	1.80	4171	3848
Z-β-Phe (rac.)	1.498	3.893	3.893	///	1.60	1.60	1.00	0.00	4983	4983
Bz-Phe (D>L)	1.499	5.474	7.041	D	2.65	3.70	1.39	4.22	4618	4455
Phenyl-Gly (rac.)	1.499	1.705	1.705	///	0.14	0.14	1.00	0.00	1551	1551
DNZ-Val (D>L)	1.499	6.867	10.981	D	3.58	6.33	1.77	7.25	4265	3660
BOC-Tyr (rac.)	1.499	4.412	4.773	D	1.94	2.18	1.12	1.29	4255	4372
Ac-Trp (rac.)	1.499	5.709	7.101	D	2.81	3.74	1.33	3.49	4305	3969
FMOC-Asn (rac.)	1.499	7.769	8.699	D	4.18	4.80	1.15	1.75	3914	3781
DNB-Pro (rac.)	1.499	6.983	6.983	///	3.66	3.66	1.00	0.00	2731	2731
FMOC-Ile (L>D)	1.499	5.070	6.419	D	2.38	3.28	1.38	3.82	4290	4162
FMOC-Gln (rac.)	1.498	1.685	1.685	///	0.12	0.12	1.00	0.00	4241	4241
Z-Ser (rac.)	1.499	5.047	5.047	///	2.37	2.37	1.00	0.00	4781	4781
FMOC-Pro (L>D)	1.499	5.580	5.717	D	2.72	2.81	1.03	0.41	5652	3396
FMOC-Aze (rac.)	1.499	6.703	7.084	D	3.47	3.73	1.07	0.93	4296	4728
DBTAMME (rac.)	1.499	7.556	8.687	S,S	4.04	4.80	1.19	2.31	4400	4407
Trolox (rac.)	1.499	4.121	4.683	S	1.75	2.12	1.21	2.05	4137	4083
Ibuprofen (rac)	1.499	2.469	2.469	///	0.65	0.65	1.00	0.00	4235	4235
Naproxen (rac.)	1.499	3.604	3.604	///	1.40	1.40	1.00	0.00	2382	2382
DNP-Mandelic acid (rac.)	1.498	26.503	33.850	R	16.69	21.60	1.29	3.46	3214	3264
Acetylmandelic acid (rac.)	1.499	5.257	5.624	S	2.51	2.75	1.10	1.10	3921	4552
Phenylbutyric acid (rac.)	1.499	2.345	2.345	///	0.56	0.56	1.00	0.00	4349	4349
TMB-Ala (rac.)	1.499	4.273	5.801	///	1.85	2.87	1.55	4.83	3986	4129
Bz-ACHSA (rac.)	1.499	6.035	6.035	///	3.03	3.03	1.00	0.00	2079	2079
MFQ.HCl (rac.)	1.499	1.376	1.376	///	-0.08	-0.08	1.00	0.00	1811	1811
BOC-Gly	1.499	1.670	///	///	0.11	///	///	///	2739	///
DNZ-Gly	1.499	10.069	///	///	5.72	///	///	///	4225	///
Vanillylmandelic acid (rac.)	1.499	7.845	8.149	///	4.23	4.44	1.05	0.67	4712	5335
Nitrophenylpropionic acid (rac.)	1.499	4.251	4.336	///	1.84	1.89	1.03	0.44	6063	9611
Hydroxyphenyllactic acid (rac.)	1.499	7.122	8.808	///	3.75	4.88	1.30	3.04	3506	3108
Tropic acid (rac.)	1.499	3.006	3.006	///	1.01	1.01	1.00	0.00	5299	5299
Fenoprofen (rac.)	1.499	3.120	3.120	///	1.08	1.08	1.00	0.00	2502	2502
Dichlorprop (rac.)	1.499	6.765	7.290	///	3.51	3.86	1.10	1.28	5140	4299
Hydroxymandelic acid (rac.)	1.499	7.972	7.972	///	4.32	4.32	1.00	0.00	3853	3853
Atrolactic acid (rac.)	1.499	5.624	5.624	///	2.75	2.75	1.00	0.00	5076	5076
Carprofen (rac.)	1.499	4.276	4.400	///	1.85	1.94	1.04	0.54	5045	6346
FMOC-Abu (rac.)	1.499	5.337	6.121	///	2.56	3.08	1.20	2.17	3810	4204
Flurbiprofen (rac.)	1.499	3.549	3.655	///	1.37	1.44	1.05	0.59	5820	7156
Bz-β-Phe (rac.)	1.499	4.035	4.491	///	1.69	2.00	1.18	1.76	4214	4425
Z-Leu (rac.)	1.498	3.982	3.982	///	1.66	1.66	1.00	0.00	5732	5732
Z-Arg (L>D)	1.499	2.316	2.316	///	0.55	0.55	1.00	0.00	4221	4221
Trp (rac.)	1.499	1.903	1.958	D	0.27	0.31	1.14	0.48	5071	4041
Tyr (rac.)	1.499	1.748	1.748	///	0.17	0.17	1.00	0.00	3339	3339
QN/QD (2:1)	1.499	1.665	1.665	///	0.11	0.11	1.00	0.00	1913	1913
Clenbuterol.HCl (rac.)	1.499	1.300	1.300	///	-0.13	-0.13	1.00	0.00	2902	2902
PI-2-56-2	1.499	8.458	11.968	///	4.64	6.98	1.50	4.16	2788	1893
PI-2-4-3	1.499	10.649	14.634	///	6.10	8.76	1.44	4.66	3664	3330
PI-2-25-1	1.499	7.707	7.707	///	4.14	4.14	1.00	0.00	3469	3469
PI-2-34-1	1.499	4.366	5.154	///	1.91	2.44	1.27	2.80	4738	4404
PI-3-67-1	1.499	6.658	8.408	///	3.44	4.61	1.34	3.92	4575	4525
PI-1-89-1	1.499	7.795	8.422	///	4.20	4.62	1.10	1.10	3148	3375
PI-2-15-1	1.499	5.858	7.071	///	2.91	3.72	1.28	2.97	4026	4005
PI-2-38-1	1.499	4.301	5.209	///	1.87	2.47	1.32	3.28	4984	4464
PI-2-87-1	1.499	4.507	5.368	///	2.01	2.58	1.29	3.02	4789	4783
P-DML-ACHSA (S,S>R,R)	1.498	6.082	6.295	R,R	3.06	3.20	1.05	0.66	6722	5198
P-DCL-ACHSA (S,S>R,R)	1.498	8.122	8.949	R,R	4.42	4.97	1.12	1.65	4468	4807

Table VI: Column 6 (150x4 mm ID, 232 µmol/g, DHQD-type CSP; injection volume: 5 µL; sample concentration: 1 mg/mL MeOH; flow rate: 1.0 mL/min; detection wavelength: 254 nm; mobile phase composition: MeOH/AcOH/NH_4OAc 99/1/0.25 (v/v/w); temperature: 25°C): different t_0-values derive from different positions of the column in the column compartment.

Analyte	t_0 [min.]	t_{r1} [min.]	t_{r2} [min.]	EO	k_1	k_2	α	R	N_1	N_2
Bz-Leu (L>D)	1.549	3.430	4.516	L	1.21	1.92	1.58	4.79	5496	4326
PFB-Leu (rac.)	1.549	3.300	3.463	L	1.13	1.24	1.09	0.82	4027	5249
A-DCL-Leu (rac.)	1.549	4.145	9.439	L	1.68	5.09	3.04	13.57	5154	4541
DNB-Leu (rac.)	1.976	8.836	31.383	L	3.47	14.88	4.29	22.90	7061	6288
DCB-Leu (rac.)	1.549	4.190	8.785	L	1.70	4.67	2.74	11.12	3104	4782
BTFMB-Leu (rac.)	1.549	2.687	4.900	L	0.73	2.16	2.94	10.37	5236	4868
DNB-N-Me-Leu (rac.)	1.549	9.183	9.183	///	4.93	4.93	1.00	0.00	1144	1144
Ac-Phe (rac.)	1.549	4.067	5.398	L	1.63	2.48	1.53	5.15	5157	5560
Z-Phe (rac.)	1.549	6.413	7.243	L	3.14	3.68	1.17	2.22	5369	5276
Phe (rac.)	1.976	2.228	2.228	///	0.13	0.13	1.00	0.00	3047	3047
DNZ-Phe (D>L)	1.976	2.921	11.830	L	0.48	4.99	10.43	20.01	3906	4875
BOC-Phe (rac.)	1.549	4.186	4.694	L	1.70	2.03	1.19	2.11	5463	5440
FMOC-β-Phe (rac.)	1.549	5.200	6.744	L	2.36	3.35	1.42	4.32	4629	4324
Z-β-Phe (rac.)	1.549	3.772	3.975	L	1.44	1.57	1.09	0.96	5270	5496
Bz-Phe (D>L)	1.549	5.948	8.164	L	2.84	4.27	1.50	5.64	5246	5084
Phenyl-Gly (rac.)	1.549	1.765	1.765	///	0.14	0.14	1.00	0.00	1775	1775
DNZ-Val (D>L)	1.549	7.455	13.255	L	3.81	7.56	1.98	9.63	4974	4482
BOC-Tyr (rac.)	1.549	4.514	5.078	L	1.91	2.28	1.19	2.09	5098	5002
Ac-Trp (rac.)	1.549	5.887	7.826	L	2.80	4.05	1.45	4.88	4790	4724
FMOC-Asn (rac.)	1.549	8.296	9.722	L	4.36	5.28	1.21	2.59	4527	4049
DNB-Pro (rac.)	1.549	8.048	8.741	D	4.20	4.64	1.11	1.42	5037	4453
FMOC-Ile (L>D)	1.549	5.351	7.570	L	2.45	3.89	1.58	6.03	5029	4837
FMOC-Gln (rac.)	1.976	2.245	2.245	///	0.14	0.14	1.00	0.00	5916	5916
Z-Ser (rac.)	1.549	5.210	5.470	L	2.36	2.53	1.07	0.95	5744	6347
FMOC-Pro (L>D)	1.549	6.038	6.477	L	2.90	3.18	1.10	1.22	4901	4746
FMOC-Aze (rac.)	1.549	7.286	7.762	L	3.70	4.01	1.08	1.14	5043	5409
DBTAMME (rac.)	1.549	7.776	8.764	R,R	4.02	4.66	1.16	2.18	5355	5261
Trolox (rac.)	1.549	4.026	4.367	R	1.60	1.82	1.14	1.50	5489	5421
Ibuprofen (rac)	1.549	2.535	2.535	///	0.64	0.64	1.00	0.00	5022	5022
Naproxen (rac.)	1.549	3.770	3.770	///	1.43	1.43	1.00	0.00	5802	5802
DNP-Mandelic acid (rac.)	1.976	28.402	42.205	S	13.37	20.36	1.52	6.38	4335	4174
Acetylmandelic acid (rac.)	1.549	5.465	5.465	///	2.53	2.53	1.00	0.00	6251	6251
Phenylbutyric acid (rac.)	1.549	2.443	2.443	///	0.58	0.58	1.00	0.00	5179	5179
TMB-Ala (rac.)	1.549	4.424	6.999	///	1.86	3.52	1.90	8.10	5516	4803
Bz-ACHSA (rac.)	1.549	6.916	7.470	///	3.46	3.82	1.10	1.44	5632	5607
MFQ.HCl (rac.)	1.549	1.387	1.387	///	-0.10	-0.10	1.00	0.00	2941	2941
BOC-Gly	1.549	1.776	///	///	0.15	///	///	///	3165	///
DNZ-Gly	1.549	11.000	///	///	6.10	///	///	///	5289	///
Vanillylmandelic acid (rac.)	1.549	8.305	8.305	///	4.36	4.36	1.00	0.00	3683	3683
Nitrophenylpropionic acid (rac.)	1.549	4.828	4.828	///	2.12	2.12	1.00	0.00	6486	6486
Hydroxyphenyllactic acid (rac.)	1.549	7.193	7.669	///	3.64	3.95	1.08	1.18	5475	5293
Tropic acid (rac.)	1.549	3.211	3.211	///	1.07	1.07	1.00	0.00	6185	6185
Fenoprofen (rac.)	1.549	3.269	3.269	///	1.11	1.11	1.00	0.00	5920	5920
Dichlorprop (rac.)	1.549	7.461	7.783	///	3.82	4.02	1.05	0.85	5985	7074
Hydroxymandelic acid (rac.)	1.549	8.080	8.080	///	4.22	4.22	1.00	0.00	2031	2031
Atrolactic acid (rac.)	1.549	5.906	5.906	///	2.81	2.81	1.00	0.00	3496	3496
Carprofen (rac.)	1.549	4.314	4.314	///	1.79	1.79	1.00	0.00	2665	2665
FMOC-Abu (rac.)	1.549	5.733	7.009	///	2.70	3.52	1.30	3.30	3867	4809
Flurbiprofen (rac.)	1.549	3.889	3.889	///	1.51	1.51	1.00	0.00	3877	3877
Bz-β-Phe (rac.)	1.549	4.233	5.184	///	1.73	2.35	1.35	3.57	4972	5027
Z-Leu (rac.)	1.549	3.808	4.058	///	1.46	1.62	1.11	1.20	5597	5820
Z-Arg (L>D)	1.549	2.063	2.063	///	0.33	0.33	1.00	0.00	3541	3541
Trp (rac.)	1.549	2.006	2.006	///	0.30	0.30	1.00	0.00	1474	1474
Tyr (rac.)	1.549	1.809	1.809	///	0.17	0.17	1.00	0.00	3743	3743
QN/QD (2:1)	1.549	1.640	1.640	///	0.06	0.06	1.00	0.00	2260	2260
Clenbuterol.HCl (rac.)	1.549	1.331	1.331	///	-0.14	-0.14	1.00	0.00	3561	3561
PI-2-56-2	1.549	9.016	9.096	///	4.82	4.87	1.01	0.17	5591	5651
PI-2-4-3	1.976	16.341	28.279	///	7.27	13.31	1.83	8.65	4423	3938
PI-2-25-1	1.549	8.224	9.675	///	4.31	5.25	1.22	2.70	4486	4421
PI-2-34-1	1.549	4.811	5.533	///	2.11	2.57	1.22	2.58	5543	5353
PI-3-67-1	1.549	7.472	9.089	///	3.82	4.87	1.27	3.54	5299	5188
PI-1-89-1	1.549	8.936	8.936	///	4.77	4.77	1.00	0.00	2160	2160
PI-2-15-1	1.549	6.160	9.310	///	2.98	5.01	1.68	7.03	4920	4611
PI-2-38-1	1.549	4.621	5.500	///	1.98	2.55	1.29	3.26	5826	5478
PI-2-87-1	1.549	5.005	5.738	///	2.23	2.70	1.21	2.51	5503	5353
P-DML-ACHSA (S,S>R,R)	1.976	8.495	9.620	S,S	3.30	3.87	1.17	2.13	4840	4585
P-DCL-ACHSA (S,S>R,R)	1.976	12.421	14.434	S,S	5.29	6.30	1.19	2.93	5873	6354

Table VII: Column 7 (150x4 mm ID, 238 µmol/g, DHQD-type CSP; injection volume: 5 µL; sample concentration: 1 mg/mL MeOH; flow rate: 1.0 mL/min; detection wavelength: 254 nm; mobile phase composition: MeOH/AcOH/NH_4OAc 99/1/0.25 (v/v/w); temperature: 25°C).

Analyte	t_0 [min.]	t_{r1} [min.]	t_{r2} [min.]	EO	k_1	k_2	α	R	N_1	N_2
PFB-Leu (rac.)	1.500	2.934	2.934	///	0.96	0.96	1.00	0.00	1786	1786
DCB-Leu (rac.)	1.500	3.853	6.870	L	1.57	3.58	2.28	5.33	1667	1199
DNB-N-Me-Leu (rac.)	1.500	8.420	8.420	///	4.61	4.61	1.00	0.00	568	568
Ac-Phe (rac.)	1.500	3.521	4.408	L	1.35	1.94	1.44	2.25	1717	1526
Z-Phe (rac.)	1.500	6.204	6.699	L	3.14	3.47	1.11	0.69	1533	1073
Phe (rac.)	1.500	1.517	1.517	///	0.01	0.01	1.00	0.00	957	957
DNZ-Val (D>L)	1.500	7.714	11.356	L	4.14	6.57	1.59	3.34	1358	1096
DNB-Pro (rac.)	1.500	7.740	8.356	D	4.16	4.57	1.10	0.72	1674	1123
FMOC-Aze (rac.)	1.500	6.643	7.126	L	3.43	3.75	1.09	0.61	1346	1096
DBTAMME (rac.)	1.500	6.946	7.982	R,R	3.63	4.32	1.19	1.10	1060	950
DNZ-Gly	1.500	12.677	///	///	7.45	///	///	///	1307	///
Hydroxyphenyllactic acid (rac.)	1.500	9.077	9.938	///	5.05	5.63	1.11	0.74	1255	890
Flurbiprofen (rac.)	1.500	3.963	3.963	///	1.64	1.64	1.00	0.00	1610	1610
Trp (rac.)	1.500	1.655	1.655	///	0.10	0.10	1.00	0.00	1894	1894
QN/QD (2:1)	1.500	1.560	1.560	///	0.04	0.04	1.00	0.00	2030	2030
Clenbuterol.HCl (rac.)	1.500	1.378	1.378	///	-0.08	-0.08	1.00	0.00	2197	2197
PI-2-56-2	1.500	8.540	9.260	///	4.69	5.17	1.10	0.63	1030	905
PI-2-15-1	1.500	4.773	6.627	///	2.18	3.42	1.57	2.93	1375	1219
P-DML-ACHSA (S,S>R,R)	1.500	5.619	5.806	S,S	2.75	2.87	1.05	0.33	1419	1862
P-DCL-ACHSA (S,S>R,R)	1.500	9.106	9.473	S,S	5.07	5.32	1.05	0.40	1228	2090

Table VIII: Column 8 (150x4 mm ID, 314 µmol/g, DHQD-type CSP; injection volume: 5 µL; sample concentration: 1 mg/mL MeOH; flow rate: 1.0 mL/min; detection wavelength: 254 nm; mobile phase composition: MeOH/AcOH/NH_4OAc 99/1/0.25 (v/v/w); temperature: 25°C).

Analyte	t_0 [min.]	t_{r1} [min.]	t_{r2} [min.]	EO	k_1	k_2	α	R	N_1	N_2
PFB-Leu (rac.)	1.602	4.952	5.155	L	2.09	2.22	1.06	0.79	5919	6613
DCB-Leu (rac.)	1.602	6.523	14.131	L	3.07	7.82	2.55	13.73	5743	5374
DNB-N-Me-Leu (rac.)	1.602	15.778	16.115	L	8.85	9.06	1.02	0.33	2854	4993
Ac-Phe (rac.)	1.602	5.901	8.008	L	2.68	4.00	1.49	5.10	4493	4580
Z-Phe (rac.)	1.602	10.543	11.859	L	5.58	6.40	1.15	2.04	4864	4828
Phe (rac.)	1.602	1.779	1.779	///	0.11	0.11	1.00	0.00	3211	3211
DNZ-Val (D>L)	1.602	12.632	22.085	L	6.89	12.79	1.86	10.03	5629	5224
DNB-Pro (rac.)	1.602	13.140	14.434	D	7.20	8.01	1.11	1.71	5646	4948
FMOC-Aze (rac.)	1.602	11.819	12.681	L	6.38	6.92	1.08	1.32	5565	5675
DBTAMME (rac.)	1.602	12.969	14.833	R,R	7.10	8.26	1.16	2.31	4759	4723
DNZ-Gly	1.602	19.328	///	///	11.07	///	///	///	6006	///
Hydroxyphenyllactic acid (rac.)	1.602	12.296	13.337	///	6.68	7.33	1.10	1.27	3962	3864
Flurbiprofen (rac.)	1.602	5.852	5.852	///	2.65	2.65	1.00	0.00	3771	3771
Trp (rac.)	1.602	2.288	2.288	///	0.43	0.43	1.00	0.00	1687	1687
QN/QD (2:1)	1.602	1.599	1.599	///	0.00	0.00	1.00	0.00	2408	2408
Clenbuterol.HCl (rac.)	1.602	1.330	1.330	///	-0.17	-0.17	1.00	0.00	3843	3843
PI-2-56-2	1.602	15.423	16.049	///	8.63	9.02	1.05	0.42	2136	1354
PI-2-15-1	1.602	9.372	14.383	///	4.85	7.98	1.64	7.19	4681	4621
P-DML-ACHSA (S,S>R,R)	1.602	9.815	11.058	S,S	5.13	5.90	1.15	2.20	5406	5499
P-DCL-ACHSA (S,S>R,R)	1.602	15.278	17.624	S,S	8.54	10.00	1.17	2.67	5392	5802

Table IX: Column 9 (150x4 mm ID, 150 µmol/g, DHQD-type CSP; injection volume: 5 µL; sample concentration: 1 mg/mL MeOH; flow rate: 1.0 mL/min; detection wavelength: 254 nm; mobile phase composition: MeOH/AcOH/NH_4OAc 99/1/0.25 (v/v/w); temperature: 25°C).

Analyte	t_0 [min.]	t_{r1} [min.]	t_{r2} [min.]	EO	k_1	k_2	α	R	N_1	N_2
PFB-Leu (rac.)	1.669	3.218	3.364	L	0.93	1.02	1.09	0.58	2991	2471
DCB-Leu (rac.)	1.669	3.821	7.708	L	1.29	3.62	2.81	8.16	2296	2391
DNB-N-Me-Leu (rac.)	1.669	7.747	7.747	///	3.64	3.64	1.00	0.00	1085	1085
Ac-Phe (rac.)	1.669	3.567	4.614	L	1.14	1.77	1.55	2.95	2096	2169
Z-Phe (rac.)	1.669	5.292	5.967	L	2.17	2.58	1.19	1.42	2246	2253
Phe (rac.)	1.669	1.854	1.854	///	0.11	0.11	1.00	0.00	768	768
DNZ-Val (D>L)	1.669	5.871	10.426	L	2.52	5.25	2.08	7.15	3031	2199
DNB-Pro (rac.)	1.669	6.326	6.846	D	2.79	3.10	1.11	0.99	3091	1937
FMOC-Aze (rac.)	1.669	5.755	6.043	L	2.45	2.62	1.07	0.69	2828	3477
DBTAMME (rac.)	1.669	6.488	7.182	R,R	2.89	3.30	1.14	1.39	2887	3104
DNZ-Gly	1.669	7.909	///	///	3.74	///	///	///	3157	///
Hydroxyphenyllactic acid (rac.)	1.669	5.518	5.518	///	2.31	2.31	1.00	0.00	812	812
Flurbiprofen (rac.)	1.669	3.376	3.376	///	1.02	1.02	1.00	0.00	2397	2397
Trp (rac.)	1.669	2.091	2.091	///	0.25	0.25	1.00	0.00	818	818
QN/QD (2:1)	1.669	1.847	1.847	///	0.11	0.11	1.00	0.00	1768	1768
Clenbuterol.HCl (rac.)	1.669	1.457	1.457	///	-0.13	-0.13	1.00	0.00	1797	1797
PI-2-56-2	1.669	7.267	7.267	///	3.35	3.35	1.00	0.00	894	894
PI-2-15-1	1.669	5.166	7.650	///	2.10	3.58	1.71	4.93	2567	2617
P-DML-ACHSA (S,S>R,R)	1.669	5.110	5.823	S,S	2.06	2.49	1.21	1.80	3038	3037
P-DCL-ACHSA (S,S>R,R)	1.669	6.854	8.164	S,S	3.11	3.89	1.25	2.45	3103	3187

Table X: Column 10 (150x4 mm ID, 138 µmol/g, DHQD-type CSP; injection volume: 5 µL; sample concentration: 1 mg/mL MeOH; flow rate: 1.0 mL/min; detection wavelength: 254 nm; mobile phase composition: MeOH/AcOH/NH_4OAc 99/1/0.25 (v/v/w); temperature: 25°C).

Analyte	t_0 [min.]	t_{r1} [min.]	t_{r2} [min.]	EO	k_1	k_2	α	R	N_1	N_2
PFB-Leu (rac.)	1.469	2.911	3.077	L	0.98	1.09	1.12	1.11	4761	8094
DCB-Leu (rac.)	1.469	3.404	6.287	L	1.32	3.28	2.49	9.98	4812	4187
DNB-N-Me-Leu (rac.)	1.469	6.543	6.543	///	3.45	3.45	1.00	0.00	1305	1305
Ac-Phe (rac.)	1.469	3.407	4.236	L	1.32	1.88	1.43	3.86	5018	5101
Z-Phe (rac.)	1.469	4.822	5.340	L	2.28	2.64	1.15	1.78	4872	4930
Phe (rac.)	1.469	1.734	1.734	///	0.18	0.18	1.00	0.00	2724	2724
DNZ-Val (D>L)	1.469	5.543	9.365	L	2.77	5.38	1.94	8.43	4598	4052
DNB-Pro (rac.)	1.469	5.899	6.353	D	3.02	3.32	1.10	1.22	4452	4198
FMOC-Aze (rac.)	1.469	5.213	5.481	L	2.55	2.73	1.07	0.87	4394	5229
DBTAMME (rac.)	1.469	5.962	6.546	R,R	3.06	3.46	1.13	1.19	4718	445
DNZ-Gly	1.469	7.757	///	///	4.28	///	///	///	4542	///
Hydroxyphenyllactic acid (rac.)	1.469	5.580	5.873	///	2.80	3.00	1.07	0.68	3188	2543
Flurbiprofen (rac.)	1.469	3.125	3.125	///	1.13	1.13	1.00	0.00	4391	4391
Trp (rac.)	1.469	1.915	1.915	///	0.30	0.30	1.00	0.00	2453	2453
QN/QD (2:1)	1.469	1.774	1.774	///	0.21	0.21	1.00	0.00	3133	3133
Clenbuterol.HCl (rac.)	1.469	1.555	1.555	///	0.06	0.06	1.00	0.00	4052	4052
PI-2-56-2	1.469	6.167	6.167	///	3.20	3.20	1.00	0.00	1327	1327
PI-2-15-1	1.469	4.223	6.025	///	1.87	3.10	1.65	3.91	1990	1969
P-DML-ACHSA (S,S>R,R)	1.469	4.594	5.093	S,S	2.13	2.47	1.16	1.23	2411	2176
P-DCL-ACHSA (S,S>R,R)	1.469	6.068	7.012	S,S	3.13	3.77	1.21	1.69	2219	2176

Table XI: Column 11 (75x4 mm ID, 477 µmol/g, DHQN-type CSP; injection volume: 5 µL; sample concentration: 1 mg/mL MeOH; flow rate: 0.5 mL/min; detection wavelength: 254 nm; mobile phase composition: MeOH/AcOH/NH_4OAc 99/1/0.25 (v/v/w); temperature: 25°C).

Analyte	t_0 [min.]	t_{r1} [min.]	t_{r2} [min.]	EO	k_1	k_2	α	R	N_1	N_2
PFB-Leu (rac.)	1.430	4.466	4.466	///	2.12	2.12	1.00	0.00	1510	1510
DCB-Leu (rac.)	1.430	7.231	12.207	D	4.06	7.53	1.86	5.22	2048	1273
DNB-N-Me-Leu (rac.)	1.430	12.657	12.657	///	7.85	7.85	1.00	0.00	844	844
Ac-Phe (rac.)	1.430	6.493	7.867	D	3.54	4.50	1.27	1.78	1303	1457
Z-Phe (rac.)	1.430	13.564	13.564	///	8.48	8.48	1.00	0.00	1153	1153
Phe (rac.)	1.430	1.637	1.637	///	0.14	0.14	1.00	0.00	1367	1367
DNZ-Val (D>L)	1.430	15.907	21.791	D	10.12	14.23	1.41	2.73	1374	1080
DNB-Pro (rac.)	1.430	14.948	14.948	///	9.45	9.45	1.00	0.00	841	841
FMOC-Aze (rac.)	1.430	13.675	14.280	D	8.56	8.98	1.05	0.52	3388	1209
DBTAMME (rac.)	1.430	15.358	18.347	S,S	9.74	11.83	1.21	1.93	1816	1977
DNZ-Gly	1.430	29.607	///	///	19.70	///	///	///	1971	///
Hydroxyphenyllactic acid (rac.)	1.430	23.298	31.504	///	15.29	21.03	1.38	2.71	1364	1262
Flurbiprofen (rac.)	1.430	7.254	7.537	///	4.07	4.27	1.05	0.53	4029	2070
Trp (rac.)	1.430	2.183	2.183	///	0.53	0.53	1.00	0.00	771	771
QN/QD (2:1)	1.430	1.349	1.349	///	-0.06	-0.06	1.00	0.00	1320	1320
Clenbuterol.HCl (rac.)	1.430	1.243	1.243	///	-0.13	-0.13	1.00	0.00	1647	1647
PI-2-56-2	1.430	19.965	19.965	///	12.96	12.96	1.00	0.00	626	626
PI-2-15-1	1.430	9.034	11.040	///	5.32	6.72	1.26	1.86	1472	1296
P-DML-ACHSA (S,S>R,R)	1.430	10.503	10.503	///	6.34	6.34	1.00	0.00	1224	1224
P-DCL-ACHSA (S,S>R,R)	1.430	17.498	17.498	///	11.23	11.23	1.00	0.00	1222	1222

Table XII: Column 11 (75x4 mm ID, 477 µmol/g, DHQN-type CSP; injection volume: 5 µL; sample concentration: 1 mg/mL MeOH; flow rate: 1.0 mL/min; detection wavelength: 254 nm; mobile phase composition: MeOH/AcOH/NH_4OAc 99/1/0.25 (v/v/w); temperature: 25°C).

Analyte	t_0 [min.]	t_{r1} [min.]	t_{r2} [min.]	EO	k_1	k_2	α	R	N_1	N_2
PFB-Leu (rac.)	0.702	2.435	2.435	///	2.47	2.47	1.00	0.00	1130	1130
DCB-Leu (rac.)	0.702	3.704	6.162	D	4.28	7.78	1.82	4.30	1389	994
DNB-N-Me-Leu (rac.)	0.702	6.284	6.284	///	7.96	7.96	1.00	0.00	696	696
Ac-Phe (rac.)	0.702	3.145	3.788	D	3.48	4.40	1.26	1.63	1284	1191
Z-Phe (rac.)	0.702	6.539	6.539	///	8.32	8.32	1.00	0.00	939	939
Phe (rac.)	0.702	0.811	0.811	///	0.16	0.16	1.00	0.00	887	887
DNZ-Val (D>L)	0.702	7.639	10.271	D	9.89	13.64	1.38	2.19	985	797
DNB-Pro (rac.)	0.702	7.082	7.082	///	9.09	9.09	1.00	0.00	681	681
FMOC-Aze (rac.)	0.702	6.680	6.680	///	8.52	8.52	1.00	0.00	510	510
DBTAMME (rac.)	0.702	7.370	8.756	S,S	9.50	11.48	1.21	1.20	857	708
DNZ-Gly	0.702	13.685	///	///	18.50	///	///	///	898	///
Hydroxyphenyllactic acid (rac.)	0.702	11.068	14.858	///	14.77	20.18	1.37	2.06	859	732
Flurbiprofen (rac.)	0.702	3.441	3.441	///	3.90	3.90	1.00	0.00	548	548
Trp (rac.)	0.702	1.030	1.030	///	0.47	0.47	1.00	0.00	744	744
QN/QD (2:1)	0.702	0.651	0.651	///	-0.07	-0.07	1.00	0.00	768	768
Clenbuterol.HCl (rac.)	0.702	0.570	0.570	///	-0.19	-0.19	1.00	0.00	732	732
PI-2-15-1	0.702	4.247	5.120	///	5.05	6.30	1.25	1.45	1039	885
P-DML-ACHSA (S,S>R,R)	0.702	5.097	5.097	///	6.26	6.26	1.00	0.00	773	773
P-DCL-ACHSA (S,S>R,R)	0.702	8.463	8.463	///	11.06	11.06	1.00	0.00	903	903

Table XIII: Column 12 (75x4 mm ID, 490 µmol/g, DHQD-type CSP; injection volume: 5 µL; sample concentration: 1 mg/mL MeOH; flow rate: 0.5 mL/min; detection wavelength: 254 nm; mobile phase composition: MeOH/AcOH/NH_4OAc 99/1/0.25 (v/v/w); temperature: 25°C).

Analyte	t_0 [min.]	t_{r1} [min.]	t_{r2} [min.]	EO	k_1	k_2	α	R	N_1	N_2
PFB-Leu (rac.)	1.412	4.896	4.896	///	2.47	2.47	1.00	0.00	1649	1649
DCB-Leu (rac.)	1.412	6.801	13.404	L	3.82	8.49	2.23	6.48	1808	1338
DNB-N-Me-Leu (rac.)	1.412	16.546	16.546	///	10.72	10.72	1.00	0.00	618	618
Ac-Phe (rac.)	1.412	6.405	8.436	L	3.54	4.97	1.41	2.77	1681	1607
Z-Phe (rac.)	1.412	12.801	14.006	L	8.06	8.92	1.11	0.85	1469	1385
Phe (rac.)	1.412	1.773	1.773	///	0.26	0.26	1.00	0.00	729	729
DNZ-Val (D>L)	1.412	15.438	23.387	L	9.93	15.56	1.57	3.73	1505	1144
DNB-Pro (rac.)	1.412	15.760	16.960	D	10.16	11.01	1.08	0.68	1589	1182
FMOC-Aze (rac.)	1.412	12.535	13.592	L	7.88	8.62	1.10	0.80	1664	1445
DBTAMME (rac.)	1.412	16.306	18.905	R,R	10.55	12.39	1.17	1.58	1835	1812
DNZ-Gly	1.412	28.428	///	///	19.13	///	///	///	1523	///
Hydroxyphenyllactic acid (rac.)	1.412	19.994	21.916	///	13.16	14.52	1.10	0.81	1311	1181
Flurbiprofen (rac.)	1.412	7.614	7.614	///	4.39	4.39	1.00	0.00	1619	1619
Trp (rac.)	1.412	2.377	2.377	///	0.68	0.68	1.00	0.00	1212	1212
QN/QD (2:1)	1.412	1.695	1.695	///	0.20	0.20	1.00	0.00	1061	1061
Clenbuterol.HCl (rac.)	1.412	1.387	1.387	///	-0.02	-0.02	1.00	0.00	1140	1140
PI-2-56-2	1.412	17.502	18.835	///	11.39	12.34	1.08	0.56	1066	830
PI-2-15-1	1.412	10.197	14.674	///	6.22	9.39	1.51	3.51	1625	1422
P-DML-ACHSA (S,S>R,R)	1.412	10.505	11.120	S,S	6.44	6.87	1.07	0.60	1439	2179
P-DCL-ACHSA (S,S>R,R)	1.412	17.645	18.402	S,S	11.49	12.03	1.05	0.42	1187	2012

Table XIV: Column 12 (75x4 mm ID, 490 µmol/g, DHQD-type CSP; injection volume: 5 µL; sample concentration: 1 mg/mL MeOH; flow rate: 1.0 mL/min; detection wavelength: 254 nm; mobile phase composition: MeOH/AcOH/NH_4OAc 99/1/0.25 (v/v/w); temperature: 25°C).

Analyte	t_0 [min.]	t_{r1} [min.]	t_{r2} [min.]	EO	k_1	k_2	α	R	N_1	N_2
PFB-Leu (rac.)	0.705	2.385	2.385	///	2.38	2.38	1.00	0.00	1144	1144
DCB-Leu (rac.)	0.705	3.338	6.535	L	3.73	8.27	2.21	5.30	1211	936
DNB-N-Me-Leu (rac.)	0.705	8.072	8.072	///	10.45	10.45	1.00	0.00	500	500
Ac-Phe (rac.)	0.705	3.026	3.983	L	3.29	4.65	1.41	2.29	1158	1100
Z-Phe (rac.)	0.705	5.887	6.425	L	7.35	8.11	1.10	0.79	1363	1270
Phe (rac.)	0.705	0.815	0.815	///	0.16	0.16	1.00	0.00	642	642
DNZ-Val (D>L)	0.705	7.536	11.353	L	9.69	15.10	1.56	3.13	1071	853
DNB-Pro (rac.)	0.705	7.662	8.223	D	9.87	10.66	1.08	0.59	1328	922
FMOC-Aze (rac.)	0.705	6.315	6.825	L	7.96	8.68	1.09	0.65	1266	1011
DBTAMME (rac.)	0.705	6.796	7.878	R,R	8.64	10.17	1.18	1.24	1139	1107
DNZ-Gly	0.705	13.213	///	///	17.74	///	///	///	1049	///
Hydroxyphenyllactic acid (rac.)	0.705	9.321	10.187	///	12.22	13.45	1.10	0.68	991	883
Flurbiprofen (rac.)	0.705	3.411	3.411	///	3.84	3.84	1.00	0.00	1113	1113
Trp (rac.)	0.705	1.043	1.043	///	0.48	0.48	1.00	0.00	860	860
QN/QD (2:1)	0.705	0.656	0.656	///	-0.07	-0.07	1.00	0.00	624	624
Clenbuterol.HCl (rac.)	0.705	0.566	0.566	///	-0.20	-0.20	1.00	0.00	651	651
PI-2-56-2	0.705	7.655	8.201	///	9.86	10.63	1.08	0.48	929	630
PI-2-15-1	0.705	4.173	5.995	///	4.92	7.50	1.53	2.78	1016	909
P-DML-ACHSA (S,S>R,R)	0.705	5.356	5.356	///	6.60	6.60	1.00	0.00	557	557
P-DCL-ACHSA (S,S>R,R)	0.705	9.065	9.065	///	11.86	11.86	1.00	0.00	598	598

Table XV: Column 13 (150x4 mm ID, app. 340 µmol/g, QN-AX type CSP; injection volume: 5 µL; sample concentration: 1 mg/mL MeOH; flow rate: 1.0 mL/min; detection wavelength: 254 nm; mobile phase composition: MeOH/AcOH/NH_4OAc 99/1/0.25 (v/v/w); temperature: 25°C): different t_0-values derive from different positions of the column in the column compartment.

Analyte	t_0 [min.]	t_{r1} [min.]	t_{r2} [min.]	EO	k_1	k_2	α	R	N_1	N_2
Bz-Leu (L>D)	1.431	3.787	7.650	D	1.65	4.35	2.64	10.59	3957	3906
PFB-Leu (rac.)	1.431	3.640	5.550	D	1.54	2.88	1.86	6.52	4016	3851
A-DCL-Leu (rac.)	1.426	4.628	34.770	D	2.25	23.38	10.41	26.28	3787	5654
DNB-Leu (rac.)	1.426	5.898	75.109	D	3.14	51.67	16.48	24.87	3841	2940
DCB-Leu (rac.)	1.426	4.889	31.016	D	2.43	20.75	8.54	21.36	3976	2919
BTFMB-Leu (rac.)	1.426	3.178	17.217	D	1.23	11.07	9.01	21.22	3925	3680
DNB-N-Me-Leu (rac.)	1.431	6.709	7.272	D	3.69	4.08	1.11	1.13	2639	3716
Ac-Phe (rac.)	1.431	4.282	5.758	D	1.99	3.02	1.52	4.73	4142	4133
Z-Phe (rac.)	1.431	6.844	8.236	D	3.78	4.76	1.26	2.60	3213	3137
Phe (rac.)	1.431	1.632	1.632	///	0.14	0.14	1.00	0.00	1124	1124
DNZ-Phe (D>L)	1.426	1.733	1.823	D	0.22	0.28	1.29	0.87	3114	6432
BOC-Phe (rac.)	1.431	4.424	5.255	D	2.09	2.67	1.28	2.76	4214	4073
FMOC-β-Phe (rac.)	1.431	4.998	6.255	D	2.49	3.37	1.35	3.33	3570	3536
Z-β-Phe (rac.)	1.431	3.731	4.066	D	1.61	1.84	1.15	1.32	3502	4103
Bz-Phe (D>L)	1.431	6.053	10.457	D	3.23	6.31	1.95	8.38	4056	3844
Phenyl-Gly (rac.)	1.431	1.631	1.631	///	0.14	0.14	1.00	0.00	997	997
DNZ-Val (D>L)	1.431	6.656	19.382	D	3.65	12.54	3.44	14.90	3962	3471
BOC-Tyr (rac.)	1.431	4.919	6.051	D	2.44	3.23	1.32	2.78	2963	2843
Ac-Trp (rac.)	1.431	6.381	10.614	D	3.46	6.42	1.86	7.37	3743	3270
FMOC-Asn (rac.)	1.431	9.141	11.825	D	5.39	7.26	1.35	3.71	3403	3322
DNB-Pro (rac.)	1.431	7.106	7.106	///	3.97	3.97	1.00	0.00	2157	2157
FMOC-Ile (L>D)	1.431	5.567	10.942	D	2.89	6.65	2.30	9.67	3639	3415
FMOC-Gln (rac.)	1.431	1.529	1.529	///	0.07	0.07	1.00	0.00	808	808
Z-Ser (rac.)	1.431	6.267	7.338	D	3.38	4.13	1.22	2.51	4057	4062
FMOC-Pro (L>D)	1.431	5.979	6.269	D	3.18	3.38	1.06	0.75	4390	3727
FMOC-Aze (rac.)	1.431	7.207	7.207	///	4.04	4.04	1.00	0.00	1954	1954
DBTAMME (rac.)	1.431	6.766	7.210	S,S	3.73	4.04	1.08	1.01	3726	4370
Trolox (rac.)	1.431	4.538	4.820	S	2.17	2.37	1.09	0.97	3830	4402
Ibuprofen (rac)	1.431	2.637	2.637	///	0.84	0.84	1.00	0.00	2359	2359
Naproxen (rac.)	1.431	3.746	3.971	S	1.62	1.77	1.10	1.00	4428	4931
DNP-Mandelic acid (rac.)	1.426	16.935	71.793	R	10.88	49.35	4.54	17.67	3741	2796
Acetylmandelic acid (rac.)	1.431	5.919	6.332	S	3.14	3.42	1.09	1.15	4469	4864
Phenylbutyric acid (rac.)	1.431	2.659	2.738	S	0.86	0.91	1.06	0.58	5001	7443
TMB-Ala (rac.)	1.426	4.564	14.036	///	2.20	8.84	4.02	15.15	3383	3693
Bz-ACHSA (rac.)	1.431	5.272	8.853	///	2.68	5.19	1.93	8.17	4239	4063
MFQ.HCl (rac.)	1.431	1.292	1.292	///	-0.10	-0.10	1.00	0.00	1994	1994
BOC-Gly	1.431	1.498	///	///	0.05	///	///	///	719	///
DNZ-Gly	1.431	11.356	///	///	6.94	///	///	///	3993	///
Vanillylmandelic acid (rac.)	1.431	9.477	9.477	///	5.62	5.62	1.00	0.00	1859	1859
Nitrophenylpropionic acid (rac.)	1.431	5.086	5.574	///	2.55	2.90	1.13	1.59	4844	4854
Hydroxyphenyllactic acid (rac.)	1.426	9.986	11.403	///	6.00	7.00	1.17	1.24	1441	1362
Tropic acid (rac.)	1.431	3.649	3.649	///	1.55	1.55	1.00	0.00	2295	2295
Fenoprofen (rac.)	1.431	3.397	3.484	///	1.37	1.43	1.04	0.52	4759	8547
Dichlorprop (rac.)	1.431	7.424	8.728	///	4.19	5.10	1.22	2.75	4527	4727
Hydroxymandelic acid (rac.)	1.431	10.953	10.953	///	6.65	6.65	1.00	0.00	1719	1719
Atrolactic acid (rac.)	1.431	7.756	9.281	///	4.42	5.49	1.24	2.30	2685	2609
Carprofen (rac.)	1.431	4.938	5.449	///	2.45	2.81	1.15	1.52	3818	3798
FMOC-Abu (rac.)	1.431	6.025	9.873	///	3.21	5.90	1.84	6.98	3093	3558
Flurbiprofen (rac.)	1.431	3.909	4.171	///	1.73	1.91	1.11	1.04	3803	4406
Bz-β-Phe (rac.)	1.431	3.935	5.672	///	1.75	2.96	1.69	5.58	3818	3788
Z-Leu (rac.)	1.431	4.101	4.935	///	1.87	2.45	1.31	2.93	3924	4164
Z-Arg (L>D)	1.431	2.005	2.186	D	0.40	0.53	1.32	1.17	2983	2855
Trp (rac.)	1.431	1.852	2.115	D	0.29	0.48	1.62	1.46	2275	1617
Tyr (rac.)	1.431	1.529	1.764	D	0.07	0.23	3.40	1.22	1009	1329
QN/QD (2:1)	1.431	1.331	1.331	///	-0.07	-0.07	1.00	0.00	1511	1511
Clenbuterol.HCl (rac.)	1.431	1.222	1.222	///	-0.15	-0.15	1.00	0.00	2145	2145
PI-2-56-2	1.431	10.945	11.932	///	6.65	7.34	1.10	0.88	1733	1616
PI-2-4-3	1.431	8.979	17.953	///	5.27	11.55	2.19	9.56	3425	3156
PI-2-25-1	1.431	6.877	8.701	///	3.81	5.08	1.33	3.33	3309	3169
PI-2-34-1	1.431	5.193	5.441	///	2.63	2.80	1.07	0.77	3757	4860
PI-3-67-1	1.426	6.512	7.306	///	3.57	4.12	1.16	1.48	2525	2791
PI-1-89-1	1.431	8.113	9.945	///	4.67	5.95	1.27	2.73	2887	2904
PI-2-15-1	1.431	5.546	8.738	///	2.88	5.11	1.78	6.47	3483	3215
PI-2-38-1	1.431	5.298	5.767	///	2.70	3.03	1.12	1.31	3744	3909
PI-2-87-1	1.426	5.216	5.216	///	2.66	2.66	1.00	0.00	2727	2727
P-DML-ACHSA (S,S>R,R)	1.426	4.574	9.802	R,R	2.21	5.87	2.66	10.82	3472	3608
P-DCL-ACHSA (S,S>R,R)	1.426	5.902	23.413	R,R	3.14	15.42	4.91	17.12	3832	2738

Table XVI: Column 14 (150x4 mm ID, app. 340 µmol/g, QD-AX type CSP; injection volume: 5 µL; sample concentration: 1 mg/mL MeOH; flow rate: 1.0 mL/min; detection wavelength: 254 nm; mobile phase composition: MeOH/AcOH/NH_4OAc 99/1/0.25 (v/v/w); temperature: 25°C): different t_0-values derive from different positions of the column in the column compartment.

Analyte	t_0 [min.]	t_{r1} [min.]	t_{r2} [min.]	EO	k_1	k_2	α	R	N_1	N_2
Bz-Leu (L>D)	1.432	3.425	7.118	L	1.39	3.97	2.85	12.51	5099	5109
PFB-Leu (rac.)	1.432	3.354	5.034	L	1.34	2.52	1.87	7.08	5058	4945
A-DCL-Leu (rac.)	1.384	4.426	30.799	L	2.20	21.25	9.67	25.32	4482	4670
DNB-Leu (rac.)	1.384	5.724	54.488	L	3.14	38.37	12.24	26.44	4735	3790
DCB-Leu (rac.)	1.384	4.504	26.209	L	2.25	17.94	7.96	24.54	4600	5046
BTFMB-Leu (rac.)	1.384	2.896	14.663	L	1.09	9.59	8.78	21.59	4263	4044
DNB-N-Me-Leu (rac.)	1.432	7.492	7.894	L	4.23	4.51	1.07	0.78	4073	3111
Ac-Phe (rac.)	1.432	3.889	5.580	L	1.72	2.90	1.69	6.52	5130	5543
Z-Phe (rac.)	1.432	6.400	8.367	L	3.47	4.84	1.40	4.85	5337	5285
Phe (rac.)	1.432	1.606	1.606	///	0.12	0.12	1.00	0.00	1714	1714
DNZ-Phe (D>L)	1.384	1.825	1.825	///	0.32	0.32	1.00	0.00	3630	3630
BOC-Phe (rac.)	1.432	4.181	5.281	L	1.92	2.69	1.40	4.12	5093	4960
FMOC-β-Phe (rac.)	1.432	4.774	6.879	L	2.33	3.80	1.63	6.13	4717	4502
Z-β-Phe (rac.)	1.432	3.576	4.269	L	1.50	1.98	1.32	3.10	4887	4965
Bz-Phe (D>L)	1.432	5.587	10.260	L	2.90	6.16	2.12	10.62	5337	5039
Phenyl-Gly (rac.)	1.432	1.593	1.593	///	0.11	0.11	1.00	0.00	1107	1107
DNZ-Val (D>L)	1.432	6.044	16.817	L	3.22	10.74	3.34	16.53	5188	4656
BOC-Tyr (rac.)	1.432	4.451	5.685	L	2.11	2.97	1.41	4.17	4807	4590
Ac-Trp (rac.)	1.432	5.577	8.467	L	2.89	4.91	1.70	6.93	4458	4620
FMOC-Asn (rac.)	1.432	7.914	9.679	L	4.53	5.76	1.27	3.26	4050	4406
DNB-Pro (rac.)	1.432	7.047	7.047	///	3.92	3.92	1.00	0.00	2318	2318
FMOC-Ile (L>D)	1.432	4.989	10.009	L	2.48	5.99	2.41	11.12	4575	4252
FMOC-Gln (rac.)	1.432	1.543	1.543	///	0.08	0.08	1.00	0.00	954	954
Z-Ser (rac.)	1.432	5.626	7.000	L	2.93	3.89	1.33	3.96	5300	5277
FMOC-Pro (L>D)	1.432	5.473	6.017	L	2.82	3.20	1.13	1.52	4382	3828
FMOC-Aze (rac.)	1.432	6.600	7.156	L	3.61	4.00	1.11	1.38	4725	4587
DBTAMME (rac.)	1.432	6.726	7.056	R,R	3.70	3.93	1.06	0.88	5900	4978
Trolox (rac.)	1.432	4.003	4.227	S	1.80	1.95	1.09	0.99	5681	4930
Ibuprofen (rac)	1.432	2.460	2.514	R,R	0.72	0.76	1.05	0.48	9898	5815
Naproxen (rac.)	1.432	3.479	3.645	R,R	1.43	1.55	1.08	0.90	6639	5313
DNP-Mandelic acid (rac.)	1.384	16.229	39.637	S	10.73	27.64	2.58	12.70	3701	3646
Acetylmandelic acid (rac.)	1.384	5.360	5.360	///	2.87	2.87	1.00	0.00	3172	3172
Phenylbutyric acid (rac.)	1.432	2.433	2.503	R,R	0.70	0.75	1.07	0.60	8727	5661
TMB-Ala (rac.)	1.384	4.236	13.261	///	2.06	8.58	4.16	17.15	4520	4327
Bz-ACHSA (rac.)	1.432	5.392	10.124	///	2.77	6.07	2.19	11.41	5720	5480
MFQ.HCl (rac.)	1.432	1.231	1.231	///	-0.14	-0.14	1.00	0.00	2677	2677
BOC-Gly	1.432	1.466	///	///	0.02	///	///	///	749	///
DNZ-Gly	1.432	10.707	///	///	6.48	///	///	///	5439	///
Vanillylmandelic acid (rac.)	1.432	7.216	7.216	///	4.04	4.04	1.00	0.00	1747	1747
Nitrophenylpropionic acid (rac.)	1.432	4.841	5.093	///	2.38	2.56	1.07	1.03	6877	6187
Hydroxyphenyllactic acid (rac.)	1.432	6.980	7.540	///	3.87	4.27	1.10	1.25	4360	3997
Tropic acid (rac.)	1.432	3.370	3.524	///	1.35	1.46	1.08	0.87	6855	5398
Fenoprofen (rac.)	1.432	3.286	3.286	///	1.29	1.29	1.00	0.00	2861	2861
Dichlorprop (rac.)	1.432	6.792	8.569	///	3.74	4.98	1.33	4.46	5976	5890
Hydroxymandelic acid (rac.)	1.432	7.850	7.850	///	4.48	4.48	1.00	0.00	2325	2325
Atrolactic acid (rac.)	1.432	6.719	6.719	///	3.69	3.69	1.00	0.00	2820	2820
Carprofen (rac.)	1.432	4.595	4.951	///	2.21	2.46	1.11	1.30	4951	4704
FMOC-Abu (rac.)	1.432	5.433	8.980	///	2.79	5.27	1.89	8.00	3937	4514
Flurbiprofen (rac.)	1.384	3.854	4.040	///	1.78	1.92	1.08	0.87	6158	4846
Bz-β-Phe (rac.)	1.432	3.690	6.333	///	1.58	3.42	2.17	9.25	4994	4856
Z-Leu (rac.)	1.432	3.712	4.706	///	1.59	2.29	1.44	4.20	5197	4927
Z-Arg (L>D)	1.432	1.906	2.033	L	0.33	0.42	1.27	0.94	3626	3214
Trp (rac.)	1.432	1.919	1.919	///	0.34	0.34	1.00	0.00	1138	1138
Tyr (rac.)	1.432	1.481	1.684	L	0.03	0.18	5.14	1.36	1417	2200
QN/QD (2:1)	1.432	1.303	1.303	///	-0.09	-0.09	1.00	0.00	2016	2016
Clenbuterol.HCl (rac.)	1.432	1.176	1.176	///	-0.18	-0.18	1.00	0.00	2426	2426
PI-2-56-2	1.432	9.594	11.246	///	5.70	6.85	1.20	2.10	2717	2896
PI-2-4-3	1.432	9.849	20.274	///	5.88	13.16	2.24	0.00	4458	4268
PI-2-25-1	1.432	6.751	9.685	///	3.71	5.76	1.55	5.74	4315	3963
PI-2-34-1	1.432	4.829	5.593	///	2.37	2.91	1.22	2.57	5028	4806
PI-3-67-1	1.432	7.011	7.401	///	3.90	4.17	1.07	0.92	4898	4441
PI-1-89-1	1.432	8.753	11.074	///	5.11	6.73	1.32	4.08	4927	4767
PI-2-15-1	1.432	5.194	9.830	///	2.63	5.86	2.23	10.19	4618	4105
PI-2-38-1	1.432	4.876	5.645	///	2.41	2.94	1.22	2.61	5152	5032
PI-2-87-1	1.432	4.975	5.612	///	2.47	2.92	1.18	2.12	5111	4803
P-DML-ACHSA (S,S>R,R)	1.384	4.822	11.079	S,S	2.48	7.01	2.82	13.18	4553	4428
P-DCL-ACHSA (S,S>R,R)	1.384	6.485	24.607	S,S	3.69	16.78	4.55	19.82	4466	4783

Table XVII: Column 16 (150x4 mm ID, 629 µmol/g, AzP-Silica type SP; injection volume: 5 µL; sample concentration: 1 mg/mL MeOH; flow rate: 1.0 mL/min; detection wavelength: 254 nm; mobile phase composition: MeOH/AcOH/NH_4OAc 99/1/0.25 (v/v/w); temperature: 25°C).

Analyte	t_0 [min.]	t_{r1} [min.]	t_{r2} [min.]	EO	k_1	k_2	α	R	N_1	N_2
PFB-Leu (rac.)	1.650	1.417	1.417	///	-0.14	-0.14	1.00	0.00	4227	4227
DCB-Leu (rac.)	1.650	1.458	1.458	///	-0.12	-0.12	1.00	0.00	4600	4600
DNB-N-Me-Leu (rac.)	1.650	1.475	1.475	///	-0.11	-0.11	1.00	0.00	4307	4307
Ac-Phe (rac.)	1.650	1.475	1.475	///	-0.11	-0.11	1.00	0.00	5188	5188
Z-Phe (rac.)	1.650	1.544	1.544	///	-0.06	-0.06	1.00	0.00	5592	5592
Phe (rac.)	1.650	1.502	1.502	///	-0.09	-0.09	1.00	0.00	3370	3370
DNZ-Val (D>L)	1.650	1.478	1.478	///	-0.10	-0.10	1.00	0.00	3660	3660
DNB-Pro (rac.)	1.650	1.486	1.486	///	-0.10	-0.10	1.00	0.00	4455	4455
FMOC-Aze (rac.)	1.650	1.521	1.521	///	-0.08	-0.08	1.00	0.00	4206	4206
DBTAMME (rac.)	1.650	1.465	1.465	///	-0.11	-0.11	1.00	0.00	3123	3123
DNZ-Gly	1.650	1.484	1.484	///	-0.10	-0.10	1.00	0.00	4279	4279
Hydroxyphenyllactic acid (rac.)	1.650	1.433	1.433	///	-0.13	-0.13	1.00	0.00	3324	3324
Flurbiprofen (rac.)	1.650	1.579	1.579	///	-0.04	-0.04	1.00	0.00	5249	5249
Trp (rac.)	1.650	1.540	1.540	///	-0.07	-0.07	1.00	0.00	3601	3601
QN/QD (2:1)	1.650	1.874	1.874	///	0.14	0.14	1.00	0.00	5263	5263
Clenbuterol.HCl (rac.)	1.650	1.631	1.631	///	-0.01	-0.01	1.00	0.00	5644	5644
PI-2-56-2	1.650	1.476	1.476	///	-0.11	-0.11	1.00	0.00	4154	4154
PI-2-15-1	1.650	1.504	1.504	///	-0.09	-0.09	1.00	0.00	4652	4652
P-DML-ACHSA (S.S>R.R)	1.650	1.499	1.499	///	-0.09	-0.09	1.00	0.00	4959	4959
P-DCL-ACHSA (S.S>R.R)	1.650	1.475	1.475	///	-0.11	-0.11	1.00	0.00	4527	4527

Table XVIII: Loading study Column 12 (75x4 mm ID, 490 µmol/g, DHQD-type CSP; injection volume: 5-100 µL (0.5-10 mg); sample concentration: 100 mg/mL Ac-Phe in MeOH; flow rate: 0.5 mL/min; detection wavelength: 270 nm; mobile phase composition: MeOH/AcOH/NH_4OAc 99/1/0.25 (v/v/w); temperature: 25°C) and Column 15 (75x4 mm ID, app. 340 µmol/g, QD-AX type CSP); injection volume: 5-100 µL (0.5-10 mg); sample concentration: 100 mg/mL Ac-Phe in MeOH; flow rate: 0.5 mL/min; detection wavelength: 270 nm; mobile phase composition: MeOH/AcOH/NH_4OAc 99.46/0.43/0.11 (v/v/w); temperature: 25°C).

Column	Inj. Vol. [µL]	Inj. Mass [mg]	t_0 [min.]	t_{r1} [min.]	tr2 [min.]	k_1	k_2	α	R	N_1	N_2
12	5	0.5	1.459	6.260	8.049	3.29	4.52	1.373	2.012	1231	841
	8	0.8	1.459	6.171	7.900	3.23	4.42	1.367	1.745	983	631
	10	1.0	1.459	6.025	7.698	3.13	4.28	1.366	1.564	804	513
	12	1.2	1.459	6.016	7.683	3.12	4.27	1.366	1.472	714	456
	14	1.4	1.459	5.958	7.606	3.08	4.21	1.366	1.369	620	396
	16	1.6	1.459	5.889	7.511	3.04	4.15	1.366	1.285	552	349
	18	1.8	1.459	5.822	7.422	2.99	4.09	1.367	1.217	494	318
	20	2.0	1.459	5.758	7.337	2.95	4.03	1.367	1.146	439	283
	22	2.2	1.459	5.691	7.251	2.90	3.97	1.369	1.079	388	253
	24	2.4	1.459	5.634	7.187	2.86	3.93	1.372	1.034	352	231
	25	2.5	1.459	5.522	7.025	2.79	3.82	1.370	0.944	317	180
	30	3.0	1.459	5.475	6.966	2.75	3.78	1.371	0.788	264	82
	50	5.0	1.459	4.933	6.207	2.38	3.26	1.367	0.533	118	55
	60	6.0	1.459	4.742	5.923	2.25	3.06	1.360	0.472	104	42
	70	7.0	1.459	4.571	5.679	2.13	2.89	1.356	0.458	113	31
	80	8.0	1.459	4.382	5.383	2.00	2.69	1.342	0.451	131	23
	90	9.0	1.459	4.242	5.173	1.91	2.55	1.334	0.449	146	19
	100	10.0	1.459	4.109	4.970	1.82	2.41	1.325	0.449	162	17
15	5	0.5	1.565	5.915	8.230	2.78	4.26	1.532	3.526	2532	1183
	10	1.0	1.565	5.689	7.835	2.64	4.01	1.520	2.276	1067	579
	20	2.0	1.565	5.288	7.296	2.38	3.66	1.539	1.418	356	276
	25	2.5	1.565	5.120	7.080	2.27	3.52	1.551	1.206	249	202
	30	3.0	1.565	4.977	6.897	2.18	3.41	1.563	1.051	187	151
	40	4.0	1.565	4.699	6.540	2.00	3.18	1.587	0.836	117	92
	50	5.0	1.565	4.450	6.240	1.84	2.99	1.620	0.693	78	59
	60	6.0	1.565	4.233	5.938	1.70	2.79	1.639	0.585	58	39
	70	7.0	1.565	4.220	5.602	1.70	2.58	1.521	0.462	57	29
	80	8.0	1.565	3.832	5.291	1.45	2.38	1.644	0.504	55	25
	90	9.0	1.565	3.658	4.882	1.34	2.12	1.585	0.442	60	16
	100	10.0	1.565	3.492	4.636	1.23	1.96	1.594	0.456	71	13